SEISMIC BEHAVIOUR EVALUATION OF INVERTED-V BRACED FRAMES

A THESIS SUBMITTED TO THE GRADUATE SCHOOL OF APPLIED SCIENCES OF NEAR EAST UNIVERSITY

By
MOHAMMAD ALKHATTAB

In Partial Fulfilment of the Requirements for the Degree of Master of Science in Civil Engineering

NICOSIA, 2019

MOHAMMAD ALKHATTAB
SEISMIC BEHAVIOUR EVALUATION OF INVERTED-V BRACED FRAMES
NEU 2019

SEISMIC BEHAVIOUR EVALUATION OF INVERTED-V BRACED FRAMES

A THESIS SUBMITTED TO THE GRADUATE SCHOOL OF APPLIED SCIENCES OF NEAR EAST UNIVERSITY

By
MOHAMMAD ALKHATTAB

In Partial Fulfilment of the Requirements for the Degree of Master of Science in Civil Engineering

NICOSIA, 2019

Mohammad ALKHATTAB: **SEISMIC BEHAVIOUR EVALUATION OF INVERTED-V BRACED FRAMES**

Approval of Director of Graduate School of Applied Sciences

Prof.Dr. Nadire ÇAVUŞ

We certify that, this thesis is satisfactory for the award of the degree of Master of Science in Civil Engineering

Examining Committee in Charge:

Prof. Dr. Kabir Sadeghi	Department of Civil Engineering, Near East University
Assit. Prof. Dr.Çiğdem Çağnan	Department of Architecture, Near East University
Assoc. Prof. Dr. Rifat Reşatoğlu	Supervisor, Department of Civil Engineering, Near East University

I hereby declare that all information in this document has been obtained and presented in accordance with academic rules and ethical conduct. I also declare that, as required by these rules and conduct, I have fully cited and referenced all material and results that are not original to this work.

Name, Last name: Mohammad ALKHATTAB
Signature:
Date:

ACKNOWLEDGEMENTS

I am deeply grateful to my supervisor Assoc.Prof.Dr. Rifat Reşatoğlu for his invaluable support patience and technical suggestions during this thesis works. I would like also to thank to all the members of the civil engineering department in Near East University.

My special appreciation and thanks goes to my family for encouraging and supporting me during my study

To my parents...

ABSTRACT

Cyprus is located in a region with high seismic activity which inquires buildings to have systems to resist the lateral imposed loads. Bracing elements in structural system plays vital role in structural behaviour during earthquake. There are plenty of bracing systems and are thoroughly studied in the literature. However, there are insufficient studies regarding inverted-V bracing system in accordance with NCSC-2015. In this study, the seismic performance of steel structures equipped with various types of inverted-V bracing systems are investigated for multi-storey buildings in accordance with NCSC-2015 in order to achieve the objective. Steel structure buildings are analysed under different loading conditions using ETABS2016 software package. For this purpose, Linear static (ELFM), non-linear static (Pushover) and non-linear dynamic (T.H) analysis were adopted. Results indicate that inverted-V bracing systems dramatically enhance the performance of the steel structure more particularly when the earthquake is applied perpendicular to the minor axis of the columns. This indicates that inverted-V bracing systems are an effective solution to resist the lateral applied loads while maintaining the functionality of the building.

Keywords: Inverted-V steel bracing system; equivalent lateral force method; pushover analysis method; dynamic time history analysis method; NCSC-2015

ÖZET

Kıbrıs, binaları yandan uygulanan yüklere karşı koyacak sistemlere sahip olmak isteyen, yüksek sismik faaliyet gösteren bir bölgede yer almaktadır.Yapı sistemlerinde destekleme elemanları, deprem sırasındaki yapısal davranışta hayati bir rol oynar. Literatürde ayrıntılı olarak incelenmiş bol miktarda destekli sistemler vardır. Ancak, NCSC-2015 uyarınca ters V destekli sistemle ilgili yeterli çalışma bulunmamaktadır. Bu çalışmada, amaca ulaşmak için muhtelif tipte ters V bağlantılı sistemlere sahip çelik yapıların sismik performansı çok katlı binalar için NCSC-2015 uyarınca incelenmiştir. ETABS2016 yazılım paketi kullanılarak farklı yükleme koşullarında çelik yapı binaları analiz edilmiştir. Bu amaçla Doğrusal statik (EÇY), doğrusal olmayan statik (statik itme) ve doğrusal olmayan dinamik (Z.T) analizleri tatbik edilmiştir. Sonuçlar, ters V bağlantılı sistemlerin, özellikle deprem kuvvetlerinin kolonların zayıf eksenine dik olarak uygulandığında, çelik yapının performansını büyük ölçüde artırdığını göstermektedir. Bu, ters V bağlantılı sistemlerinin, binanın işlevselliğini korurken, yanal uygulanan yüklere karşı koymak için de etkili bir çözüm olduğunu gösterir.

Anahtar kelimeler: Ters V çelik bağlantılı sistemleri;eşdeğer yanal kuvvet yöntemi; statik itme analizi metodu; dinamik zaman tanım alanında analiz yöntemi; NCSC-2015

TABLE OF CONTENTS

ACKNOWLEDGEMENTS …….. ii
ABSTRACT …… iv
ÖZET …….. v
TABLE OF CONTENTS …….. vi
LIST OF TABLES ……. ix
LIST OF FIGURES ……... xi
LIST OF ABBREVIATIONS ……... xiv
LIST OF SYMBOLS ……. xvi

CHAPTER 1: NTRODUCTION
1.1 Background …… 1
1.2 Problem Statement ……...…….. 3
1.3 Objective and Scope …….. 3
1.4 Outline of the Document ……..…. 4

CHAPTER 2 : LITERATURE REVIEW
2.1 Overview …… 5

CHAPTER 3: METHODOLOGY
3.1 Overview …… 9
3.2 Analysis Strategy…… 9
3.3 Location of the Case Study……. 10
3.4 Modelling of Steel Framed Structures…… 11
3.5 Structural Elements and Slab Properties……. 14
3.5.1 Column Cross-Section…… 14
3.5.2 Beam cross-section……. 14
3.5.3 Bracing cross-section…….. 15
3.5.4 Knee cross-section…….. 16
3.5.5 Slab type……. 16
3.6. Inverted-V Bracing Types……. 16

3.6.1 Concentric inverted-V bracing (CIV)……. 16
3.6.2 Eccentric inverted-V Bracing (EIV)……... 17
3.6.3 Inverted-V with knee (KIV1&2)…… 19
3.7 Types of Seismic Analysis Methods...……...……. 20
3.7.1 Equivalent lateral force method…….. 20
3.7.2 Non-linear static pushover analysis…… 21
3.7.2.1 Target displacement calculation……. 21
3.7.2.2 Pushover curve…… 23
3.7.2.3 Plastic hinges…….. 25
3.7.3 Time history analysis…….. 26
3.7.3.1 Ground motion scaling methods……. 27
3.7.3.2 Scaling of real acceleration to fit NCSC-2015 spectrum…… 27
3.8 Modal Analysis……... 28
3.8.1 Eigen-vector analysis…….. 28
3.8.2 Ritz-vector analysis…… 29
3.9 Design Assumptions……... 29
3.9.1 Gravity loads……... 29
3.9.2 Wind loads…….. 30
3.9.3 Earthquake load parameters…… 30
3.9.4 Load combination……... 31
3.10 Non-Linear Analysis of the Case Study……..……. 32
3.10.1 Pushover analysis of the case study…..…… 32
3.10.2 Time history analysis of the case study…… 34

CHAPTER 4: RESULTS AND DISCUSSIONS

4.1 Overview……. 36
4.2 Equivalent Lateral Force Method (ELFM)……. 36
4.2.1 Base shear……... 36
4.2.2 Top storey displacement……. 38
4.2.3 Storey drift…….. 40
4.2.4 Mass of the structural buildings…….. 44

4.3 Non-Linear Static Pushover Analysis……. 46
4.3.1 Base shear at the target displacement……. 46
4.3.2 Lateral stiffness……... 48
4.3.3 State of plastic hinges……. 53
4.3.4 Displacement ductility factor…….. 55
4.4 Time History Analysis…… 57
4.4.1 Base shear……... 57
4.4.2 Roof displacement…….……. 62
4.4.3 Roof acceleration…… 67

CHAPTER 5: CONCLUSIONS & RECOMMENDATIONS
5.1 Overview……. 73
5.2 Summary of the Results…….. 73
5.3 Recommendations……... 75

REFERENCES……..... 76

APPENDICES
Appendix 1: Seismic Zones in Cyprus …… 81
Appendix 2: Soil Investigation in Famagusta City …….. 83
Appendix 3: Materials and Slab Deck Properties……. 85
Appendix 4: Earthquake Parameters According to NCSC-2015…….. 87
Appendix 5: (Stiffness-Base Shear) Displacement Curves…….. 93
Appendix 6: Response Spectrum Curves…….. 100

LIST OF TABLES

Table 3.1: Modification factor C_0 according to FEMA-356……. 22
Table 3.2: Modification factor C_2 according to FEMA-356……. 23
Table 3.3: Ductility reduction Factor (R)……. 30
Table 3.4: Earthquake parameters used in this study……... 31
Table 3.5: Design load combinations……... 32
Table 3.6: Plastic hinges Properties…….. 33
Table 3.7: Target displacement in X direction……. 33
Table 3.8: Target displacement in Y direction……. 34
Table 3.9: Details of the selected ground motion records…… 35
Table 4.1: The percent variation in the base shear compared with the moment resisting frame (ELFM)…….. 38
Table 4.2: The percent variation in the roof displacement compared with the moment resisting frame (ELFM)……... 40
Table 4.3: Total mass of the structural systems (ELFM)……. 45
Table 4.4: The difference between elements weight of braced and MRF G+4 buildings (ELFM)……... 45
Table 4.5: The difference between elements weight of braced and MRF G+9 buildings (ELFM)……... 46
Table 4.6: The percent variation in the initial and final stiffness for G+4 buildings compared with the moment resisting frame (Pushover)……. 52
Table 4.7: The percent variation in the initial and final stiffness for G+9 buildings compared with the moment resisting frame (Pushover)……. 53
Table 4.8: Plastic hinges for G+4 buildings (Pushover)……... 55
Table 4.9: Plastic hinges for G+9 buildings (Pushover)……... 55
Table 4.10: Displacement ductility factor in X and Y directions for G+4 buildings (Pushover)…….. 56
Table 4.11: Displacement ductility factor in X and Y directions for G+9 buildings (Pushover)…….. 57
Table 4.12: The percent variation in the base shear compared with the moment resisting frame (K.E)…… 61

Table 4.13: The percent variation in the base shear compared with the moment resisting frame (S.E)…… 61
Table 4.14: The percent variation in the base shear compared with the moment resisting frame (E.E)…… 62
Table 4.15: The percent reduction in the roof displacement compared with the moment resisting frame (K.E)……. 66
Table 4.16: The percent reduction in the roof displacement compared with the moment resisting frame (S.E)…….. 66
Table 4.17: The percent reduction in the roof displacement compared with the moment resisting frame (E.E)…….. 67
Table 4.18: The percent increment in the roof acceleration compared with the moment resisting frame (K.E)……. 71
Table 4.19: The percent increment in the roof acceleration compared with the moment resisting frame (S.E)…….. 71
Table 4.20: The percent increment in the roof acceleration compared with the moment resisting frame (E.E)…….. 72

LIST OF FIGURES

Figure 1.1: Concentric steel bracings types……..……... 2
Figure 1.2: Eccentric steel bracings types……..... 2
Figure 1.3: Steel bracings with knee types……... 2
Figure 1.4: Inverted-v bracing types …… 2
Figure 3.1: Flow chart of the research program……..……... 10
Figure 3.2: location of the structural steel building (Google maps 2019)..……. 11
Figure 3.3: Seismic map zoning according to NCSC 2015 (Chamber of Civil Engineers, 2015)……. 11
Figure 3.4: Floor plan for regular steel framed buildings……..…….. 12
Figure 3.5: Floor plan for irregular steel framed buildings……..……... 12
Figure 3.6: Three dimensional model of G+4 storey regular steel framed building with (CIV) bracing……. 13
Figure 3.7: Three dimensional model of G+4 storey irregular steel framed building with (CIV) bracing……. 13
Figure 3.8: Schematic view of the HEB cross-section……. 14
Figure 3.9: Schematic view of the IPE cross-section……... 15
Figure 3.10: Schematic view of the CHS cross-section……... 15
Figure 3.11: Schematic view of the Aldeck 70/915 cross-section……..… 16
Figure 3.12: Concentric inverted-V Bracing (CIV)……..…….. 17
Figure 3.13: Eccentric steel bracing system (EIV)……..…… 17
Figure 3.14: Rotation angels for eccentric steel bracing……..……... 18
Figure 3.15: Inverted-V with knee bracing system (KIV)…… 19
Figure 3.16: Seismic analysis methods..……..…… 20
Figure 3.17: Relationship between lateral forces and latera deflection..…...……... 24
Figure 3.18: chart of plastic hinge phases…..……..……... 25
Figure 3.19: Mode shapes components to determine the total response (CSI, 2014).. 29
Figure 3.20: Ground acceleration records……..……. 35
Figure 4.1: Base shear in X and Y directions for G+5 buildings (ELFM)……... 37
Figure 4.2: Base shear in X and Y directions for G+9 buildings (ELFM)……... 37
Figure 4.3: Roof displacement in X and Y directions for G+5 buildings (ELFM)….. 39

Figure 4.4: Roof displacement in X and Y directions for G+9 buildings (ELFM)….. 39
Figure 4.5: Storey drift in X direction for G+5 regular buildings (ELFM)…….. 41
Figure 4.6: Storey drift in Y direction for G+5 regular buildings (ELFM)…….. 41
Figure 4.7: Storey drift in X direction for G+5 irregular buildings (ELFM)……... 42
Figure 4.8: Storey drift in Y direction for G+5 irregular buildings (ELFM)……... 42
Figure 4.9: Storey drift in X direction for G+9 regular buildings (ELFM)…….. 43
Figure 4.10: Storey drift in Y direction for G+9 regular buildings (ELFM)…… 43
Figure 4.11: Storey drift in X direction for G+9 irregular buildings (ELFM)……. 44
Figure 4.12: Storey drift in Y direction for G+9 irregular buildings (ELFM)……. 44
Figure 4.13: Base shear in X and Y directions for G+4 buildings (Pushover)……. 47
Figure 4.14: Base shear in X and Y directions for G+9 buildings (Pushover)……. 47
Figure 4.15: Stiffness - displacement curves in X direction for (Regular-G+4) buildings……...…… 48
Figure 4.16: Stiffness - displacement curves in Y direction for (Regular-G+4) buildings……...…… 49
Figure 4.17: Stiffness - displacement curves in X direction for (IRegular-G+4) buildings……...…… 49
Figure 4.18: Stiffness - displacement curves in Y direction for (IRegular-G+4) buildings……...… 50
Figure 4.19: Stiffness - displacement curves in X direction for (Regular-G+9) buildings……...…… 50
Figure 4.20: Stiffness - displacement curves in Y direction for (Regular-G+9) buildings……...…… 51
Figure 4.21: Stiffness - displacement curves in X direction for (IRegular-G+9) buildings……...…... 51
Figure 4.22: Stiffness - displacement curves in Y direction for (Regular-G+9) buildings……...… 52
Figure 4.23: First and final step plastic hinges occurring in Y direction for (R-CIV-5) building…… 54
Figure 4.24: First and final step plastic hinges occurring in Y direction for (R-CIV-10) building…….. 54

Figure 4.25: Base shear in X and Y directions for G+4 buildings (K.E)……. 58
Figure 4.26: Base shear in X and Y directions for G+9 buildings (K.E)……. 58
Figure 4.27: Base shear in X and Y directions for G+4 buildings (S.E)…….. 59
Figure 4.28: Base shear in X and Y directions for G+9 buildings (S.E)…….. 59
Figure 4.29: Base shear in X and Y directions for G+4 buildings (E.E)…….. 60
Figure 4.30: Base shear in X and Y directions for G+9 buildings (E.E)…….. 60
Figure 4.31: Roof displacement in X and Y directions for G+4 buildings (K.E)…… 63
Figure 4.32: Roof displacement in X and Y directions for G+9 buildings (K.E)…… 63
Figure 4.33: Roof displacement in X and Y directions for G+4 buildings (S.E)……. 64
Figure 4.34: Roof displacement in X and Y directions for G+9 buildings (S.E)……. 64
Figure 4.35: Roof displacement in X and Y directions for G+9 buildings (E.E)……. 65
Figure 4.36: Roof displacement in X and Y directions for G+9 buildings (E.E)……. 65
Figure 4.37: Roof acceleration in X and Y direction for G+4 buildings (K.E)…… 68
Figure 4.38: Roof acceleration in X and Y direction for G+9 buildings (K.E)…… 68
Figure 4.39: Roof acceleration in X and Y direction for G+4 buildings (S.E)…… 69
Figure 4.40: Roof acceleration in X and Y direction for G+9 buildings (S.E)…… 69
Figure 4.41: Roof acceleration in X and Y direction for G+4 buildings (E.E)…… 70
Figure 4.42: Roof acceleration in X and Y direction for G+9 buildings (E.E)…… 70

LIST OF ABBREVIATIONS

R:	Regular Building
IR:	Irregular building
G:	Ground floor
IV:	Inverted-V Bracing
CIV:	Concentric Inverted-V
EIV:	Eccentric Inverted-V
KIV:	Inverted-V with Knee
MRF:	Moment Resisting Frame
AISC:	The Australian Industry and Skills Committee
LRFD:	Load and Resistance Factor Design
ASCE:	American Society of Civil Engineers
BNBC:	Bangladesh National Building Code
STAAD PRO:	Stands For Structural Analysis and Designing Program
SAP:	Structural Analyses Programme
IS:	Indian Standard
UC:	Universal Column
UB:	Universal Beam
UFC:	Unified Facilities Criteria
EC 3:	Design of Steel Structures
NCSC-2015:	Northern Cyprus Seismic Code
FEMA:	Federal Emergency Management Agency Code
ELFM:	Equivalent Lateral Force Method
T.H:	Dynamic Time History Analysis
ETABS:	Extended Three Dimensional Analysis of Building System
PEER:	Pacific Earthquake Engineering Research
T.D:	Target Displacement
RU:	Ready for Usage
LS:	Life Safety
IQ:	Immediate Occupancy
CP:	Collapse Prevention

PC:	Pre-Collapse
F:	Force
D:	Displacement
FNA:	Fast Non-Linear Analysis
HEB:	European Standard Wide Flange H Steel Beams, Type (B)
HEA:	European Standard Wide Flange H Steel Beams, Type (A)
IPE:	European Standard I Sections With Parallel Flange
CHS:	Circular Hollow Section
(K.E, S.E, E.E):	(Kocaeli, Sakarya, Erzincan) Earthquake

LIST OF SYMBOLS

DL:	Dead load
LL:	Live load
A (T):	Spectral Acceleration Coefficient
$\boldsymbol{A_0}$**:**	Effective Ground Acceleration Coefficient
S (T):	Spectrum Coefficient
($\boldsymbol{T_A}$**,** $\boldsymbol{T_B}$**):**	Spectrum Characteristic Periods
Mp:	Bending moment capacity calculated at the bottom end of the column
Vp:	Shear force capacity
e:	Link length
L:	Span length
γp:	Turning Angle of the Bond Beam
Op:	The Angle of Story Drift
Δi:	Storey Drift
H:	Storey Height
B:	Frame width
h:	Knee Part Height
b:	Knee Part Width
I:	Building Importance Factor
T:	Building Natural Period
Z:	Local Site Class
R:	Structural Behaviour Factor
Vt:	Total Equivalent Seismic Load
W:	Total building weight
Ra:	Seismic Load Reduction Factor
Wi:	Storey weight
qi:	Total live load at i'th storey of a building
n:	Live Load Participation Factor,
ΔFN:	Additional equivalent seismic load
Fi:	Design seismic load acting at i'th storey in Equivalent Seismic Load Method

N:	Total number of stories of building from the foundation level
g:	Acceleration of Gravity
Te:	Effective Fundamental Period of the Building
Ts:	Characteristic Period of the Response Spectrum
SaR(T):	Acceleration spectrum ordinate for the r'th natural vibration mode
Sae(T):	Elasticity spectrum ordinate
Sa:	Response spectrum acceleration
K:	Lateral Stiffness
μ:	Displacement Ductility Factor
Δmax:	Maximum Displacement
Δy:	Displacement of First Yielding
P:	Axial Force
M2, M3:	Bending moments
Ku:	Stiffness-Displacement Matrix
Cú:	Damping-Velocity Matrix
Mü:	Diagonal Mass-Acceleration Matrix
r:	Applied load
Mw:	Moment magnitude
Vs30:	Shear Wave Velocity
Ω^2:	Diagonal Matrix of Eigenvalue
Φ:	Matrix of the G
W^2:	Eigenvalue
F:	Cyclic Frequency
Rjb:	The Horizontal Displacement Between Rupture Plane and The Station
Rrup:	The Direct Displacement Between Rupture Plane and The Station

CHAPTER 1

INTRODUCTION

1.1 Background

For the past millennium, earthquakes can be considered as one of the most dangerous natural disasters that threatened the lives of human race. It has been estimated that around 500,000 seismic activities take place around the world. However, only 100,000 of which can be felt (Ozmen et al. 2008). Earthquake can result in a catastrophic events, which can lead to a large number of casualties and significant damages in both superstructure and infrastructure. Thus, designing a structure that can withstand these events is a major concern for engineers. There are plenty of systems that can enhance the ability of structure to the lateral forces such as;

1- Base isolation.
2- Tuned mass damper.
3- Viscous and friction damper.

However, such system requires skilled labours and hard to apply in developing countries not to mention the tremendous cost of shipping and instillation. Hence, cheaper and applicable system such as shear walls or bracing system are more desirable in such countries.

Steel bracings are designated to repel the lateral forces that might be exerted on a given structure. There are plenty types of steel bracing systems such as;

- X-bracing.
- Diagonal-bracing
- V-bracing
- K-bracing

These bracing systems minimise the ability of creating openings along the elevation of the building, where openings are quite essential in Northern Cyprus for the purpose of natural ventilation. Ultimately, Inverted-V bracing systems have good advantages in this aspect.

Figure 1.1-1.3 present a schematic plots of the most widely used bracing systems altogether with their structural classifications.

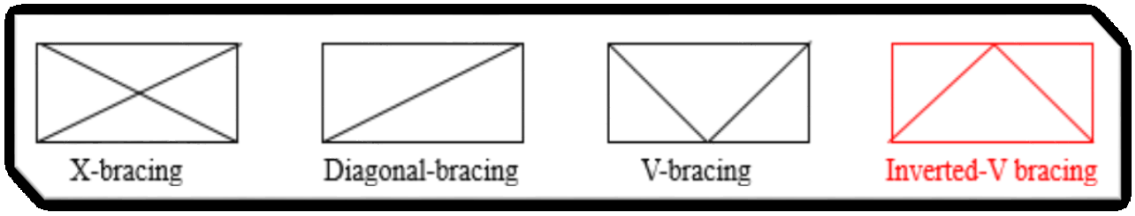

Figure 1.1: Concentric steel bracings types

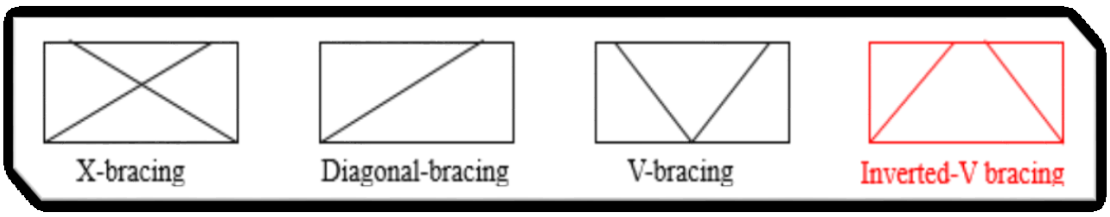

Figure 1.2: Eccentric steel bracings types

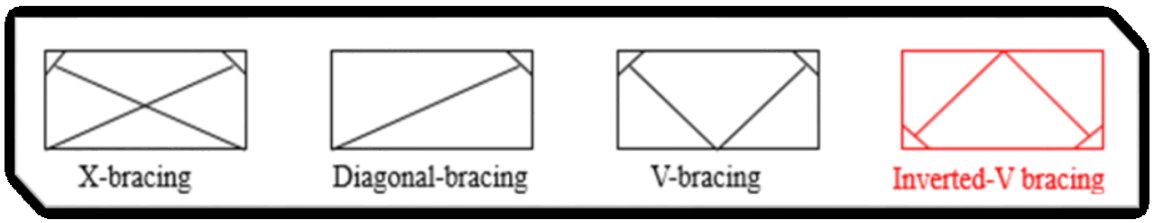

Figure 1.3: Steel bracings with knee types

(a) Concentric inverted-v bracing (b) Eccentric inverted-v bracing

Figure 1.4: Inverted-v bracing types

Northern Cyprus is one of the developing countries that are threatened by seismic activities. Since it is located within the plate boundary between the Anatolian, Nubian and Sinai faults. Thus, the development of an applicable and inexpensive systems that can survive the sever ground motion is extremely vital.

1.2 Problem Statement

The usage of shear walls and bracing system in the enhancement of building performance to resist the lateral forces is extensively investigated in the literature. On the other hand, the documented literature on the performance of inverted-V bracing systems in accordance with the Northern Cyprus Seismic Code (NCSC-2015) does not exist yet. In addition, the optimum type of inverted-V bracing systems to accommodate with the intense peak ground acceleration in the Northern Cyprus is not studied yet.

1.3 Objective and Scope

Three different analysis methods are utilized to investigate the performance of various types of inverted-V bracing systems on steel structures in accordance with NCSC-2015. The adopted analysis methods includes;

1. Linear static (Equivalent lateral force method).
2. Non-linear static (Pushover).
3. Non-linear dynamic (Time history analysis).

In order to make this research more comprehensive, both medium rise and high rise buildings are implemented, which will enable the study to decide on the most efficient inverted-V bracing systems in terms of the following parameters:

- Total mass of the structure
- The resulted base shear
- The imposed storey drift and displacement
- The lateral stiffness
- Displacement ductility factor

1.4 Outline of the Thesis

This dissertation is organized in six main chapters. This chapter gives a general information about the seismicity of Northern Cyprus (i.e. seismic risk of Northern Cyprus). It also introduces the motivation of this dissertation. Finally, the outline of the document is described.

Chapter 2 discusses previous the studies within the literature that shares similar interests with this study.

Chapter 3 concentrates on the seismic analysis methods.

Chapter 4 presents an overview of the case study, describing the geometry and section properties and explains the methods to model the structures.

Chapter 5 presents the results and discussions of the analysed models by means of the structure performance.

Chapter 6 presents the main conclusion and provides recommendation for future developments.

CHAPTER 2

LITERATURE REVIEW

2.1 Overview

This chapter contains some of articles which are related to steel bracing systems with the revelation of brief overview. In accordance to past published researches in earthquake resisting methods, there are different standards and method of analysis which investigates the impact of steel bracing systems on the seismic performance of buildings.

Nourbakakhsh (2011) has presented a comparative study among three different eccentric steel bracings types. Where each of v, inverted v and diagonal bracing in different buildings height (4, 8, 12 storey). The building are designed according to AISC LRFD (1999) steel code and Iranian seismic code (2800). In this study the frames are assessed by pushover analysis based on FEMA 440 standard to evaluate the buildings in terms of weight and plastic hinges classification. The analysis done by using ETABS software, where the results show that diagonal braced frames have better performance among these types.

Tafheem & Khusru (2013) have presented a comparative study between concentric and eccentric steel bracing systems. In this study six storey steel structural buildings are modelled and analysed due to wind loading lateral earthquake loading in addition to dead load and live load. Each concentric x- bracing and eccentric v bracing are performed in the same steel building. In this study the wind loads are calculated according to ASCE 7-05 and earthquake lateral loads are calculated according to Bangladesh national building code BNBC 2006. The performance of the buildings are evaluated in terms of storey drift, displacement, axial forces and bending moment by using ETABS software. From this study it is found that more lateral displacement reduced by concentric x bracing with greater structure stiffness.

Siddiqi, Hameed & Akmal (2014) have presented a study investigated the comparison of different bracing systems in tall buildings. In this study five types of steel bracing systems are investigated in terms of structure weight, lateral displacement and lateral stiffness. Where each of concentric diagonal braced frames, concentric x braced frames, concentric inverted-v braced frames and eccentric inverted-v braced frames are modelled and analysed by using STAAD Pro. For the reason of this study non-linear static analysis is performed. From the results that obtained from this study eccentric inverted-v obtained minimum value of lateral displacement. However, the minimum weight obtained in case of cross x bracing.

Patil & Sangle (2015) have presented a study investigated a comparative study aimed to compare the seismic behaviour for each of v-braced frames, inverted-v braced frames, x-braced frames and zipper braced frames in high rise 2-D steel building. To investigate these types pushover analysis were carried out to assess the performance of steel bracings in high rise steel buildings of 15, 20, 25, 30 and 35 storey, where the buildings are designed by using SAP200 software according to IS1893:2002 and IS 800:2007 codes. The size of all columns and beams in all the buildings are the same as in the moment resisting building and all bracings types have same steel size. The results show that all the bracings types are performed well and lead to enhance the performance of the moment resisting frames, inverted-v braced frames show lower story displacement and story drift with seismic response similar in term of base shear.

Khaleel & Kumar (2016) have presented a study investigated the effect of seismic forces on regular and irregular steel structural buildings with different steel bracing systems, where each of moment resisting frame, x-bracing, v-bracing, inverted-v bracing, k-bracing and knee bracing systems are investigated according to IS 1983-2002 code. The structural buildings with G+9 storey are designed and analysed using ETABS software. The parameters such as base shear and displacement are studied where the analysis carried out by equivalent lateral force method. The results show that for both cases regular and irregular buildings X-bracing is the beast bracing system for reducing the story displacement , in addition x-bracing has high base share because of increased the stiffness.

Kulkarni, Ghandak, Devtale & Sayyed (2016) have present a study about steel bracing as a method to resist the lateral forces. In this study G+9 storey steel buildings are designed with respect to Indian standard 800-2007 by using each of UC and UB British sections.to resist earthquake, wind and gravity loads. Different types of steel bracing are investigated in this study, where each of x-bracing, v-bracing, inverted-v bracing and k-bracing are modelled with the structure by using STAAD Pro (v8i) software. The results from this study show that, maximum lateral deflection observed in k braced building and minimum weight is observed in case of v-braced building.

Mapar & Ghugal (2017) have present a study about the seismic performance of high rise steal buildings in case of MRF and braced frames. For the aim of this study each of cross, v , k and inverted-v bracing types are selected and introduced within 25 storey structure. The dynamic analysis is investigated by using ETABS 2013 software. The results according to base shear roof displacement and modal period show that cross bracing is the optimum bracing system.

Haque, Masum, Ratuland & Tafheem (2018) have present an investigation about the effectiveness of different braced buildings, where each of eccentric inverted-v, v and x braced structures are selected for this study and compared with unbraced structure. The comparative in this study based on storey drift, story displacement and moment on the beams The buildings have been analysed by using ETABS 2015 software with respect to Bangladesh National Building code BNBC 2006. From the results that obtained in this study X bracing is the optimum type among the selected types.

Mahmoud, Hassan, Mourad & Sayed (2018) have present a study investigated the progressive collapse, which is caused by seismic loads for five steel MRF and braced frames with different columns removal section. These frames are designed with respect to Egyptian standard with applying of alternate path method according to UFC guideline. For the popups of this study time history analysis is conducted by using SAP200 software.

Hashemi & Alirezaei (2018) have investigated the seismic performance of eccentric diagonal bracing by adding knee element within the system. To achieve the aim of this study finite element software is used to do a numerical modelling. Hence, the knee elements dissipate the energy through plastic deformation with remaining in plastic range for the other structural elements, the deformation of knee element is stand by using stopper. The results of the study show that the stiffness and strength are enhanced.

Mahmoudi, Montazeri & Jailili (2018) have presented an investigation about the performance of cross bracing with adding knee element and shape memory alloy bars. To achieve the purpose of this investigation three, five and seven storey frames are modelled. 12 different diameter of shape memory alloy are investigated by using pushover and time history analysis. From the results of this study the seismic response of the frames are increased by adding shape memory alloy where this enhancing is related to increasing of the diameter.

Yang, Sheikh & Tobber (2019) have investigated a study about the effect of steel bracing configuration on the response of steel frames conducted by concentric bracing. For the aim of this study five storey buildings, which located in Vancouver Canada are investigated by using five different configurations, the models designed according to the national building code in Canada. The comparative which done according to initial and life cycle cost shows that cross bracing is the most expensive type and expanded cross type which consist of v and inverted-v bracing is the most economical type.

CHAPTER 3

METHODOLOGY

3.1 Overview

This chapter presents the selected case study and discusses the modelling of steel structural buildings and explore the variations in the results obtained.

3.2 Analysis Strategy

The aim of this study is to investigate the influence of various types of inverted-V bracing systems on the seismic performance of steel frame buildings at Famagusta city. In order to meet this objective, 20 models of steel frame buildings that are consisted of both G+4 and G+9 floors, with 4 different types of bracing systems, considering both regular and irregular plans.

In order to make the study more comprehensive, three different methods of analyses are conducted which are listed below;

1- Equivalent lateral force method (ELFM) in accordance with NCSC-2015.
2- Non-linear static pushover analysis method in accordance with FEMA-356.
3- Non-linear time history analysis method (T.H) by using three different ground motion records.

Figure 3.1 briefly presents the analysis strategy in the form of flow chart.

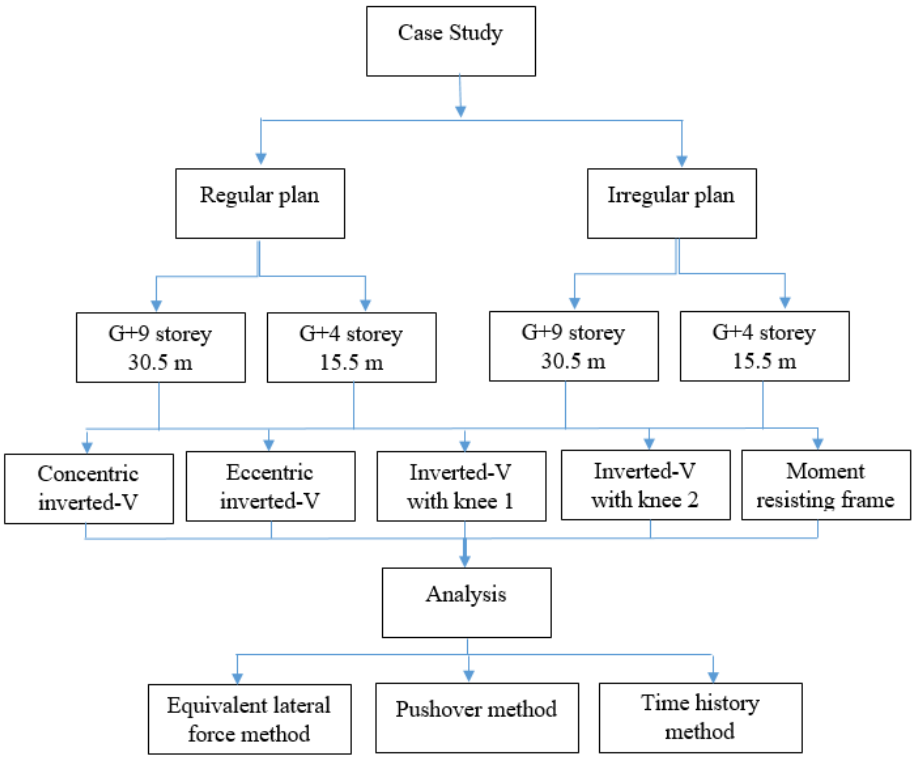

Figure 3.1: Flow chart of the research strategy

3.3 Location of the Case Study

The location of the steel structural building is assumed to be at Famagusta (Gazimağusa) city in northern Cyprus as shown in Figure 3.2. This location has characterized with a peak ground acceleration ranging between 0.3-0.35g. This can be seen in Figure 3.3 which shows the seismic zoning map that has been adopted for the northern part of the island.

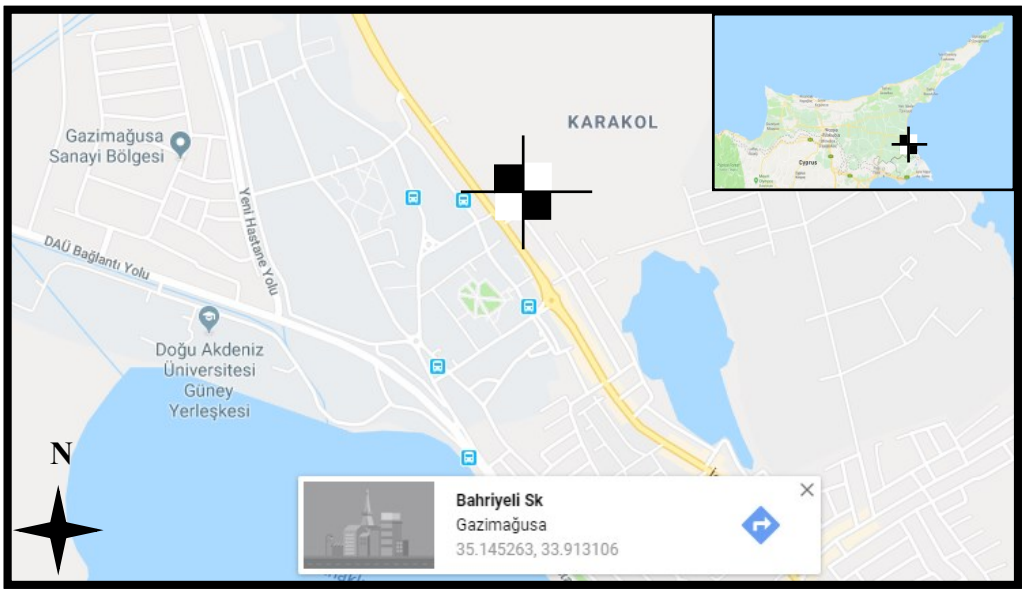

Figure 3.2: Location of the structural steel building (Google Maps 2019)

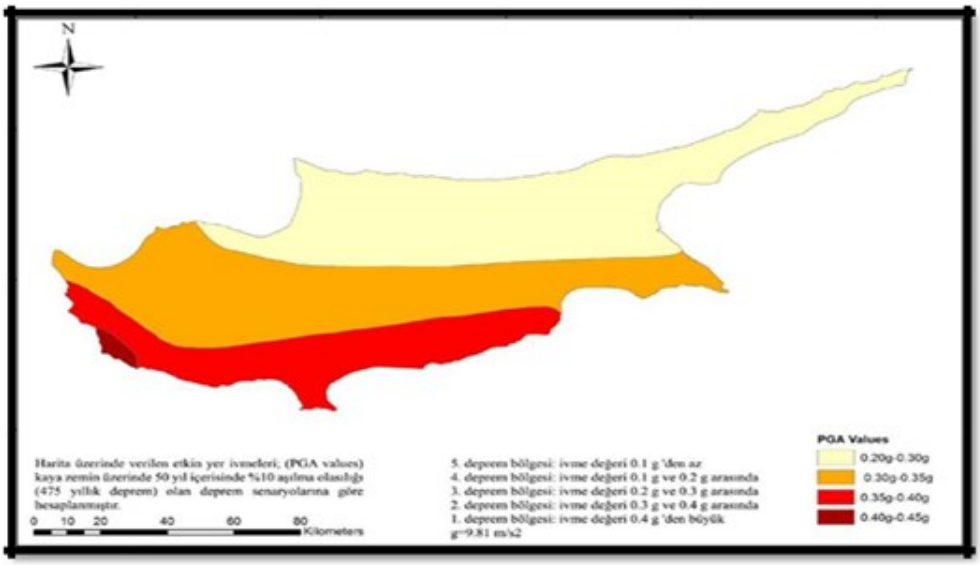

Figure 3.3: Seismic zoning map according to NCSC 2015 (Chamber of Civil Engineers, 2015)

3.4 Modelling of Steel Framed Structures

Buildings are modelled, analysed and designed using ETABS2016 software. The column arrangement and the spans length are presented in Figure 3.4 and Figure 3.5 for both regular and irregular buildings respectively. All the buildings are consisted of a ground floor with an elevation of 3.5 m from ground level. Ultimately, the typical storey height is 3 m. The three dimensional representation of the buildings are presented in Figure 3.6 and Figure 3.7

for both regular and irregular building respectively. All the structural element are connected with rigid connection except bracings and secondary beams where they are hinged at both ends.

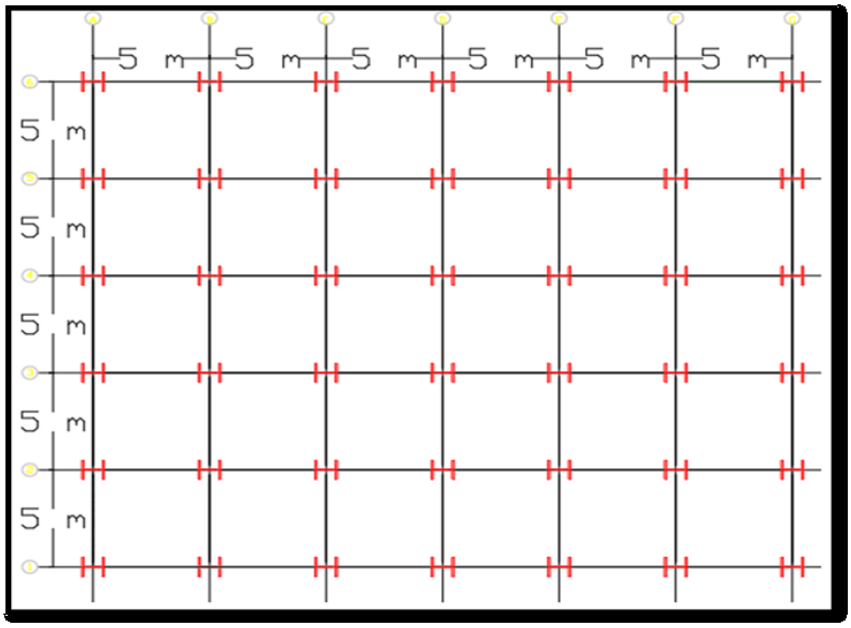

Figure 3.4: Floor plan for regular steel framed buildings

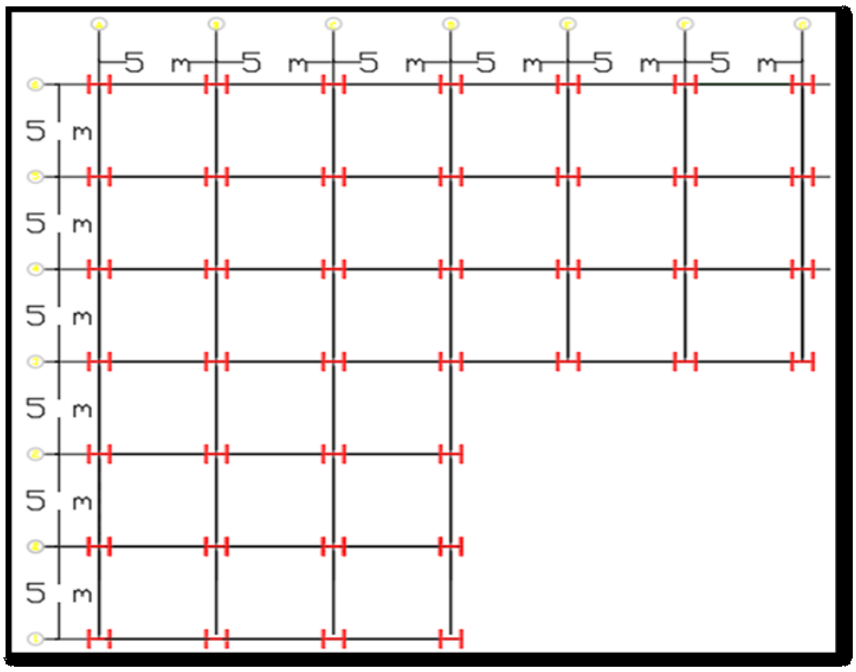

Figure 3.5: Floor plan for irregular steel framed buildings

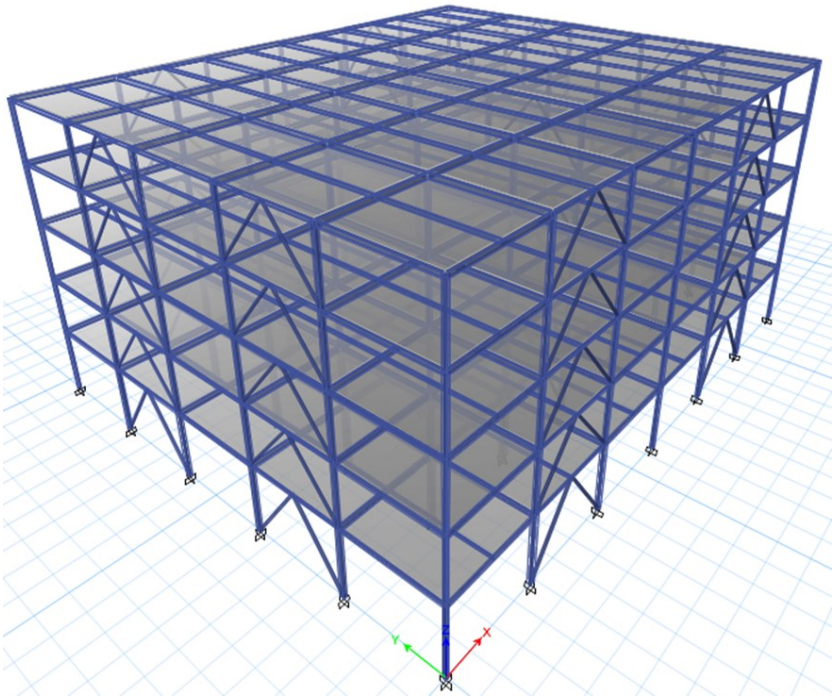

Figure 3.6: Three dimensional model of G+4 storey regular steel framed building with (CIV) bracing

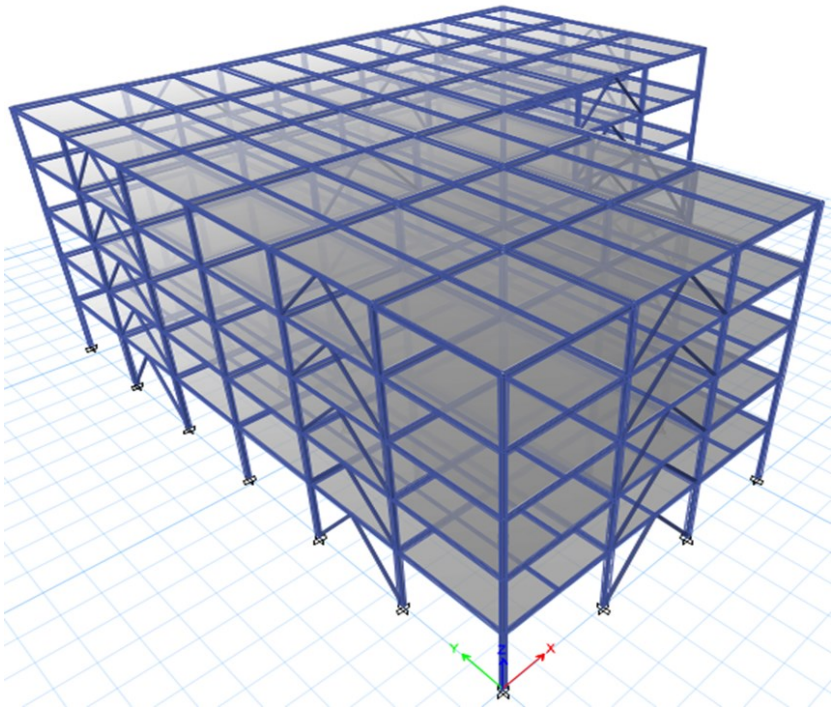

Figure 3.7: Three-dimensional model of G+4 storey irregular steel framed building with (CIV) bracing

3.5 Structural Elements and Slab Properties

The study focus on the behaviour of steel building in northern Cyprus. Hence, only steel cross-section available at the market, are considered. The available cross-section are mainly European section with a yielding stress of 275 MPa. Further information regarding the used material and the slab properties are presented in APPENDIX 3.

3.5.1 Column Cross-Section

The selected column cross-section is HEB since it provides higher ductility compared with the HEA cross-section. Since the flange thickness is relatively high. Figure 3.8 presents an overview of the HEB cross-section.

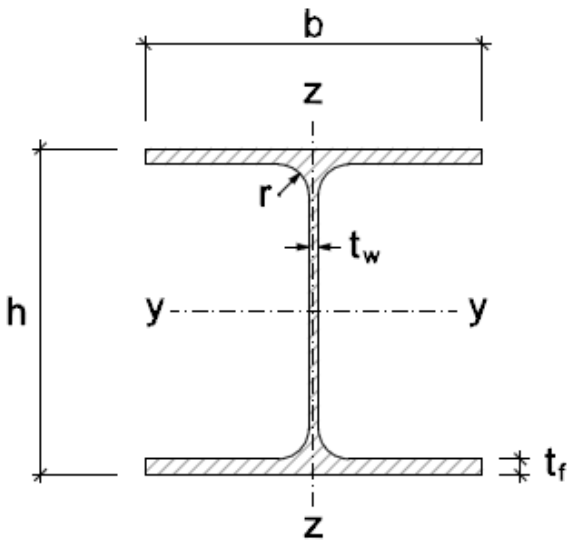

Figure 3.8: Schematic view of the HEB cross-section

3.5.2 Beam cross-section

The selected beam cross-section is IPE, since steel beams mainly resist bending moment and shear along the major axis of the element. Since the steel deck provides additional restrains to the beam. Figure 3.9 presents an overview of the IPE cross-section.

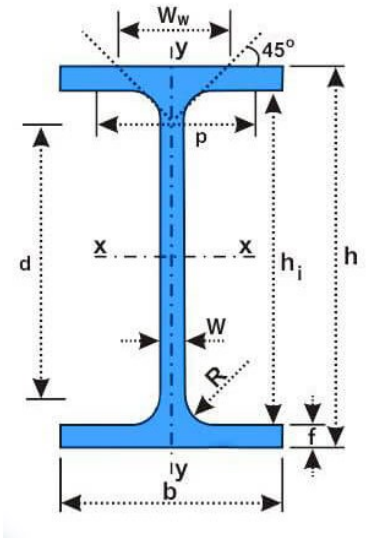

Figure 3.9: Schematic view of the IPE cross-section

3.5.3 Bracing cross-section

The bracing elements are mainly tension or compression element that carry uniaxial stress. Hence, symmetrical cross-section along both major and minor axes serve the best. Thus, CHS section is adopted in this research. Figure 3.10 presents an overview of the CHS cross-section.

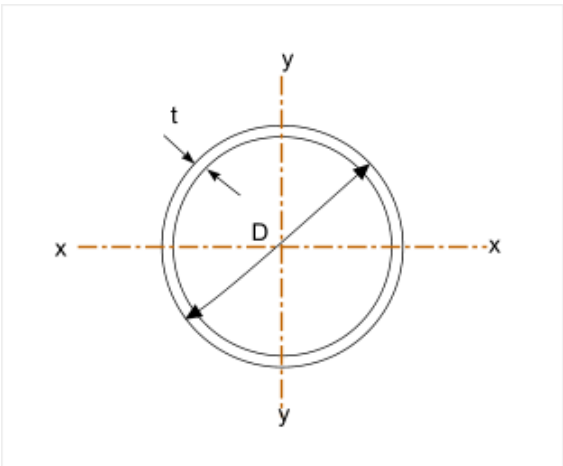

Figure 3. 10: Schematic view of the CHS cross-section

3.5.4 Knee cross-section

The axial load in the bracing element is transferred to the knee as point load which leads to the development of high shear and bending moment along the major axis of the section. Hence, IPE cross-section is used.

3.5.5 Slab type

The selected type of slab is light metal gauge steel deck. The deck is connected to the beams with the help of shear stud. The steel deck is filled with concrete that has a compressive strength of 25 MPa. The selected deck section is Aldeck 70/915 which gives a maximum span 3.5 m. Figure 3.11 presents an overview of the Aldeck 70/915 cross-section.

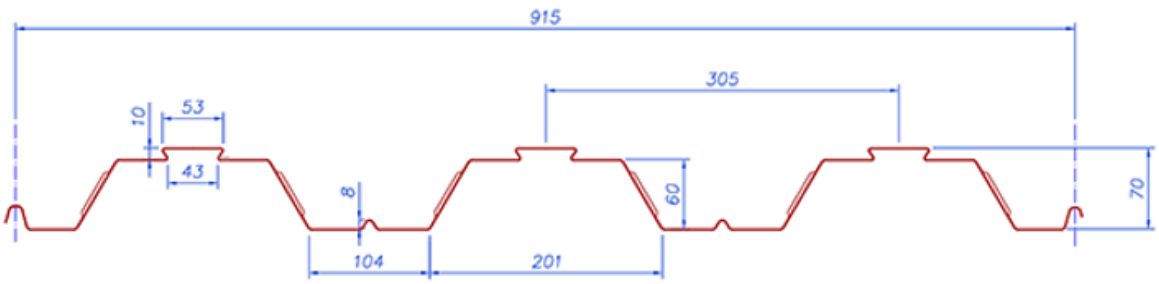

Figure 3.11: Schematic view of the Aldeck 70/915 cross-section

3.6. Inverted-V Bracing Types

There are many types of inverted-V bracing system. However, this study focus on three types which are commonly used.

3.6.1 Concentric inverted-V bracing (CIV)

Two bracing element are connected at the midpoint of the top primary beam where the other ends are joint to the lower corner of the frame as shown in Figure 3.12.

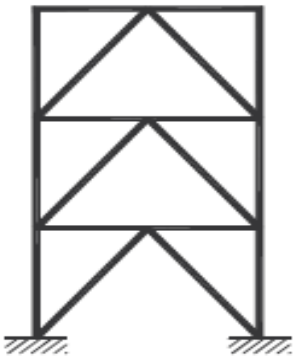

Figure 3.12: Concentric inverted-V bracing (CIV)

3.6.2 Eccentric inverted-V Bracing (EIV)

For the case of eccentric steel bracing system elements which are connected to each other eccentrically to a loop point at the frame with link length (e) as shown in Figure 3.13. It is not easy to determine the optimal length for this elements, therefor according to (NCSC-2015) the link length (e) can be determined by Equations 3.1.

$$1.Mp/Vp \leq e \leq 5.Mp/Vp \tag{3.1}$$

where;

- Mp: Is the bending moment.
- Vp: Shear stress capacity.

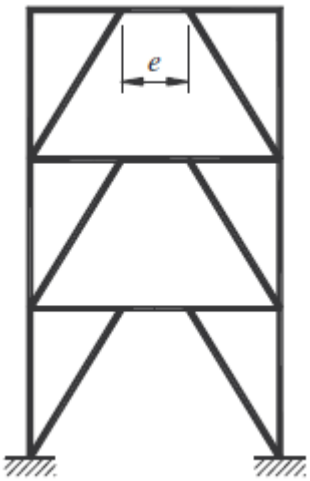

Figure 4.13: Eccentric steel bracing system (EIV)

The turning angle (Op) which occurs between brace-beam and story level is shown in Figure 3.14 and it shall not exceed these two values presented in Equation 3.2.

$$0.1 \text{ radian} \leq \gamma\, p = \frac{L}{e}\, Op \leq 0.03 \text{ radian} \tag{3.2}$$

Where;

- Op: The angle of storey drift determined by Equation 3.3.

$$Op = R\frac{\Delta i}{hi} \tag{3.3}$$

Note: sense it is difficult to determine the link length the angel of the inverted V eccentric bracing system should be between 35° and 60° and the initial link length is estimated to be 0.15L (Egor et al, 1987).

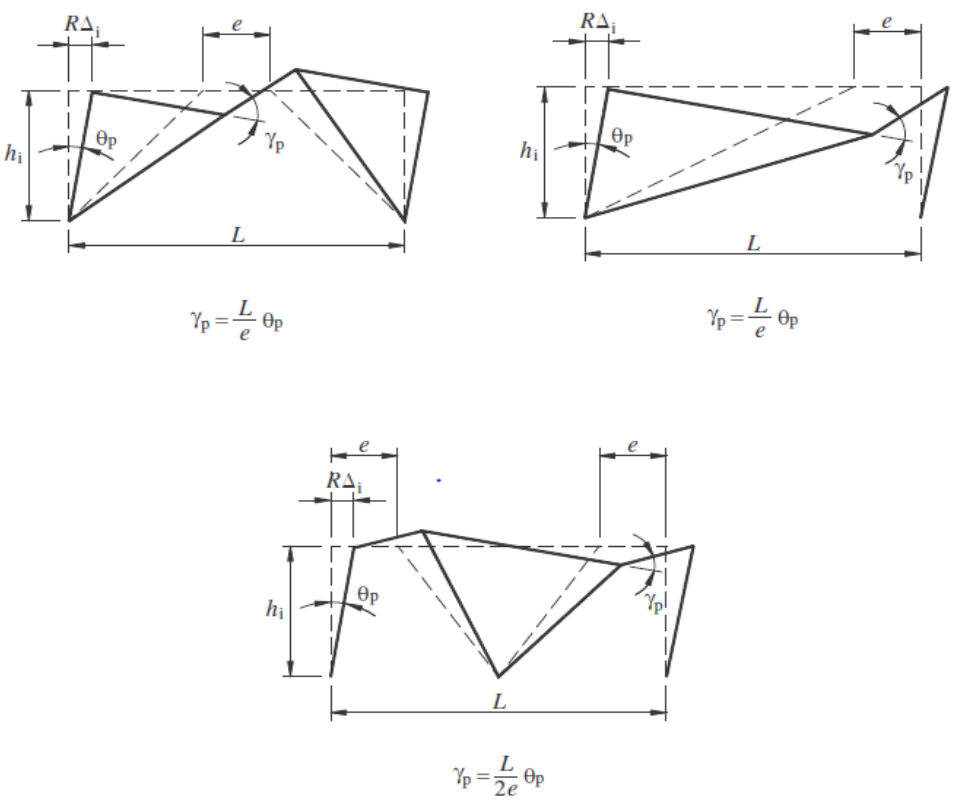

Figure 3.14: Rotation angels for eccentric steel bracing (Chamber of Civil Engineers, 2015)

3.6.3 Inverted-V with knee (KIV1&2)

Similar with the concentric bracing but it connect with knees rather than the corner as shown in Figure 3.15. The length of the knee part can be calculated using Equations 3.4-3.5.

$$0.2 \leq h/H \leq 0.3 \tag{3.4}$$

$$b/h = K.(B/H) \tag{3.5}$$

(K) ration in Equation 4.5 is equal to 1 for the optimal knee. Which makes the knee elements parallel to the diagonal direction of the frame or it can be taken as (0.5) which make the knee elements parallel to the diagonals inverted-v elements. In this study both cases are discussed, where for K=1 the model name is (KIV1) and for K=0.5 the model name is (KIV2).

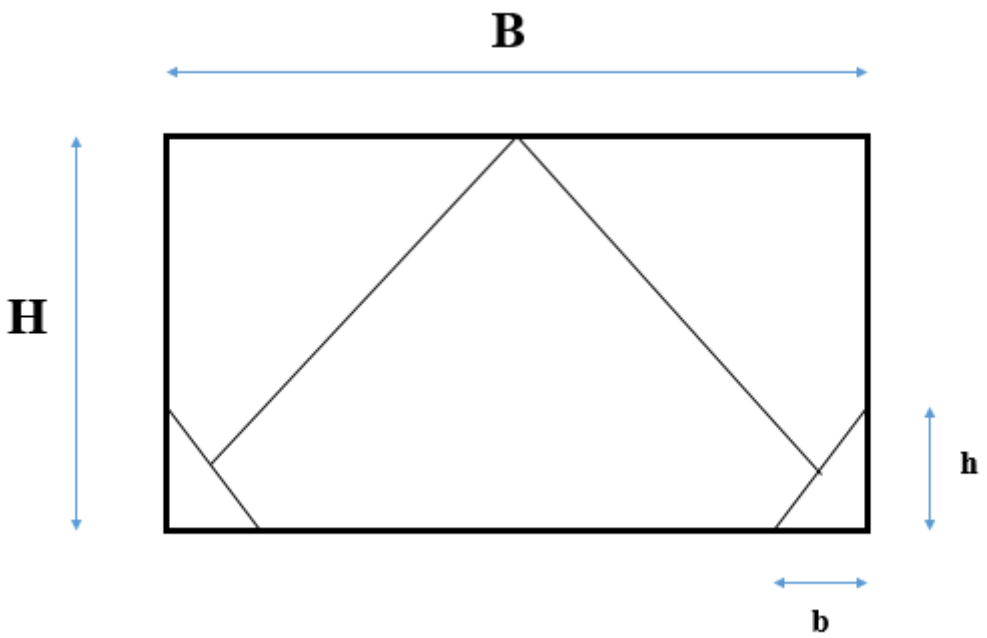

Figure 4. 15: Inverted-V with knee bracing system (KIV)

3.7 Types of Seismic Analysis Methods

Engineers aim to design their buildings in such that the internal stresses within the structural elements do not exceed the yielding stress of the building material (linear analysis), which is a faster method and requires small amount of computational effort. However, under unexpected severe loading conditions (i.e. seismicity with high magnitude) the stresses within the structural elements may exceed the yielding stress of the building material causing the structural elements to act in non-linear conditions. Thus, researchers and scientists developed both linear and non-linear analysis methods that can simulates the various behaviour of the structural elements within a given building. Figure 3.16 presents a flowchart that summarize the various types of seismic analysis methods.

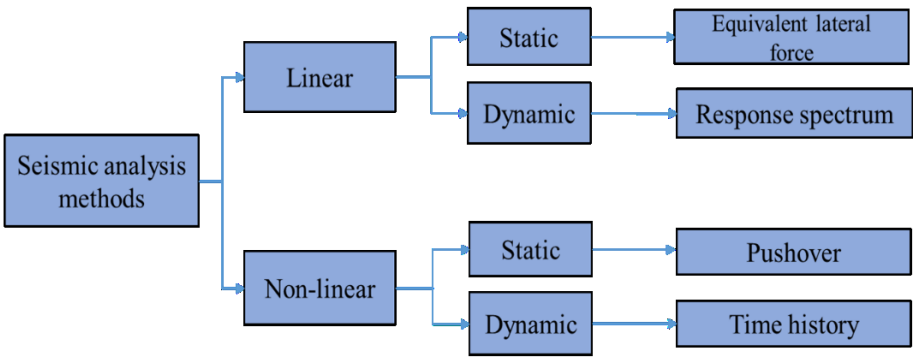

Figure 3.16: Seismic analysis methods

3.7.1 Equivalent lateral force method

The aim of this method is to substitute the dynamic earthquake forces with an equivalent static lateral forces. This method basically estimate the base shear with respect to the total weight of the building, the fundamental period in the considered direction, the response acceleration transmitted to the building and the ductility of the building. Equation 3.6 presents the base shear calculation formula in accordance with NCSC-2015.

$$Vt = \frac{WA(T_1)}{Ra(T_1)} \geq 0.10\ A0\ I\ W \tag{3.6}$$

Then the calculated base shear is distributed along the elevation of the building at the centres of the rigid or semi rigid diaphragms as shown in Equation 3.7.

$$Fi = (Vt)\frac{wi\ Hi}{\sum_{i=1}^{N} wi\ Hi} \tag{3.7}$$

where,

- W: The total weight of the structure.

3.7.2 Non-linear static pushover analysis

The nonlinear behavior of a structure is usually determined using the non-linear static pushover analysis method. This methods requires high computational effort unlike the linear static method, since the stiffness matrix of the structure varies with respect to the applied loads. It is an iterative method where forces are applied in a predetermined number of steps. At each step the internal stresses within each primary elements are checked and the stiffness matrix is modified accordingly. This iterative approach continues until the limit state is reached (target displacement). There are many standard and procedure about the performance of the non-linear static pushover analysis. Nevertheless, Federal Emergency Management Agency (FEMA) standards have the highest repetition among the researchers community. In addition to the fact that FEMA is fully implemented within ETABS 2016. Hence, the non-linear analysis procedure suggested by FEMA is followed within the content of this research.

3.7.2.1 Target displacement calculation

Target displacement (δt) is one of the limiting states of the pushover analysis. Where beyond this displacement the performance of the structure is not considered by researchers and engineers. Equation 3.8 presents the target displacement calculation.

$$\delta t = C_0 C_1 C_2 C_3 Sa \frac{T^2 e}{4\pi 2}\ g \tag{3.8}$$

(C_0): The modification factor to relate spectral displacement of an equivalent to the roof displacement of the structure. There are several ways of calculating the modification factor as shown in Table 3.1.

Table 3.1: Modification factor C_0 according to FEMA-356

	Shear structure		**Other structures**
Storey number	**Triangular Load Pattern**	**Uniform Load Pattern**	**Any Load Pattern**
1	1	1	1
2	1.2	1.15	1.2
3	1.2	1.2	1.3
5	1.3	1.2	1.4
10+	1.3	1.2	1.5

(C_1): Defined as the modification factor to relating expected maximum inelastic displacements to the displacements calculated for linear elastic response, it is calculated according to Equation 3.9.

$$\begin{aligned} C_1 &= 1 && T_e \geq T_s \\ C_1 &= (1 + (R-1)T_s/T_e)/R && T_e < T_s \end{aligned} \tag{3.9}$$

where,

- (T_e): defined as effective fundamental period of the structure in the consider direction.
- (T_s): defined as characteristic period according to the response spectrum.

(C_2): Which defined as modification factor to represent the effect of pinched hysteretic shape, strength deterioration and stiffness degradation on maximum displacement response. The value of this factor for different framing systems and structural performance levels can be obtained from Table 3.2.

Table 3.2: Modification factor C_2 according to FEMA-356

	$T \leq 0.1\ second$		$T \geq T_S\ second$	
Structural Building	Frame	Frame	Frame	Frame
Performance Level	Type1	Type2	Type1	Type2
IO	1	1	1	1
LS	1.3	1	1.1	1
CP	1.5	1	1.2	1

where,

- Fame type 1: Includes ordinary moment-resisting frames, concentrically-braced frames, shear-critical, piers, unreinforced masonry walls, frames with partially-restrained connections, tension-only braces, and spandrels of reinforced concrete or masonry.
- Fame type 1: Two includes all frames types that not assigned to framing type one.

(C_3): Has no influence if the second order elastic analysis is not significant.

(Sa): Spectral acceleration at the fundamental period of the structure in g units (NCSC-2015).

3.7.2.2 Pushover curve

The results of the nonlinear static pushover analysis can be presented by plotting the base shear relative displacement, as shown in Figure 3.17. This curve plays an important rule since it is used to evaluate both of lateral stiffness and structure ductility.

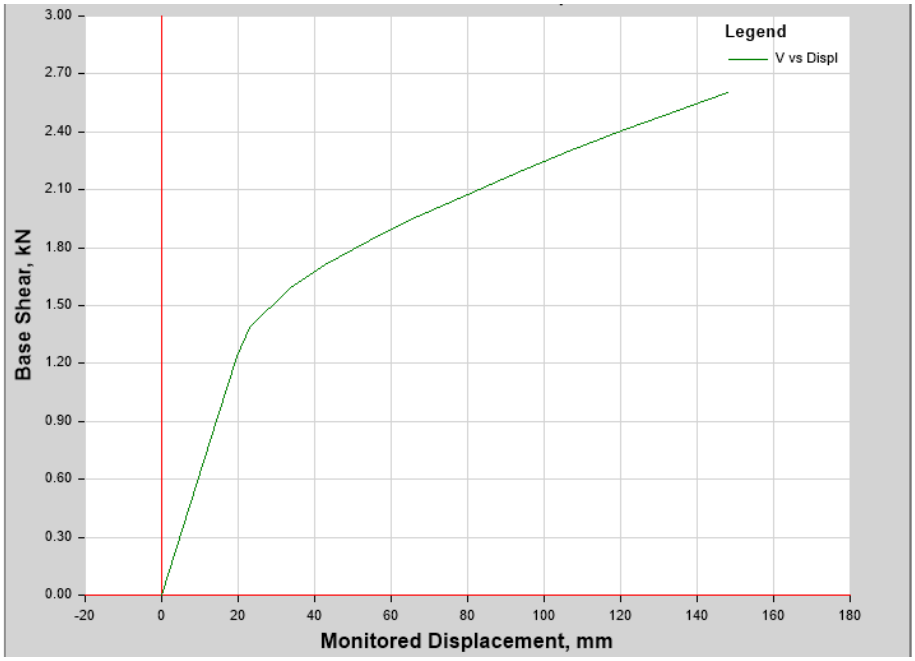

Figure 3.17: Relationship between lateral forces and lateral deflection

Lateral stiffness

The magnitude of force required to achieve one unit displacement is referred as lateral stiffness. Lateral stiffness is one of the most important parameters regarding the design of building that are exposed to high lateral forces. However. Increasing the stiffness may results in a brittle performance which is not desirable. In structural engineering, stiffness refers to the rigidity of the buildings. This stiffness is constant in the elastic region. However, as the building displacement approaches the plastic region of the curve the lateral stiffness is reduced dramatically, the lateral stiffness (K) of the structure can be determined according to Equation 3.10.

$$K = \frac{F}{D} \tag{3.10}$$

Ductility

Ductility is the capacity of the structure to bear a large deformation without significant loss in the stiffness or strength, which is an essential factor especially for building that are exposed to severe ground motion. Ductility is basically a shock absorber within the structure.

Ductility refers to the ratio of the displacement just before the ultimate displacement or collapses, to the value of the displacement at the first damage or yield. The displacement ductility factor (μ) can be calculated as shown in Equation 3.11

$$\mu = \frac{\Delta max}{\Delta y} \tag{3.11}$$

3.7.2.3 Plastic hinges

Plastic hinge refers to the case where the bending moment within an element exceeds the yielding stress. Hence, the structural element loose its ability to resist high bending moment and it behaves partially like a hinge. Plastic hinges can be divided into 3 main categories which are listed below;

1- Immediate occupancy: the structural element undamaged.
2- Life safety: the structural elements is partially damaged.
3- Collapse prevention: the structural element is extremely damaged or even collapsed.

The performance level of each plastic hinge can be determined according to the chart of plastic hinge phases as shown in Figure 3.18

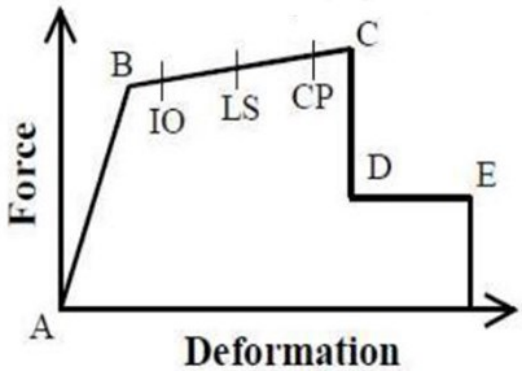

Figure 3.18: chart of plastic hinge phases

3.7.3 Time history analysis

This type of analysis is steps analysis of dynamical response of a structure to a particular loading that vary with the time. Time history analysis could be linear or non-linear. Equation 3.12 presents the general equation of motion which is used to solve the structural system for both linear and non-linear case.

$$Ku\,(t) + C\acute{u}\,(t) + M\ddot{u}\,(t) = r(t) \qquad (3.12)$$

where,

- K: Stiffness matrix.
- C: Damping matrix.
- M: Diagonal mass matrix.
- U: The displacements.
- Ú: The velocities.
- Ü: The accelerations.
- R: Is the applied load.

To determine the type of the time history analysis, there are several options as:

- Linear time history analysis or non-linear time history analysis
- To solve the equilibrium equation there are two different methods (modal and direct integration), where both of which yields same results for a given problem.
- Transient analysis and periodic analysis, where transient analysis considers the applied load with a beginning and end like one time event. However, parodic analysis is only limited to linear modal analysis considering the applied load with unlimited cycles.
- Rits and Eigen modal: generally both of them could be used. However, for the case of non-linear modal (FNA) Ritz analysis is used when Eigen vectors analysis fails to calculate the structural modes.

3.7.3.1 Ground motion scaling methods

Ground motion record requires for them to match a given design spectrum. There are two main method for scaling the record which are listed below

Scaling in frequency domain:

This method based on the ratio of the target response spectrum to response spectrum of the time series with keeping the Fourier phase of the motion constant. This method is sample. However, it does not have a good convergence characteristics. In addition this method often lead to change the character of the time series until a degree where it not look like a time series from an earthquake. Matching using this method always tend to increase the total energy in the ground motion.

Scaling in time domain:

Generally this method considered a better method for matching. Since it gives matched function with the target response spectrum without changing the frequency content. This approach depends on adjusting the acceleration of the ground record in time domain by adding wavelets. Where wavelets are mathematical functions which define waveform with limited duration that has a zero average. The wavelet amplitude oscillates up and down passing the zero.

3.7.3.2 Scaling of real acceleration to fit NCSC-2015 spectrum

According to NCSC-2015 the spectral ordinate to be taken into n' th vibration mode, can be determined by Equation 3.13.

$$Sar\ (Tn)\ =\ \frac{Sae\ (Tn)}{Ra\ (Tn)} \tag{3.13}$$

$$Sae\ (T)\ =\ A\ (T)\ .\ g \tag{3.14}$$

Where, Sae (Tn) is the ordinate of elastic acceleration spectrum calculated according to equation 3.14. This spectral acceleration is designed for a probability of 10% exceedance within 50 years. However, for the case of 2% probability of exceedance the spectral acceleration will be magnified by 50%.

3.8 Modal Analysis

Modal analysis are used to determine the natural vibration modes of the structure. These methods can be used like basis for the modal superposition in response spectrum analysis and modal load cases for time history analysis. To define a modal load case there are two types of modal analysis (Eigen and Ritz victors).

3.8.1 Eigen-vector analysis

This analysis determines the frequencies and undamped free vibration modes of the system, these natural modes give very good view for the behaviour of the structure. Eigen vectors analysis modes can be used for all types of analysis. However, Ritz vectors are recommended for the basis of response spectrum and time history analysis. This analysis include the solution of the generalized eigenvalue problem.

$$(K - \Omega^2 M)\,\phi = 0 \qquad (3.15)$$

where,

- Ω^2: Diagonal matrix of eigenvalues
- Φ: Eigen vectors matrix.

Each natural vibration modes shape determined by pair of (eigenvector-eigenvalue) which identified by numbers (1) to (n). Figure 3.19. The eigenvalue (ω^2) is the square of the circular frequency (ω), Equations 3.16-3.17.

$$F = \omega / 2\pi \qquad (3.16)$$

$$T = 1/f \tag{3.17}$$

where,

- f : The cyclic frequency and
- T: The period of the mode.

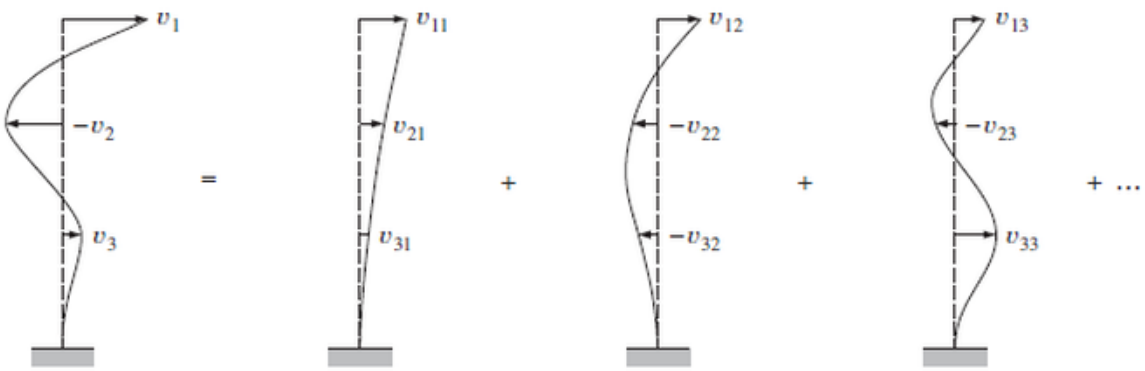

Figure 3.19: Mode shapes components to determine the total response (CSI, 2014)

3.8.2 Ritz-vector analysis

The natural free vibration modes are not the best in terms of superposition analysis of structures subjected to dynamic loads. On the other hand, Ritz vector analysis yields more accurate results, compared with the natural mode shapes. That is because Ritz vectors are taking into account the spatial distribution of the dynamic loading, unlike the free vibration modes where it is neglected.

3.9 Design Assumptions

The steel structural buildings presented in this study are designed in accordance with Design of steel structures, Eurocode 3 (EC 3). The buildings are designed to yield the smallest sections that can withstand the applied loads. The building are subjected to various types of loading which are listed as follow;

3.9.1 Gravity loads

The gravity loads includes the self-weight of the structural elements and slabs. In addition, to the acting loads on the slabs which is consisted of the loads of the screed and marble

which is assumed as 1.5 kN/m^2 (additional dead load), also the live loads which is equivalent to 2 kN/m^2 (TS 498 for residential buildings).

3.9.2 Wind loads

The buildings are designed to withstand the lateral loads created by wind. The maximum wind speed is found as 50 kmph (Metroblue 2019). The loads are calculated in accordance with TS 498 and applied at the centre of the semi-rigid diaphragm. Assuming that the building has no openings in order to simulate the worst scenario.

3.9.3 Earthquake load parameters

The buildings are designed to resist seismic lateral load with 10% probability of exceedance as provisioned by NCSC2015. The parameters are selected in accordance with the building location and its function. Hence, the peak ground acceleration is taken as $A_0 = 0.3$ with a site class of Z2. Since the building is residential, the building importance factor is I=1. The buildings ductility reduction factors vary between 6 and 8 as shown in Table 3.3. Summary of the selected seismic parameters from NCSC2015 are listed in Table 3.4.

Table 3.3: Ductility reduction factor (R)

Structural system type	Bracing type	System with high ductility steel
Structures in seismic loads are fully resisted by frames	MRF	R=8
Structures in which seismic loads are jointly resisted by structural steel braced (concentric braced frame)	CIV	R=6
Structures in which seismic loads are jointly resisted by structural steel braced (eccentric braced frame)	EIV-KIV	R=8

Table 3.4: Earthquake parameters used in this study

Earthquake seismic parameters	**Value**
Case study location	Northern Cyprus –Famagusta city
Earthquake seismic zone	Zone 2
Effective ground acceleration coefficient , (A_o)	0.3 g
Site class	Z2
Ground soil type	B
Importance factor, (I)	1
Live load reduction factor	0.3
Spectrum characteristic periods,(T_A, T_B)	(0.15 , 0.4)sec
Damping ratio	5%
Structural behaviour factor R	6 - 8

The seismic loads are automatically calculated using ETABS2016 and applied in both orthogonal directions at the centre of the semi-rigid diaphragm with an additional eccentricity equals to ± 0.05 as suggested by NCSC-2015.

3.9.4 Load combination

The load combinations used in the design of the steel structural buildings are listed in Table 3.5.

Table 3.5: Design load combinations

Gravity and Wind Loads Combinations	Earthquake Combinations	
DL + LL	DL + LL + EX + 0.3EY	±0.05 eccentricity
1.4DL +1.6 LL	DL + LL + EX - 0.3EY	±0.05 eccentricity
DL + LL + WX	DL + LL - EX + 0.3EY	±0.05 eccentricity
DL + LL - WX	DL + LL - EX - 0.3EY	±0.05 eccentricity
DL + LL + WY	DL + LL + EY + 0.3EX	±0.05 eccentricity
DL + LL - WY	DL + LL + EY - 0.3EX	±0.05 eccentricity
0.9DL + WX	DL + LL - EY + 0.3EX	±0.05 eccentricity
0.9DL - WX	DL + LL - EY - 0.3EX	±0.05 eccentricity
0.9DL + WY	0.9DL + EX + 0.3EY	±0.05 eccentricity
0.9DL - WY	0.9GDL + EX - 0.3EY	±0.05 eccentricity
	0.9DL - EX + 0.3EY	±0.05 eccentricity
	0.9DL - EX - 0.3EY	±0.05 eccentricity
	0.9D + EY + 0.3EX	±0.05 eccentricity
	0.9DL + EY - 0.3EX	±0.05 eccentricity
	0.9DL - EY + 0.3EX	±0.05 eccentricity
	0.9DL - EY - 0.3EX	±0.05 eccentricity

3.10 Non-Linear Analysis of the Case Study

The structural steel buildings performance under high seismic activity is evaluated by means of pushover analysis and nonlinear time history analysis. The followed methods in conducted these types of analysis are listed as follow;

3.10.1 Pushover analysis of the case study

The nonlinear static pushover analysis is conducted in accordance with FEMA365. Where plastic hinges at both ends of the structural elements are assigned. The properties of the plastic hinges are listed in Table 3.6. Earthquake load case with a probability of 2% exceedance within 50 years is used to push the building. The lateral force are applied at the centre of the semi-rigid diaphragm with an additional eccentricity of ± 0.05. The lateral loads are applied in 200 steps until the target displacement is reached. Further information

regarding the target displacements of each structural system are presented in Table 3.7 and Table 3.8 for x-direction and y-direction respectively.

Table 3.6: Plastic hinges properties

Structural element	Stresses regarding hinge formation
Column	Axial stress and bending moments in both major and minor axes (P,M3,M2)
Beam	Bending moment along the major axis (M3)
Bracing	Axial stress (P)
Knee	Bending moment along the major axis (M3)

Table 3.7: Target displacement in X direction

Model name	Ti (sec)	C_0	C_1	C_2	C_3	Sa	$\frac{T^2}{4*\pi^2}$ g	δ(m)	δ(mm)
R-CIV-5	0.773	1.4	1	1.1	1	0.699	0.149	0.160	160
R-EIV-5	1.088	1.4	1	1	1	0.497	0.294	0.205	205
R-KIV-5	1.195	1.4	1	1	1	0.452	0.355	0.225	225
R-MRF-5	1.34	1.4	1	1.1	1	0.403	0.447	0.277	277
IR-CIV-5	0.687	1.4	1	1.1	1	0.787	0.117	0.142	142
IR-EIV-5	1.01	1.4	1	1	1	0.535	0.254	0.190	190
IR-KIV-5	1.074	1.4	1	1	1	0.503	0.287	0.202	202
IR-MRF-5	1.367	1.4	1	1.1	1	0.395	0.465	0.283	283
R-CIV-10	1.525	1.5	1	1.1	1	0.354	0.578	0.338	338
R-EIV-10	1.912	1.5	1	1	1	0.283	0.909	0.386	386
R-KIV-10	1.95	1.5	1	1	1	0.277	0.946	0.393	393
R-MRF-10	2.415	1.5	1	1.1	1	0.224	1.451	0.536	536
IR-CIV-10	1.379	1.5	1	1.1	1	0.392	0.473	0.306	306
IR-EIV-10	1.784	1.5	1	1	1	0.303	0.792	0.360	360
IR-KIV-10	1.833	1.5	1	1	1	0.295	0.836	0.370	370
IR-MRF10	2.42	1.5	1	1.1	1	0.223	1.457	0.537	537

Table 3.8: Target displacement in Y direction

Model name	Ti (sec)	C_0	C_1	C_2	C_3	Sa	$\frac{T^2}{4*\pi^2}$ g	δ(m)	δ(mm)
R-CIV-5	0.715	1.4	1	1.1	1	0.756	0.127	0.148	148
R-EIV-5	1.105	1.4	1	1	1	0.489	0.304	0.208	208
R-KIV-5	1.295	1.4	1	1	1	0.417	0.417	0.244	244
R-MRF-5	2.146	1.4	1	1.1	1	0.252	1.146	0.444	444
IR-CIV-5	0.747	1.4	1	1.1	1	0.724	0.139	0.155	155
IR-EIV-5	1.125	1.4	1	1	1	0.480	0.315	0.212	212
IR-KIV-5	1.286	1.4	1	1	1	0.420	0.411	0.242	242
IR-MRF-5	1.964	1.4	1	1.1	1	0.275	0.959	0.407	407
R-CIV-10	1.491	1.5	1	1.1	1	0.363	0.553	0.331	331
R-EIV-10	1.985	1.5	1	1	1	0.272	0.980	0.400	400
R-KIV-10	2.165	1.5	1	1	1	0.250	1.166	0.437	437
R-MRF-10	3.267	1.5	1	1.1	1	0.165	2.655	0.725	725
IR-CIV-10	1.538	1.5	1	1.1	1	0.351	0.588	0.341	341
IR-EIV-10	2.037	1.5	1	1	1	0.265	1.032	0.411	411
IR-KIV-10	2.219	1.5	1	1	1	0.244	1.225	0.448	448
IR-MRF-10	3.325	1.5	1	1.1	1	0.163	2.750	0.738	738

3.10.2 Time history analysis of the case study

In order to perform the nonlinear time history analysis 3 different ground motion records are selected aiming to cover large range of frequencies as suggested by NCSC2015. The details of the selected ground motion records are presented in Table 3.9 and the ground acceleration resulted of these earthquakes are shown in Figure 4.16 ,where the data are collected from the Pacific Earthquake Engineering Research centre (PEER) ground motion data base,(https://ngawest2.berkeley.edu). The ground motion records are scaled so they have a similar behaviour of earthquake spectra with a probability of 2% exceedance within 50 years. Plastic hinge properties are identical to the pushover analysis. All the details about spectral acceleration curves which are used given in APPENDIX 6.

Table 3.9: Details of the selected ground motion records

Earthquake Name	Kocaeli, Turkey	Duzce, Turkey	Erzincan, Turkey
Station Name	Duzce	Sakarya	Erzincan
Year	1999	1999	1992
Magnitude, Mw	7.51	7.14	6.69
Shear-wave velocity ,Vs30 (m/sec)	281.86	414.91	352.05
Rjb (km)	13.6	45.16	0
Rrup (km)	15.37	45.16	4.38

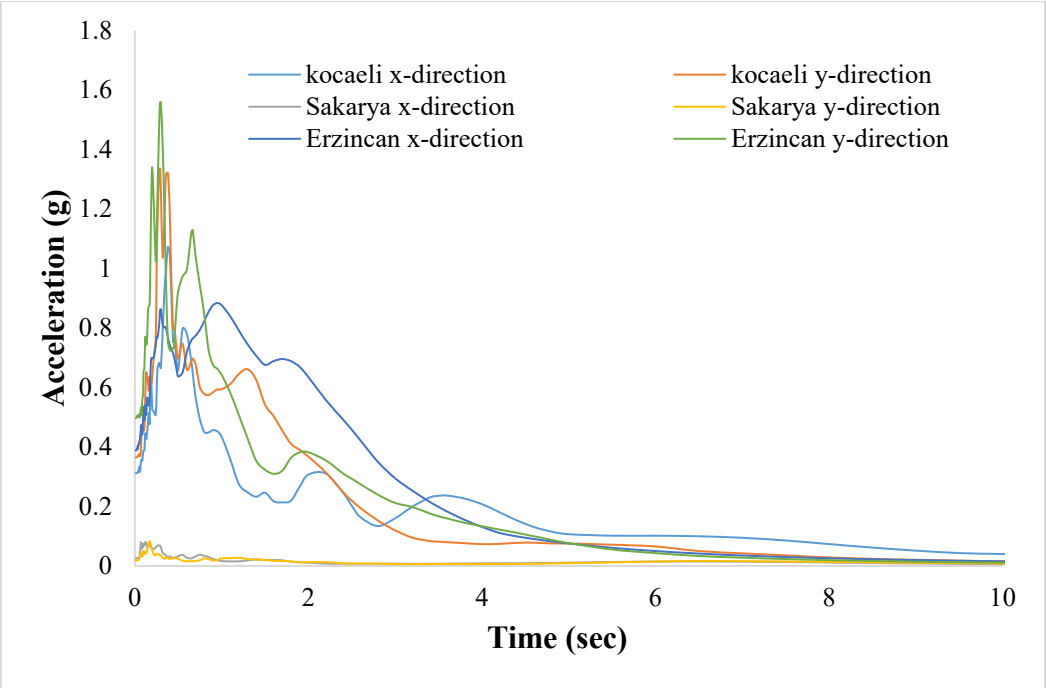

Figure 3.20: Ground acceleration records

CHAPTER 4

RESULTS AND DISCUSSIONS

4.1 Overview

This chapter presents the outcomes and the discussions of the analyses methods in terms of base shear, lateral displacement, storey drift, total mass of the buildings, lateral stiffness and displacement ductility factor, in both orthogonal directions.

4.2 Equivalent Lateral Force Method (ELFM)

This section of the thesis presents and discusses the obtained results regarding the seismic lateral loading applied using ELFM.

4.2.1 Base shear

The analysis results of the steel structural buildings in both orthogonal directions show that, concentric inverted-V bracing has the highest magnitude of the developed base shear, where the base shear is almost twice as much the base shear resulted for moment resisting frame. Ultimately, eccentric and knee types of bracing show no significant variation. This behaviour can be linked to the lower ductility reduction factor that concentric bracing system has(R=6) compared with the other system(R=8). These variation among the eccentric, knee and moment resisting system are related to the variation in the structural elements masses and the different natural periods. This behaviour is observed in all analysed models. Figure 4.1 and Figure 4.2 presents the resulted base shear in accordance with ELFM for the G+4 and G+9 buildings respectively. Also Table 4.1 presents the percent variation in the base shear compared with the moment resisting frame.

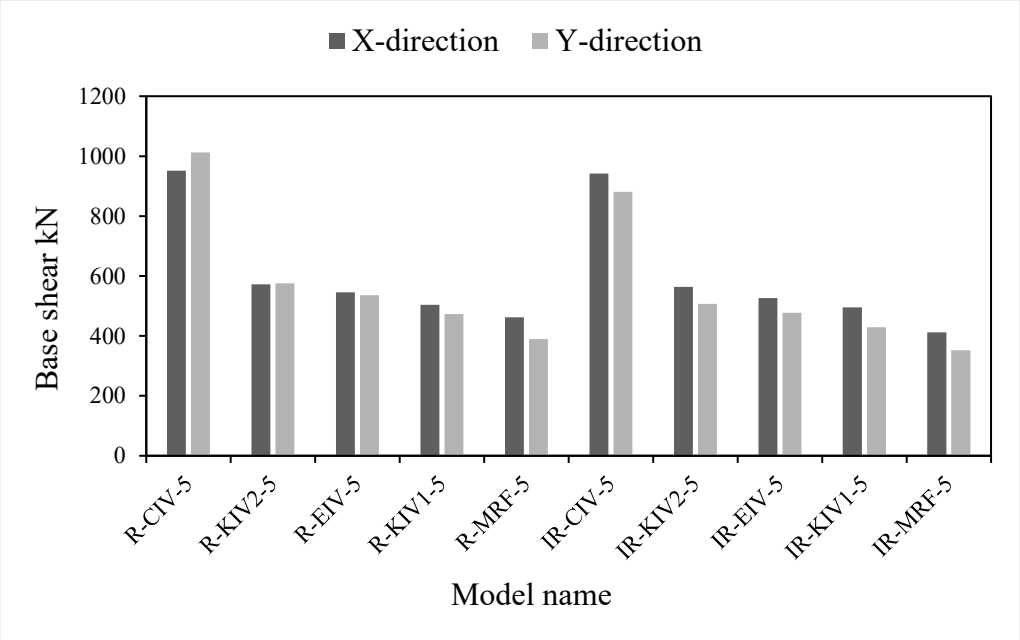

Figure 4.1: Base shear in X and Y directions for G+5 buildings (ELFM)

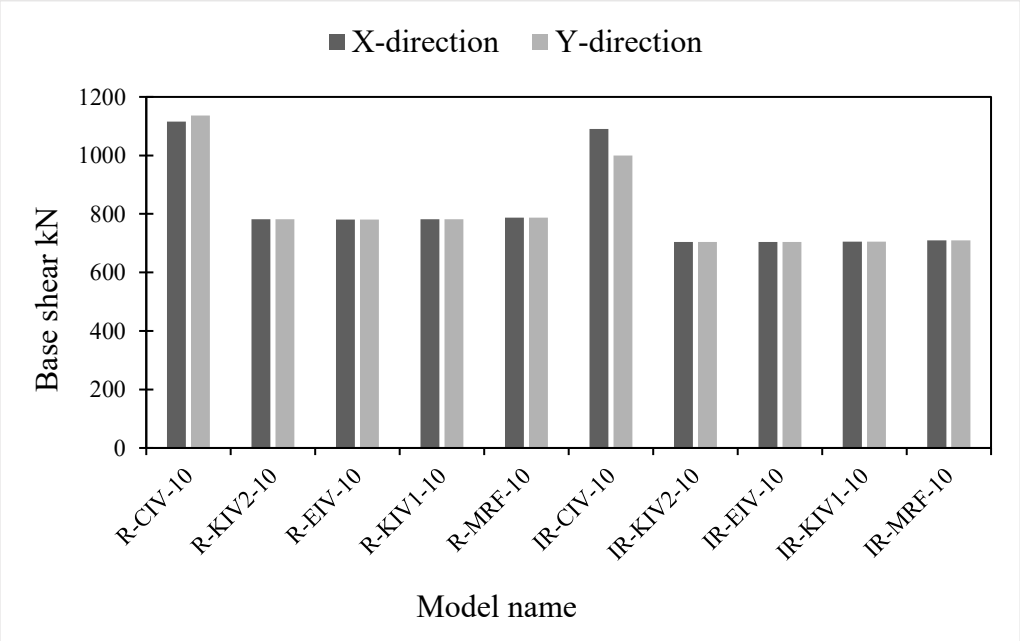

Figure 4.2: Base shear in X and Y directions for G+9 buildings (ELFM)

Table 4.1: The percent variation of base shear compared with the moment resisting frame (ELFM)

Model Name	*(%) in (G+4)-X-direction	*(%) in (G+4) Y-direction	*(%) in (G+9) X-direction	*(%) in (G+9) Y-direction
R-CIV	105.67	160.19	41.8	44.42
R-EIV	23.62	47.88	0.69	0.69
R-KIV1	17.82	37.8	0.77	0.77
R-KIV2	8.87	21.49	0.64	0.64
IR-CIV	129.2	150.35	53.81	40.95
IR-EIV	37.09	44.15	0.62	0.62
IR-KIV1	28.06	35.39	0.68	0.68
IR-KIV2	20.39	21.73	0.53	0.53

$$*(\%) = \frac{Bracing\ base\ shear - MRF\ base\ shear}{MRF\ base\ shear} \times 100$$

4.2.2 Top storey displacement

The analyses in regards with ELFM of the structural steel buildings show that moment resistant frame has the highest roof displacement compared with other system. This can be linked to the high ductility of the moment resistant frame. On the other hand, CIV and KIV2 bracing systems resulted in the least displacement. Which emphasize that these types poses the highest lateral stiffness. Also the buildings are exposed to high displacement in Y-direction. Which can be related to the orientation of the columns' major axis, where they are oriented parallel to X-direction. Figure 4.3 and Figure 4.4 presents the resulted top roof displacement in accordance with ELFM for the G+4 and G+9 buildings respectively. Also Table 4.2 presents the percent variation in the top storey displacement compared with the moment resisting frame.

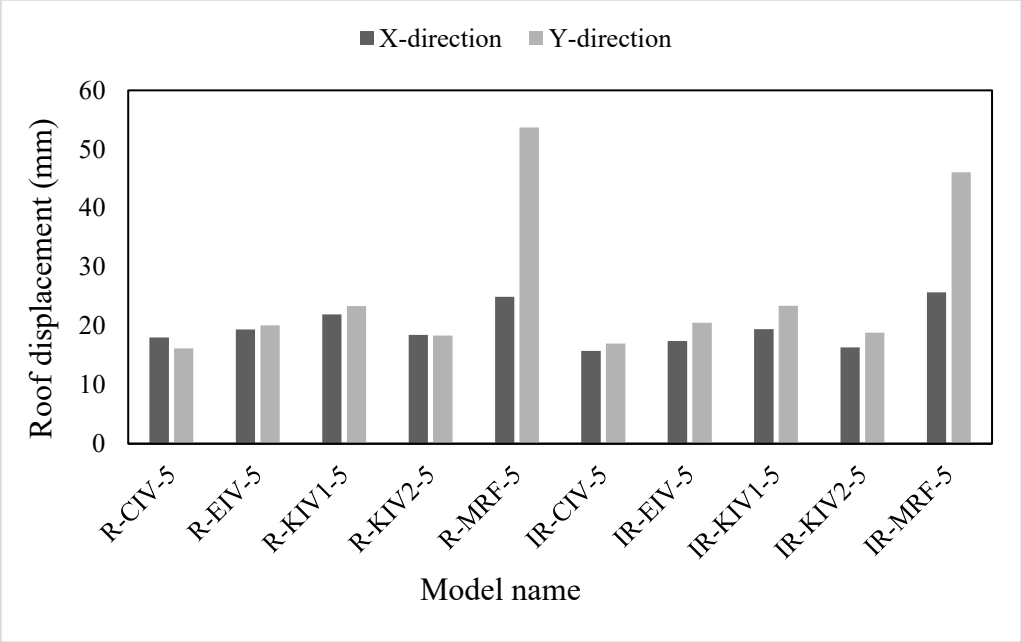

Figure 4.3: Roof displacement in X and Y directions for G+5 buildings (ELFM)

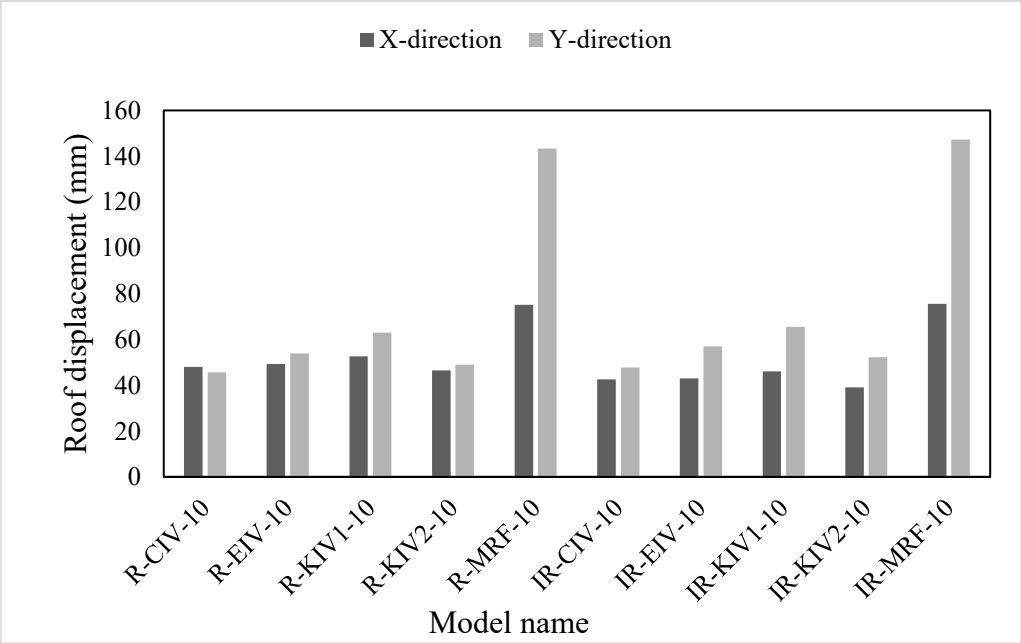

Figure 4.4: Roof displacement in X and Y directions for G+9 buildings (ELFM)

Table 4.2: The percent variation of roof displacement compared with the moment resisting frame (ELFM)

Model Name	*(%) in (G+4)-X-direction	*(%) in (G+4) Y-direction	*(%) in (G+9) X-direction	*(%) in (G+9) Y-direction
R-CIV	27.7	69.9	36.2	68.1
R-EIV	22.2	62.6	34.4	62.4
R-KIV1	12.0	56.5	30.1	56.1
R-KIV2	25.9	65.8	38.1	65.8
IR-CIV	38.7	63.1	43.7	67.6
IR-EIV	32.2	55.4	43.1	61.3
IR-KIV1	24.2	49.2	39.1	55.5
IR-KIV2	36.3	59.1	48.3	64.5

$*(\%) = \left| \frac{Bracing\ disp - MRF\ disp}{MRF\ disp} \times 100 \right|$

4.2.3 Storey drift

The analysed models show that the storey drift ratio are inconsistent, epically the moment resistant frame where it shows a multi-curvature plots. This can be related to the design process where columns cross-sections varies along the elevation of the building. In addition the storey drift ratio is the least at the top storey. This can be related to the fact that the lateral story forces are higher towards the base of structure and lower towards the roof, and the reason behind the low storey drift at the base is the support fixities. Ultimately, CIV and KIV2 bracing systems resulted in the least inter storey drift. This is valid for all of the analysed cases. This can be clearly seen in all figures between Figure 4.5 until Figure 4.12.

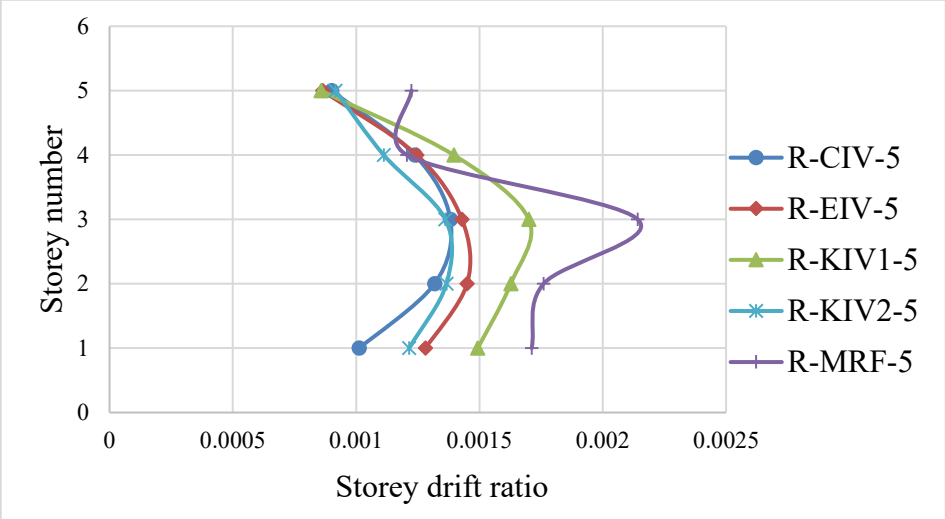

Figure 4.5: Storey drift in X direction for G+5 regular buildings (ELFM)

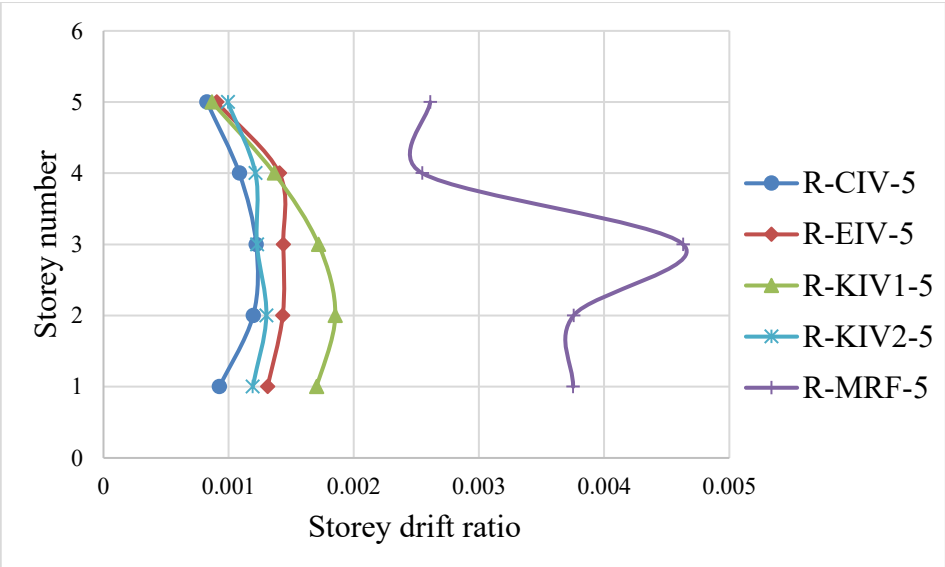

Figure 4.6: Storey drift in Y direction for G+5 regular buildings (ELFM)

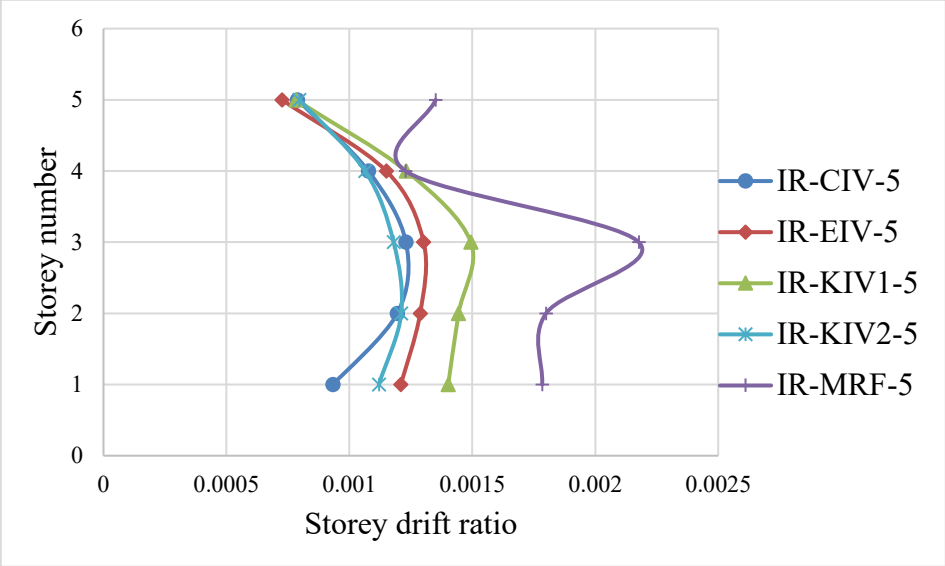

Figure 4.7: Storey drift in X direction for G+5 irregular buildings (ELFM)

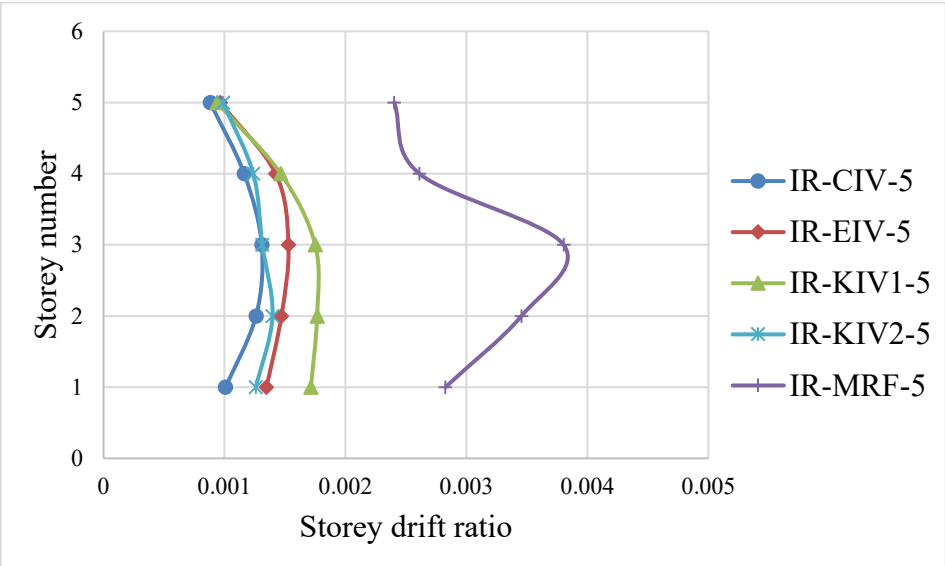

Figure 4.8: Storey drift in Y direction for G+5 irregular buildings (ELFM)

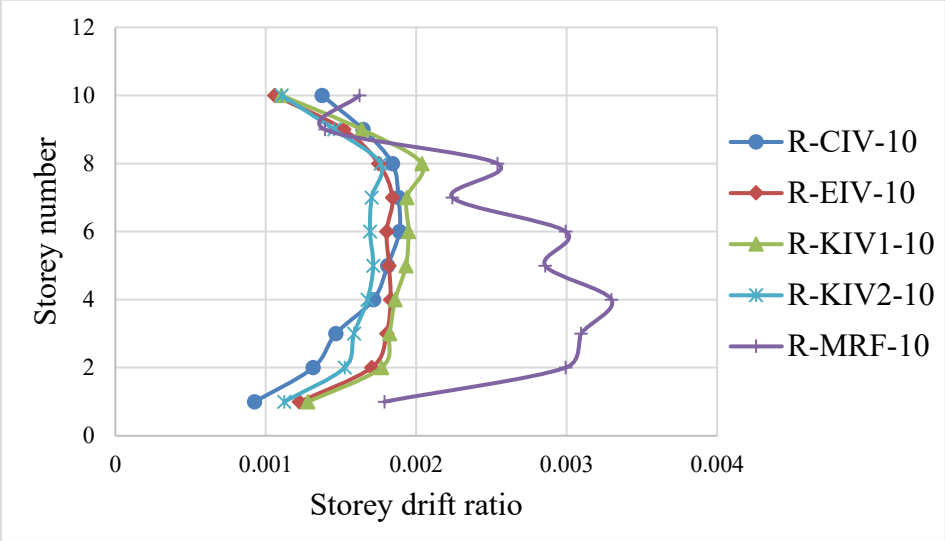

Figure 4.9: Storey drift in X direction for G+9 regular buildings (ELFM)

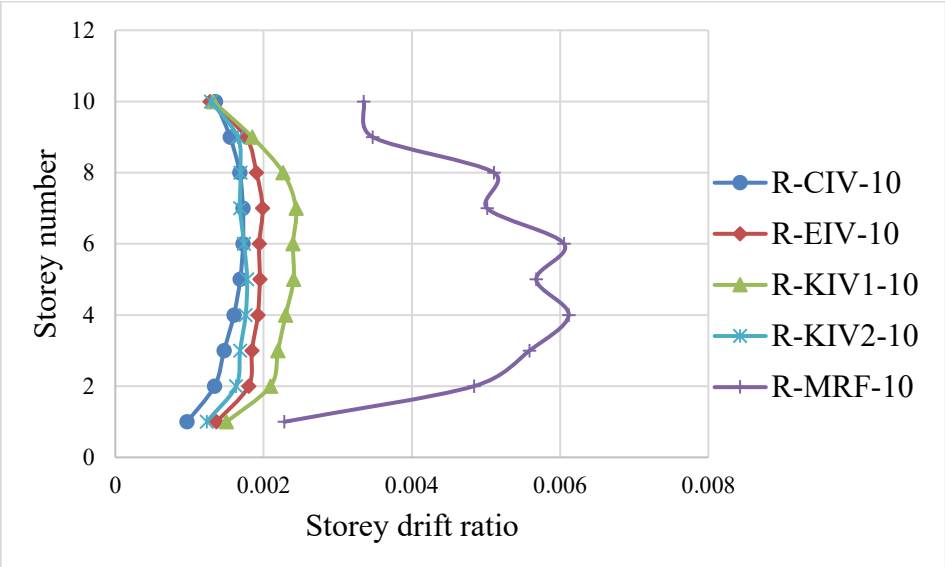

Figure 4.10: Storey drift in Y direction for G+9 regular buildings (ELFM)

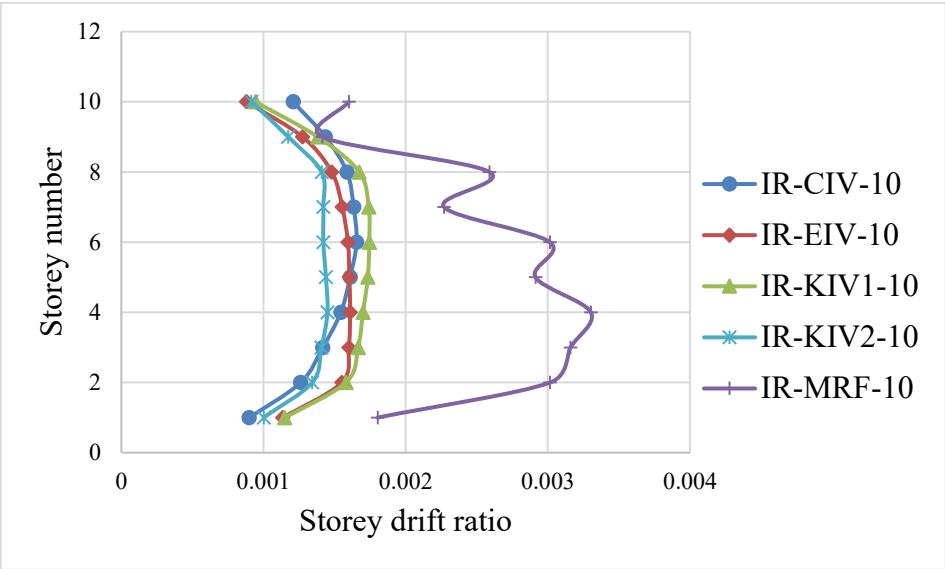

Figure 4.11: Storey drift in X direction for G+9 irregular buildings (ELFM)

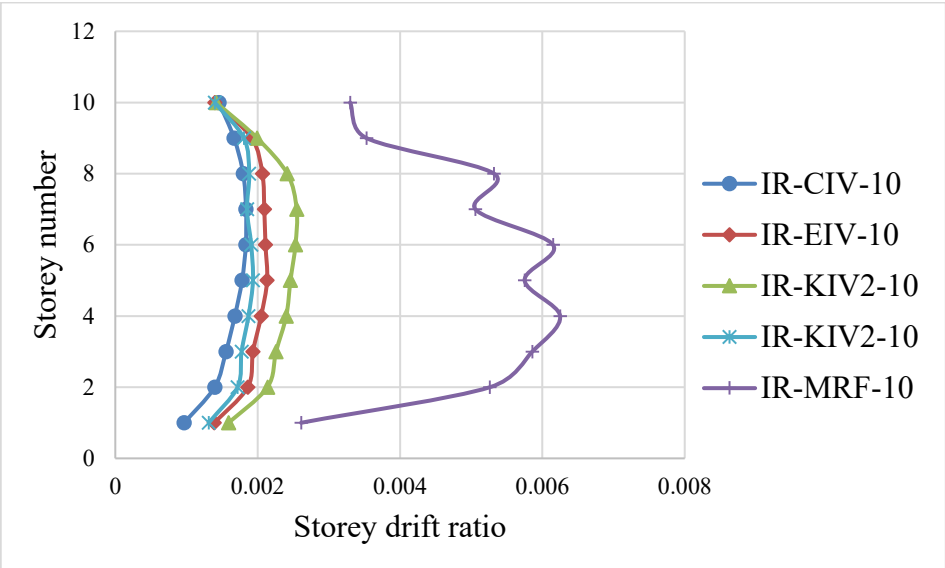

Figure 4.12: Storey drift in Y direction for G+9 irregular buildings (ELFM)

4.2.4 Mass of the structural buildings

Beyond the analysis of the steel structural building the cost of the suggested systems is extremely important. The cost of the steel buildings are directly related to the mass of the steel which is used. All buildings are designed using the smallest sections that can withstand the resulted internal stresses. The results show that moment resistant frame is the heavyset although it has lower number of the structural elements compared with buildings equipped

with the bracing systems this can be clearly seen in Table 4.3 which presents the total mass of the steel structural buildings. The main reduction is observed in the columns masses where the reduction in beams masses are insignificant. Table 4.4 and Table 4.5 summarise the reduction in the structural elements compared with the moment resistant frame system for both G+4 and G+9 respectively.

Table 4.3: Total mass of the structural systems (ELFM)

Model name	G+4 mass (ton)	G+9 mass (ton)
R-CIV	1089.5	2204.4
R-EIV	1089.6	2202.4
R-KIV1	1090.2	2206.3
R-KIV2	1089.4	2204.3
R-MRF	1098.1	2224.5
IR-CIV	982.7	1988.5
IR-EIV	983.2	1987.1
IR-KIV1	984	1991.1
IR-kIV2	982.9	1988.2
IR-MRF	994	2004.8

Table 4.4: The difference between elements weight of braced and MRF G+4 buildings (ELFM)

Model name	Columns (ton)	Beams (ton)	Bracing (ton)	Total (ton)
R-CIV-5	11.8	0.5	-3.8	8.6
R-EIV-5	12.1	-0.3	-3.3	8.5
R-KIV1-5	12.3	0.5	-4.9	7.9
R-KIV2-5	12.4	0.5	-4.2	8.8
IR-CIV-5	14.4	0.6	-3.7	11.3
IR-EIV-5	14.3	-0.3	-3.3	10.7
IR-KIV1-5	14.2	0.7	-4.9	10
IR-kIV2-5	14.7	0.5	-4.2	11

Table 4.5: The difference between elements weight of braced and MRF G+9 buildings (ELFM)

Model name	Columns (ton)	Beams (ton)	Bracing (ton)	Total (ton)
R-CIV-10	24.1	3.4	-7.4	20.1
R-EIV-10	28.1	0.5	-6.5	22.1
R-KIV1-10	24.9	3.6	-10.2	18.2
R-KIV2-10	25.3	3.4	-8.4	20.2
IR-CIV-10	19.5	3.9	-7.2	16.2
IR-EIV-10	23.2	1	-6.5	17.7
IR-KIV1-10	19.8	4.1	-10.2	13.7
IR-KIV2-10	21.2	3.7	-8.4	16.5

4.3 Non-Linear Static Pushover Analysis

The pushover analysis results of all models are presented in this segment of the research where results of base shear, lateral stiffness, plastic hinges status and displacement ductility factor are taken at the target displacement.

4.3.1 Base shear at the target displacement

The nonlinear static pushover analysis results of the base shear at the target displacement show that MRF systems have the least base shear this can be linked to the high ductility and low lateral stiffness. Hence, low force is required to push the building to the target displacement. Also this indicate that MRF is more likely exposed to the development of plastic hinges, which explained the loss in its strength although it has the highest target displacement compared with the other systems. On the other hand, KIV1 has the highest base shear this can be linked to various number of reasons which are listed below;

1- High target displacement compared with the other bracing systems.
2- The structural system mass is relatively higher.
3- The system has higher lateral stiffness compared with the MRF.

Also it can be concluded that KIV1 system has low probability to develop collapse prevention hinges since it didn't lose it lateral strength upon pushing. In addition, base shear

along Y-direction is relatively lower than X-direction which is related to the orientation of the column major axis. Figure 4.13 and Figure 4.14 summarized the results of the base shear at the target displacement of G+4 and G+9 respectively.

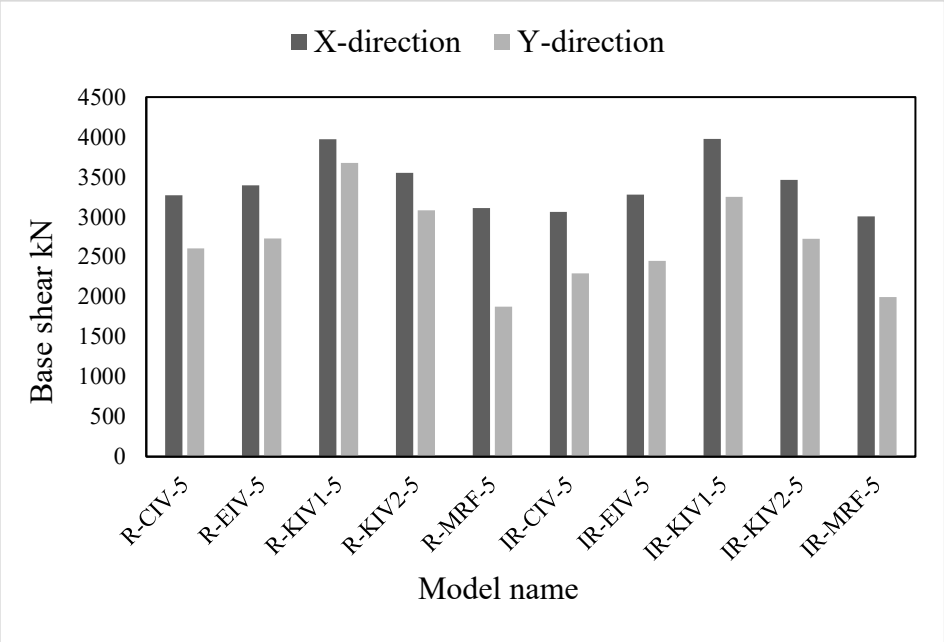

Figure 4.13: Base shear in X and Y directions for G+4 buildings (Pushover)

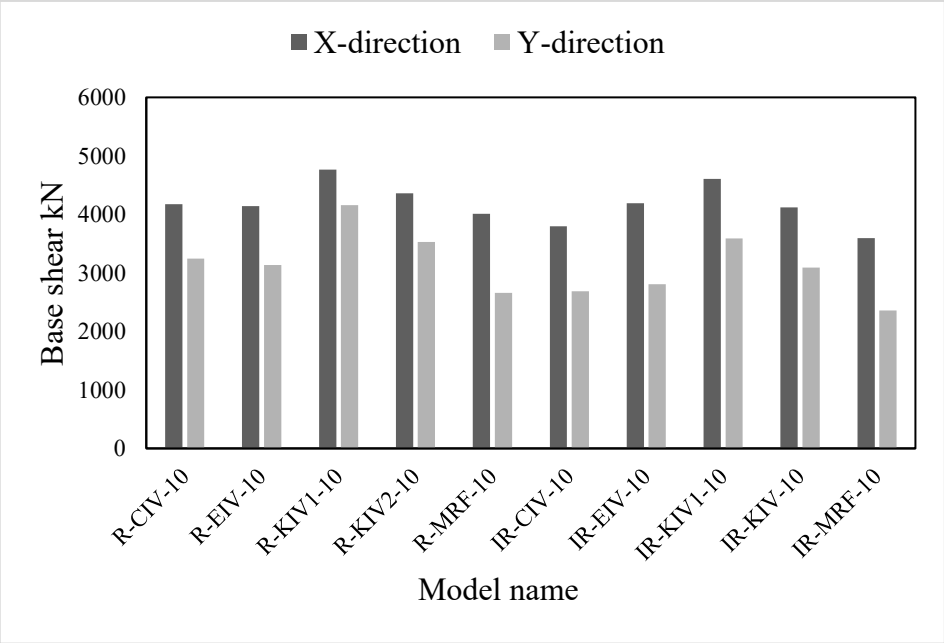

Figure 4.14: Base shear in X and Y directions for G+9 buildings (Pushover)

4.3.2 Lateral stiffness

The lateral stiffness results obtained from the nonlinear static pushover analysis show that at low monitored displacement the lateral stiffness is constant this can be linked to the fact that the structural elements did not exceed their yielding stress and the behaviour of the structure is rather linear. However, the lateral stiffness reduces upon the increment of the monitored displacement. This behaviour indicates the initial formation of the plastic hinges where the internal stresses within some of the structural elements exceeds the yielding stress. The results also show that CIV bracing system has the highest initial stiffness compared with the other systems. However, upon the formation of the plastic hinges this stiffness is dramatically reduced, where lateral stiffness level becomes almost equal with the other systems. Ultimately MRF has the least lateral stiffness and the drop in its stiffness is not as quit severe as the bracing system. This behaviour can be clearly observed in all cases from Figure 4.15 until Figure 4.22. The enhancement of the building performance upon the addition of the bracing system is listed in Table 4.6 and Table 4.7 where CIV bracing system gives the higher initial and final stiffness enhancement. For more information which include (stiffness-base shear) displacement curves (APPENDIX 5).

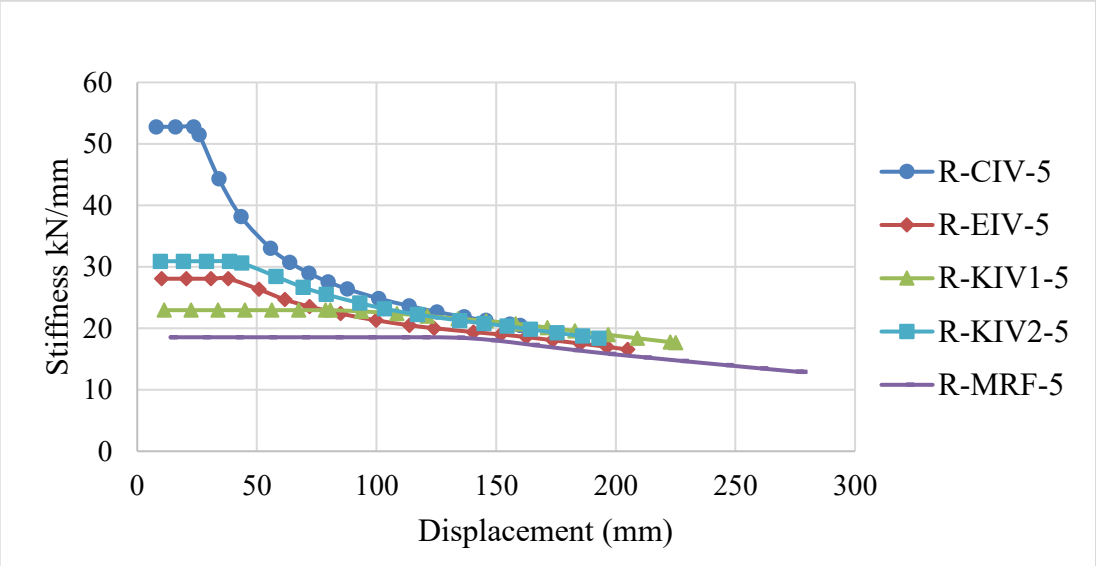

Figure 4.15: Stiffness - displacement curves in X direction for (Regular-G+4) buildings

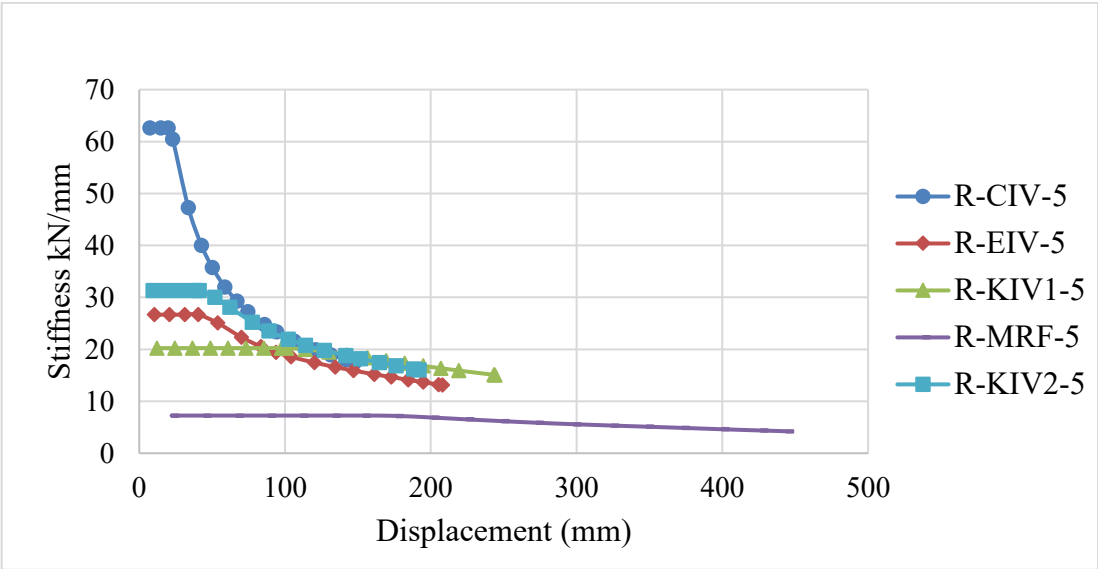

Figure 4.16: Stiffness - displacement curves in Y direction for (Regular-G+4) buildings

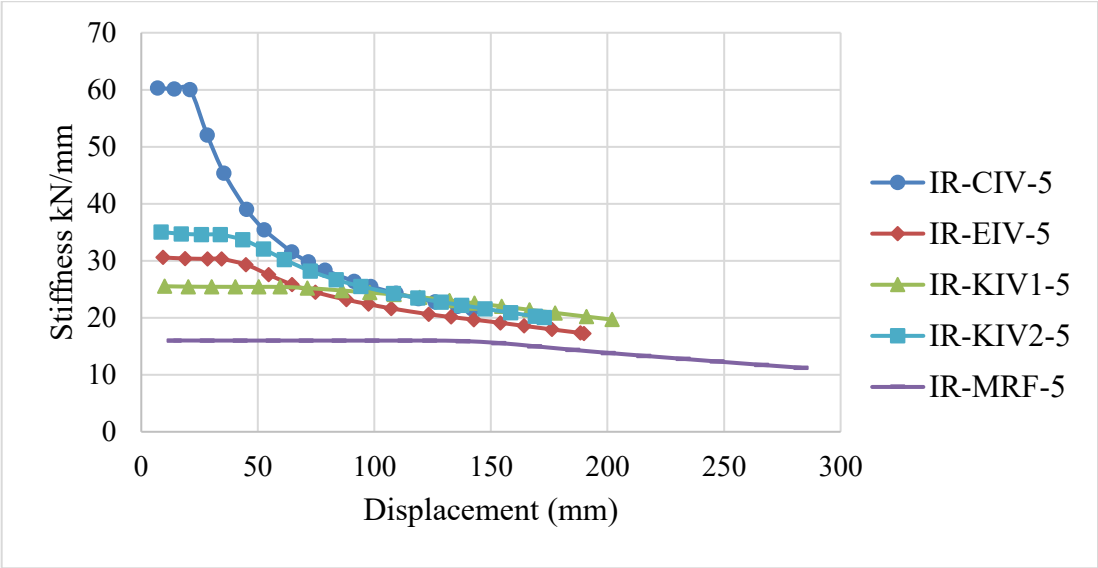

Figure 4.17: Stiffness - displacement curves in X direction for (Irregular-G+4) buildings

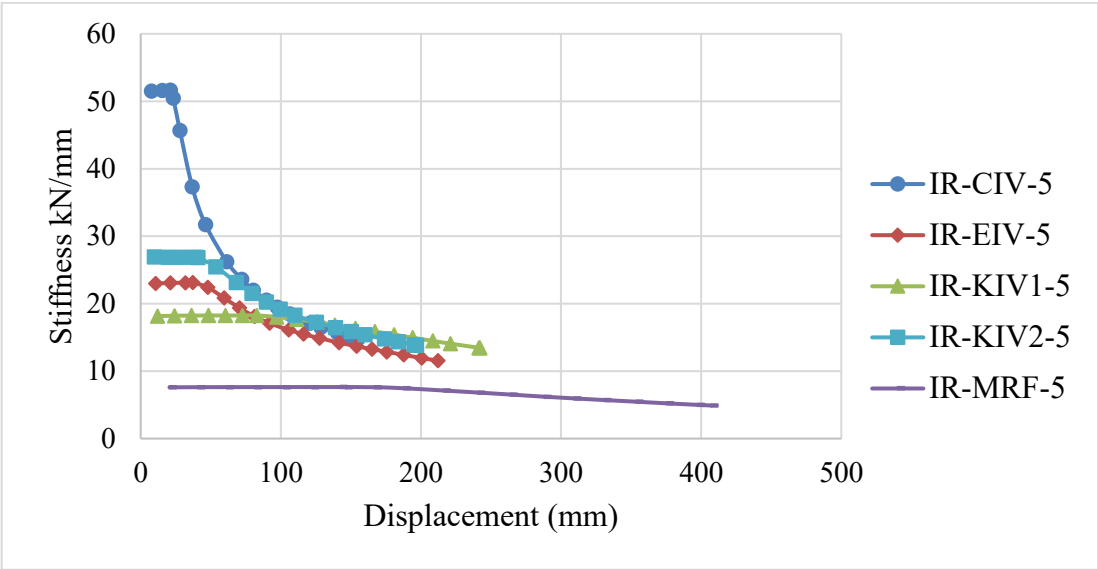

Figure 4.18: Stiffness - displacement curves in Y direction for (Irregular-G+4) buildings

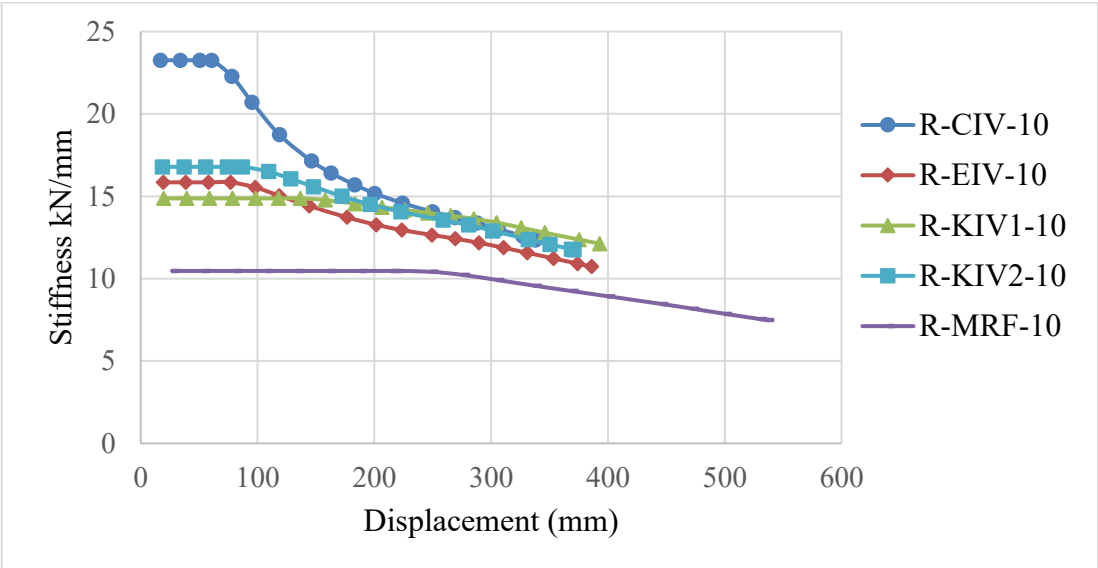

Figure 4.19: Stiffness - displacement curves in X direction for (Regular-G+9) buildings

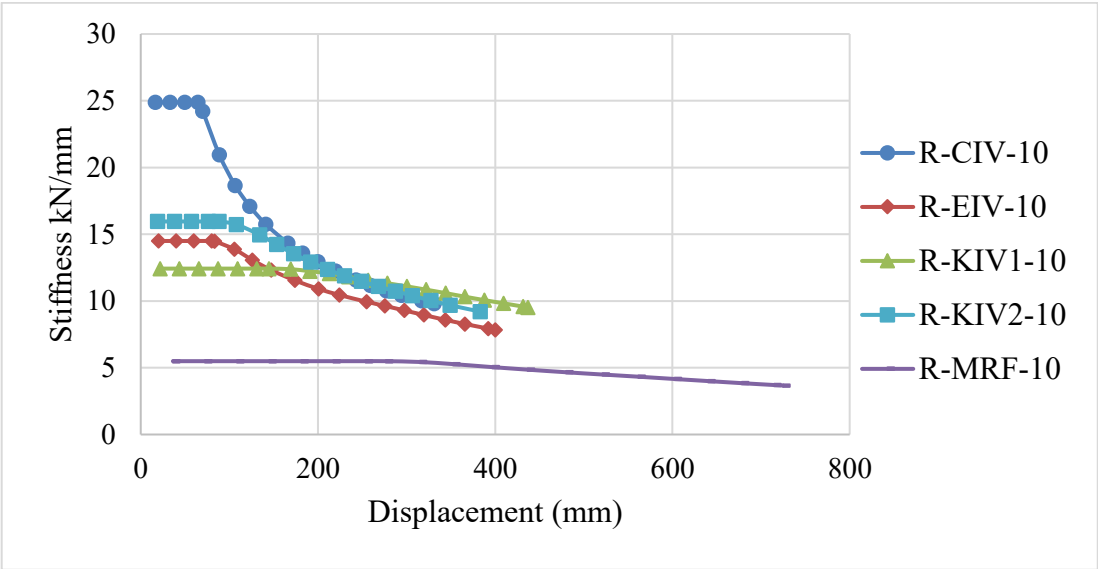

Figure 4.20: Stiffness - displacement curves in Y direction for (Regular-G+9) buildings

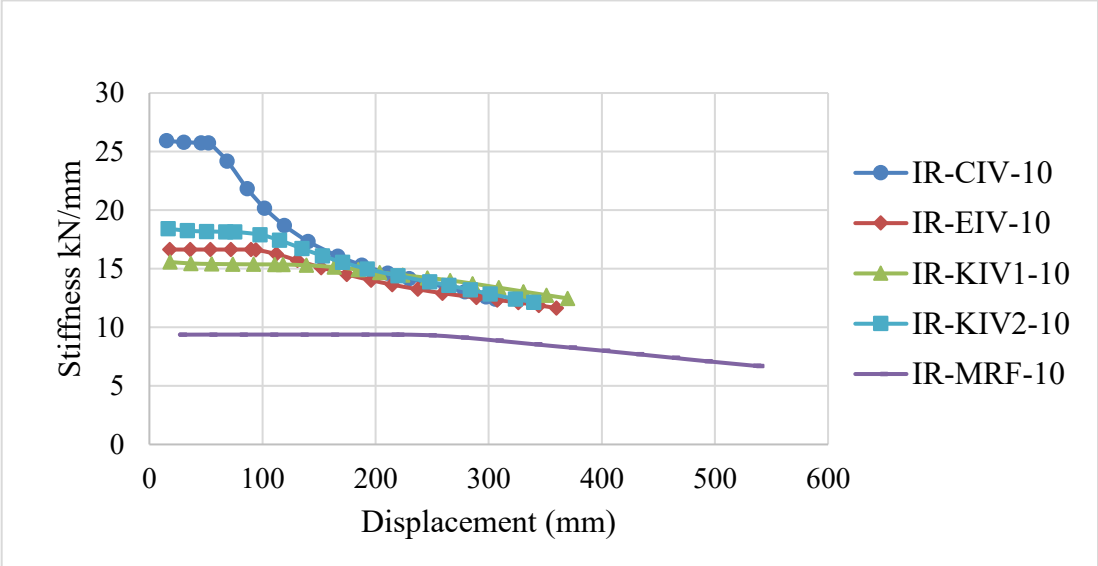

Figure 4.21: Stiffness - displacement curves in X direction for (Irregular-G+9) buildings

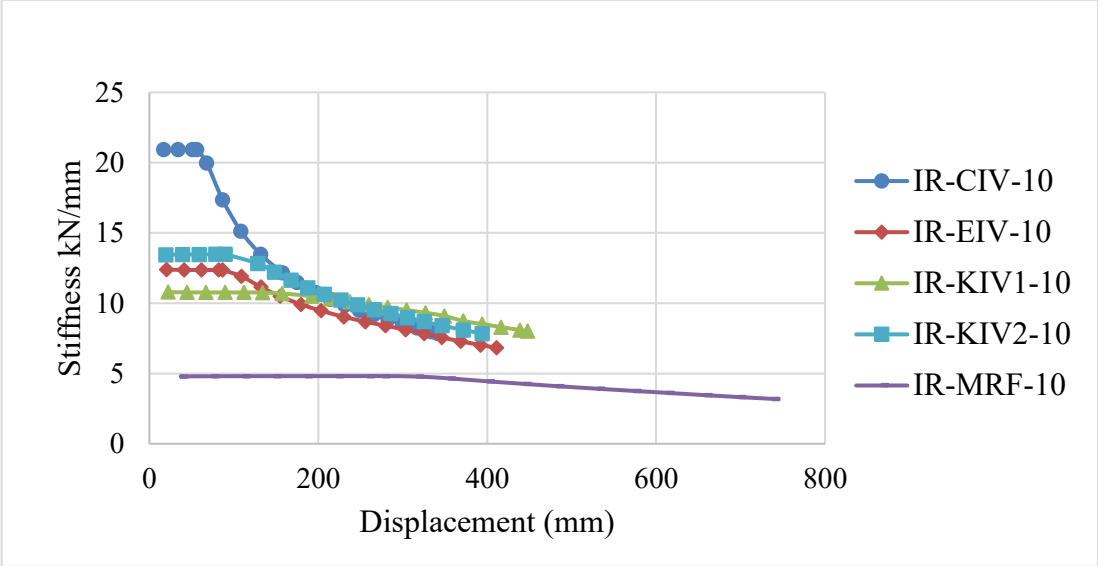

Figure 4.22: Stiffness - displacement curves in Y direction for (Irregular-G+9) buildings

Table 4.6: The percent variation of initial and final stiffness for G+4 buildings compared with the moment resisting frame (Pushover)

	Initial stiffness		**Final stiffness**	
Model Name	***(%) in X-direction**	***(%) in Y-direction**	***(%) in X-direction**	***(%) in Y-direction**
R-CIV	184.7	763.4	58.6	316.3
R-EIV	51.3	267.9	28.4	210.4
R-KIV1	23.8	179.2	36.9	256.3
R-KIV2	66.7	332.0	42.6	279.9
IR-CIV	276.6	578.8	92.2	202.0
IR-EIV	90.9	202.9	53.8	135.7
IR-KIV1	59.4	139.3	75.3	174.3
IR-KIV2	118.9	254.5	78.5	182.4

$*(\%) = \frac{Bracing\ K - MRF\ K}{MRF\ K} \times 100$

Table 4.7: The percent variation of initial and final stiffness for G+9 buildings compared with the moment resisting frame (Pushover)

	Initial stiffness		Final stiffness	
Model Name	***(%) in X-direction**	***(%) in Y-direction**	***(%) in X-direction**	***(%) in Y-direction**
R-CIV	122.2	353.2	64.8	167.0
R-EIV	51.4	164.1	43.4	113.6
R-KIV1	42.0	126.4	61.9	159.4
R-KIV2	60.4	190.7	56.9	151.0
IR-CIV	176.7	336.7	85.2	146.7
IR-EIV	77.6	158.7	73.7	114.1
IR-KIV1	66.3	125.3	86.1	151.1
IR-KIV2	96.6	180.8	81.0	145.8

$*(\%) = \frac{Bracing\ K - MRF\ K}{MRF\ K} \times 100$

4.3.3 State of plastic hinges

When the stress within the structural element exceeds the yielding stress plastic hinges are formed. Initially immediate occupancy (labelled in green) hinges are form as long as the rotation of the hinge relatively small however upon the incremented loading the rotation angle will increase causing the plastic hinge to change its status to life safety (labelled in blue) or collapse prevention (labelled in red) hinges. It worth to mention that initially hinges are formed in the inter-storey then the formation propagates to both base and top storeys. This can be linked to the high drift ratio of the inter-storey. Which can be clearly observed in Figure 4.23 and Figure 4.24.

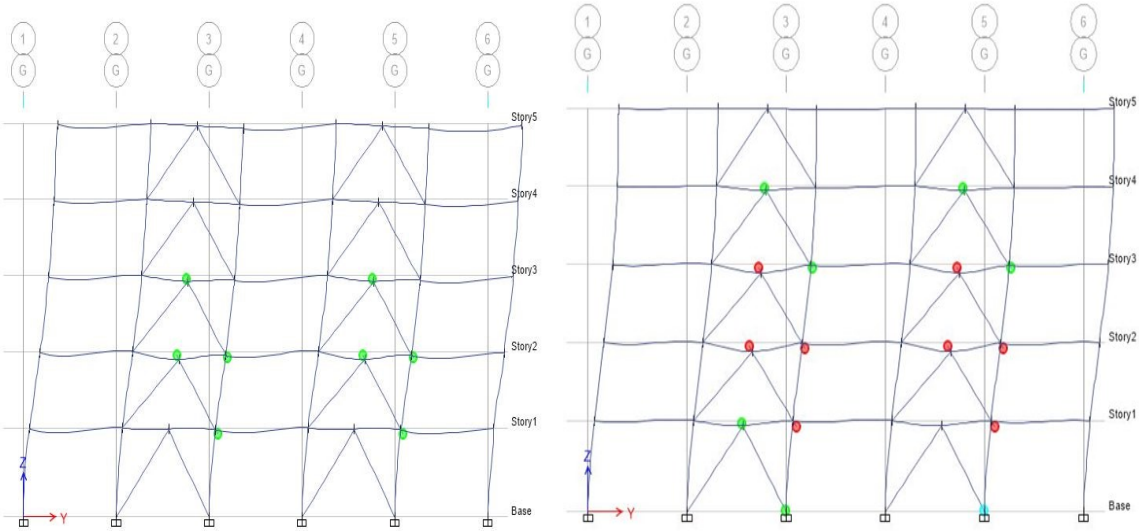

Figure 4.23: First and final step plastic hinges occurring in Y direction for (R-CIV-5) building

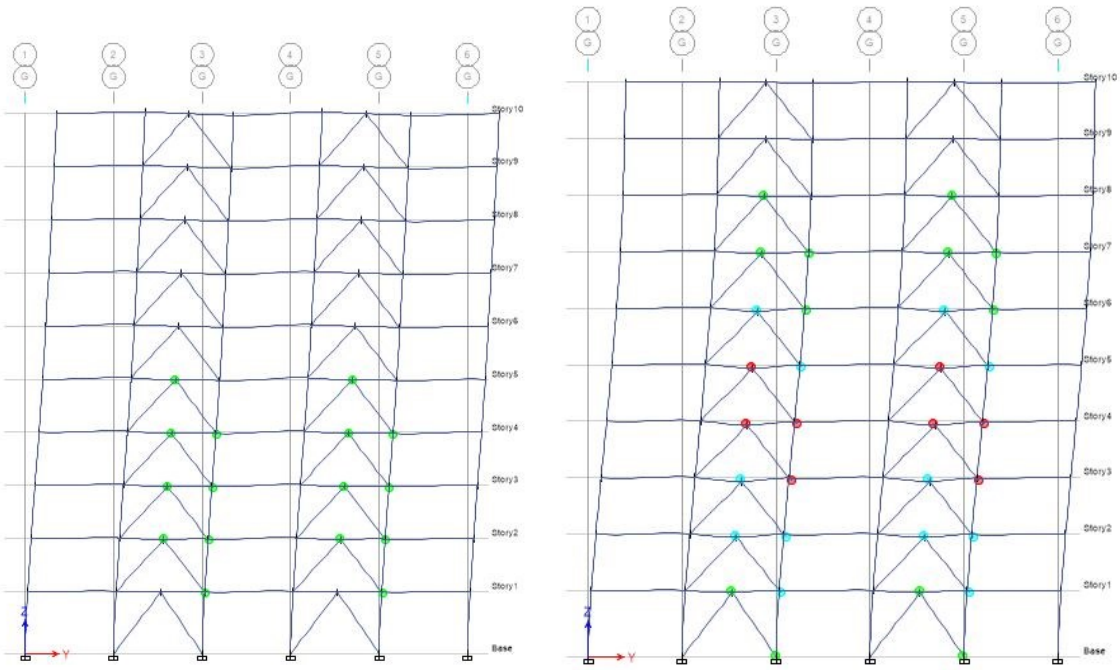

Figure 4.24: First and final step plastic hinges occurring in Y direction for (R-CIV-10) building

The best performance regarding the development of collapse prevention hinges is observed at KIV1 bracing system and the worst performance is observed at the MRF system. The

results of the developed plastic hinges are displayed in Table 4.8 and Table 4.9 for G+4 and G+9 buildings respectively.

Table 4.8: Plastic hinges for G+4 buildings (Pushover)

model name	Total	A-IO	IO-LS	LS-CP	>CP
R-CIV-5	1630	1539	48	26	17
R-EIV-5	1630	1482	102	34	12
R-KIV1-5	1830	1622	187	18	3
R-KIV2-5	1831	1682	101	36	12
R-MRF-5	1832	1586	208	0	38
IR-CIV-5	1530	1440	54	19	17
IR-EIV-5	1530	1397	88	38	7
IR-KIV1-5	1730	1561	154	8	7
IR-KIV2-5	1731	1605	84	29	13
IR-MRF-5	1732	1529	180	0	23

Table 4.9: Plastic hinges for G+9 buildings (Pushover)

model name	Total	A-IO	IO-LS	LS-CP	>CP
R-CIV-10	3260	3070	98	64	28
R-EIV-10	3260	3034	168	46	12
R-KIV1-10	3660	3445	188	24	3
R-KIV2-10	3661	3471	121	40	29
R-MRF-10	3662	3249	412	0	1
IR-CIV-10	3060	2893	91	48	28
IR-EIV-10	3060	2886	129	39	6
IR-KIV1-10	3460	3268	164	21	7
IR-KIV2-10	3461	3282	116	39	24
IR-MRF-10	3462	3075	379	0	8

4.3.4 Displacement ductility factor

Ductility plays a major role in reducing the absorbed energy from the ground motion. Since it reduces the exerted lateral forces that may act on structure. However, too ductile structure

are exposed high amount of sway which leads to the discomfort of residence and reduces the serviceability of the structure. The results of the nonlinear static pushover analysis show that MRF structure has the highest ductility. Since, its sway upon the application of lateral forces is relatively high and its yield displacement is high as well. On the other hand, all bracing system have very low yielding displacement which results in low ductility. This is valid for all cases except the KIV1 where its yield displacement is relatively high compared with the other bracing systems. Since the KIV1 has the least amount of the lateral stiffness among the other bracing types. Table 4.10 and Table 4.11 display summary of the displacement ductility factors for G+4 and G+9 buildings respectively.

Table 4.10: Displacement ductility factor in X and Y directions for G+4 buildings (Pushover)

	X-direction			**Y-direction**		
Model name	**displacement (mm)**	**D(Y) mm**	**μ**	**displacement (mm)**	**D(Y) mm**	**μ**
R-CIV-5	160	23.53	6.80	148	19.78	7.49
R-EIV-5	205	38.05	5.38	208	40.50	5.14
R-KIV1-5	225	80.77	2.78	244	97.60	2.50
R-KIV2-5	193	38.60	5.00	192	41.23	4.66
R-MRF-5	277	119.48	2.32	444	201.10	2.21
IR-CIV-5	142	20.84	6.83	155	21.30	7.26
IR-EIV-5	190	34.46	5.52	212	37.30	5.68
IR-KIV1-5	202	59.57	3.39	242	82.97	2.92
IR-KIV2-5	173	33.95	5.09	197	39.39	5.00
IR-MRF-5	283	123.70	2.29	407	142.59	2.86

Table 4.11: Displacement ductility factor in X and Y directions for G+9 buildings (Pushover)

	X-direction			Y-direction		
Model name	**displacement (mm)**	**D(Y) mm**	**μ**	**displacement (mm)**	**D(Y) mm**	**μ**
R-CIV-10	338	60.69	5.57	331	64.47	5.13
R-EIV-10	386	76.98	5.01	400	80.00	5.00
R-KIV1-10	393	136.66	2.88	437	144.58	3.02
R-KIV2-10	371	87.17	4.26	383	88.20	4.34
R-MRF-10	536	219.17	2.45	725	276.70	2.62
IR-CIV-10	306	52.40	5.84	341	55.95	6.10
IR-EIV-10	360	90.00	4.00	411	86.48	4.75
IR-KIV1-10	370	117.61	3.14	448	132.43	3.38
IR-KIV2-10	340	97.83	3.47	394	89.65	4.40
IR-MRF-10	537	214.83	2.50	738	276.74	2.67

4.4 Time History Analysis

This part of the research discusses the performance of inverted-V bracing using real ground motions records. Three records are used to cover wide range of frequency. Base shear, top storey displacement and acceleration are presented.

4.4.1 Base shear

The analysis results of the steel structural buildings under three different ground motion records show that highest developed base shear is at CIV bracing system for all cases. Ultimately, there is no significant difference in the resulted base shear for both eccentric and knee types of bracing. This behaviour can be related to the low ductility and high lateral stiffness of the concentric bracing compared with the eccentric and knee types of bracing. On the other hand, MRF resulted in the least amount of the developed base shear since it has high ductility and high natural vibration period. It is worth to mention that Erzincan earthquake records (1992) resulted in the highest base shear which may indicates that the frequency of the ground motion records and the CIV bracing system are similar in magnitude

(resonance). The results of base shear under different ground motion records are displayed in bar chart form from Figure 4.25 until Figure 4.30. Also Tables 4.12-4.13-4.14 present the percent variation in the base shear compared with the moment resisting frame.

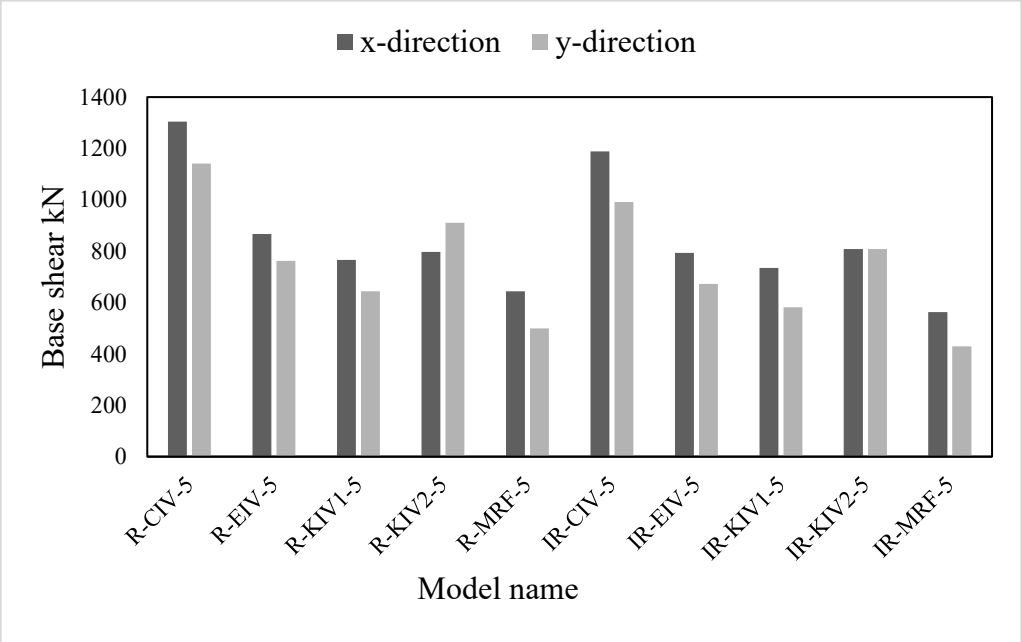

Figure 4.25: Base shear in X and Y directions for G+4 buildings (K.E)

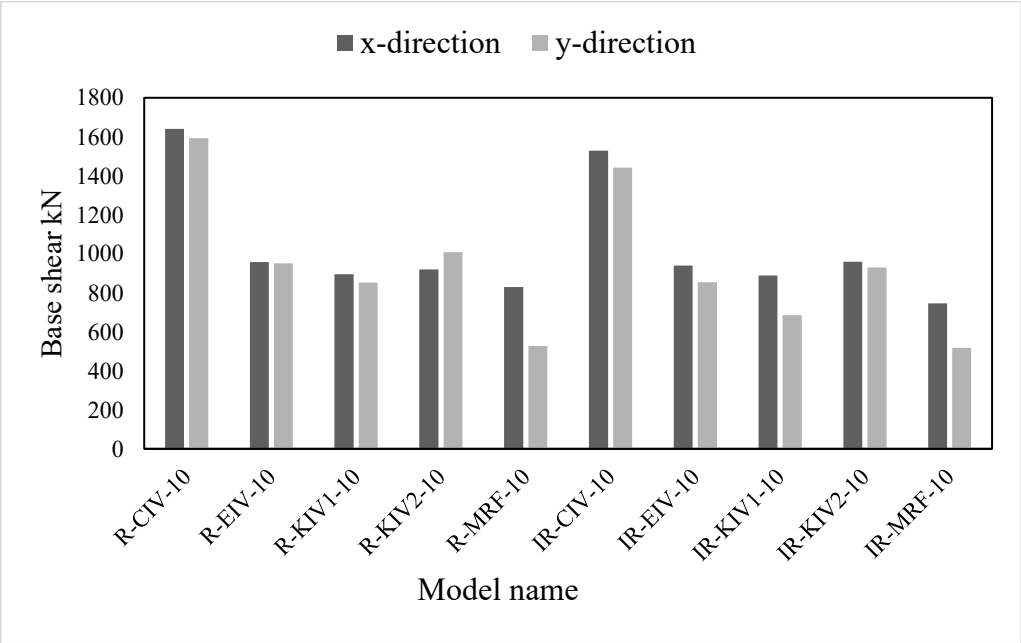

Figure 4.26: Base shear in X and Y directions for G+9 buildings (K.E)

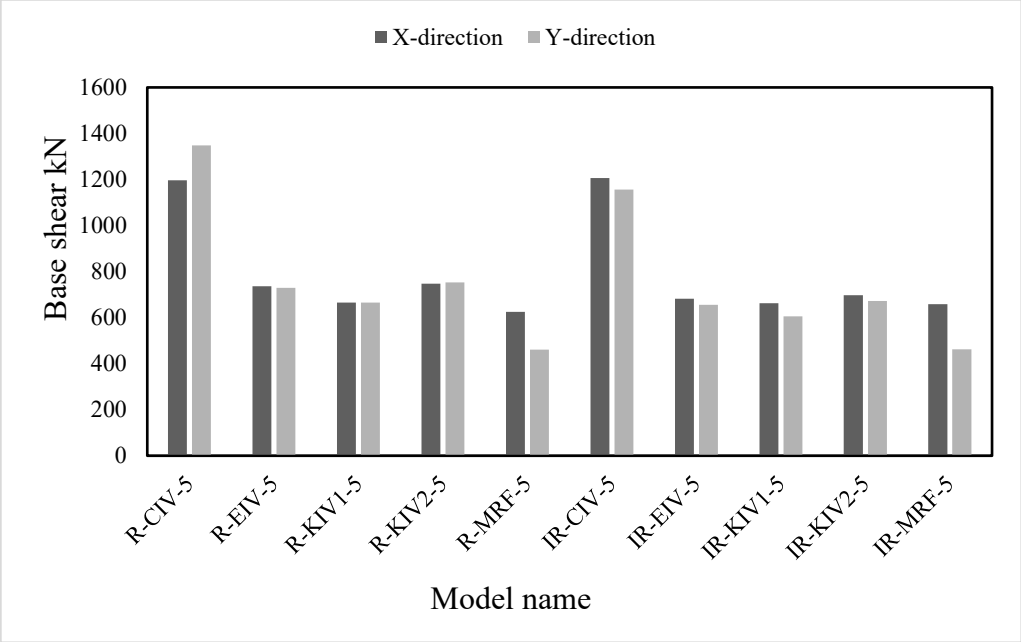

Figure 4.27: Base shear in X and Y directions for G+4 buildings (S.E)

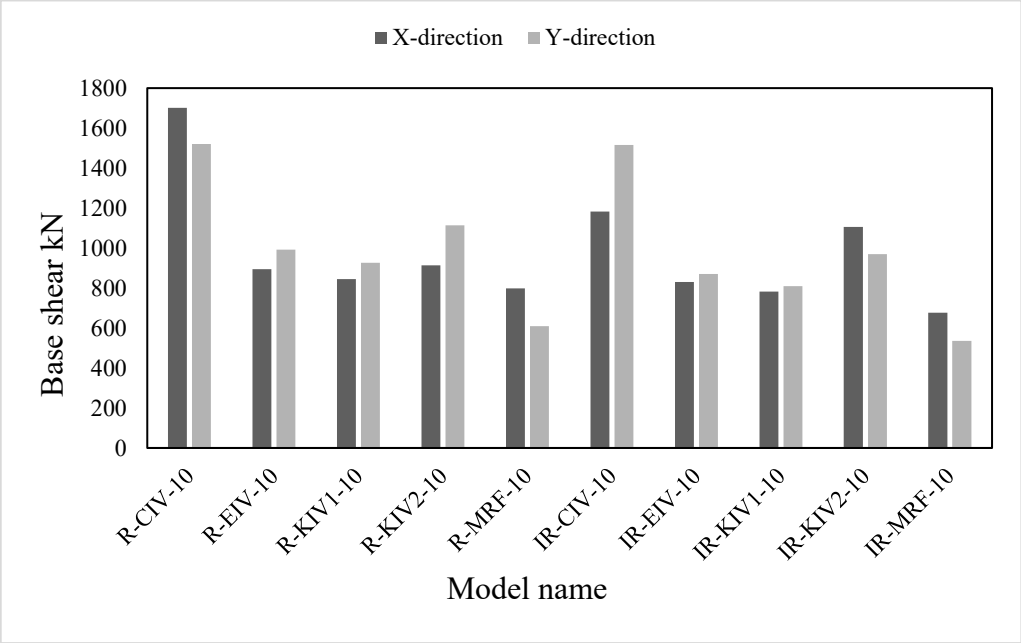

Figure 4.28: Base shear in X and Y directions for G+9 buildings (S.E)

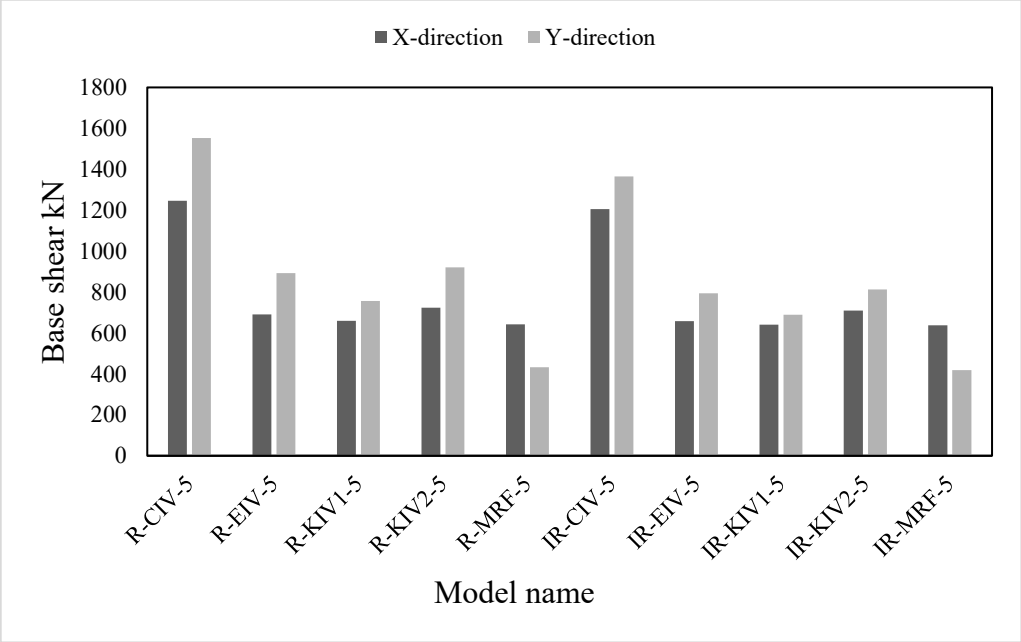

Figure 4.29: Base shear in X and Y directions for G+4 buildings (E.E)

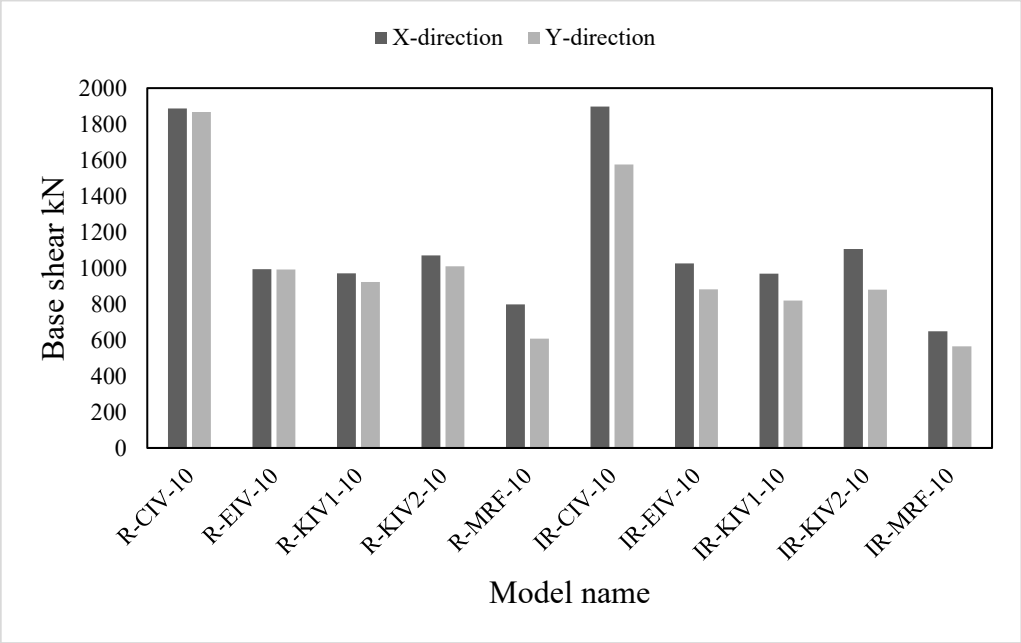

Figure 4.30: Base shear in X and Y directions for G+9 buildings (E.E)

Table 4.12: The percent variation of base shear compared with the moment resisting frame (K.E)

Model Name	*(%) in (G+4)-X-direction	*(%) in (G+4) Y-direction	*(%) in (G+9) X-direction	*(%) in (G+9) Y-direction
R-CIV	102.5	128.4	97.6	201.9
R-EIV	34.6	52.4	10.8	80.3
R-KIV1	18.8	28.6	8.0	61.4
R-KIV2	23.8	82.0	15.4	90.9
IR-CIV	111.0	130.5	104.7	178.4
IR-EIV	40.9	56.3	25.8	65.1
IR-KIV1	30.6	35.1	19.0	32.0
IR-KIV2	43.5	87.9	28.5	79.5

$$*(\%) = \frac{Bracing\ base\ shear - MRF\ base\ shear}{MRF\ base\ shear} \times 100$$

Table 4.13: The percent variation of base shear compared with the moment resisting frame (S.E)

Model Name	*(%) in (G+4)-X-direction	*(%) in (G+4) Y-direction	*(%) in (G+9) X-direction	*(%) in (G+9) Y-direction
R-CIV	91.5	192.4	113.3	149.3
R-EIV	17.8	58.4	12.2	62.6
R-KIV1	6.4	44.5	5.9	51.8
R-KIV2	19.7	63.3	14.4	82.6
IR-CIV	83.4	150.4	74.9	183.4
IR-EIV	3.6	42.0	22.8	62.6
IR-KIV1	0.8	31.2	15.8	51.2
IR-KIV2	6.1	45.7	63.5	81.3

$$*(\%) = \frac{Bracing\ base\ shear - MRF\ base\ shear}{MRF\ base\ shear} \times 100$$

Table 4.14: The percent variation of base shear compared with the moment resisting frame (E.E)

Model Name	*(%) in (G+4)-X-direction	*(%) in (G+4) Y-direction	*(%) in (G+9) X-direction	*(%) in (G+9) Y-direction
R-CIV	94.1	258.4	136.5	207.1
R-EIV	7.6	106.2	24.4	63.2
R-KIV1	2.6	74.8	21.6	51.6
R-KIV2	12.6	112.5	34.1	66.1
IR-CIV	89.2	226.6	192.9	179.3
IR-EIV	3.3	90.0	58.3	56.2
IR-KIV1	0.6	64.8	49.4	45.4
IR-KIV2	11.3	94.5	70.7	55.9

$$*(\%) = \frac{Bracing\ base\ shear - MRF\ base\ shear}{MRF\ base\ shear} \times 100$$

4.4.2 Roof displacement

The roof displacement results obtained by nonlinear time history analysis of three different ground motion records show that MRF system has the highest roof displacement especially along the y-direction this can be related to the high ductility and low lateral stiffness of the MRF system. Resonance did not take place in the case of the MRF since all ground motion records produce similar displacement in both orthogonal directions regardless of their different frequency. On the other hand, for the least roof displacement the results are inconsistent where CIV perform the best in the case of G+4 buildings. However, for the G+9 buildings KIV2 resulted in a lower displacement. This argument is valid for all the cases of the ground motion records. This might indicates that CIV bracing systems of the G+9 buildings have near natural vibration periods with the oscillated ground motion acceleration. However, these displacement are not as quit extreme since CIV bracing system has high lateral stiffness. This behavior can be seen in Figures 4.31-4.32-4.33-4.34-4.35-4.36. In addition the percent reduction in the imposed roof displacement of the MRF system are displayed in Tables 4.15-4.16-4.17.

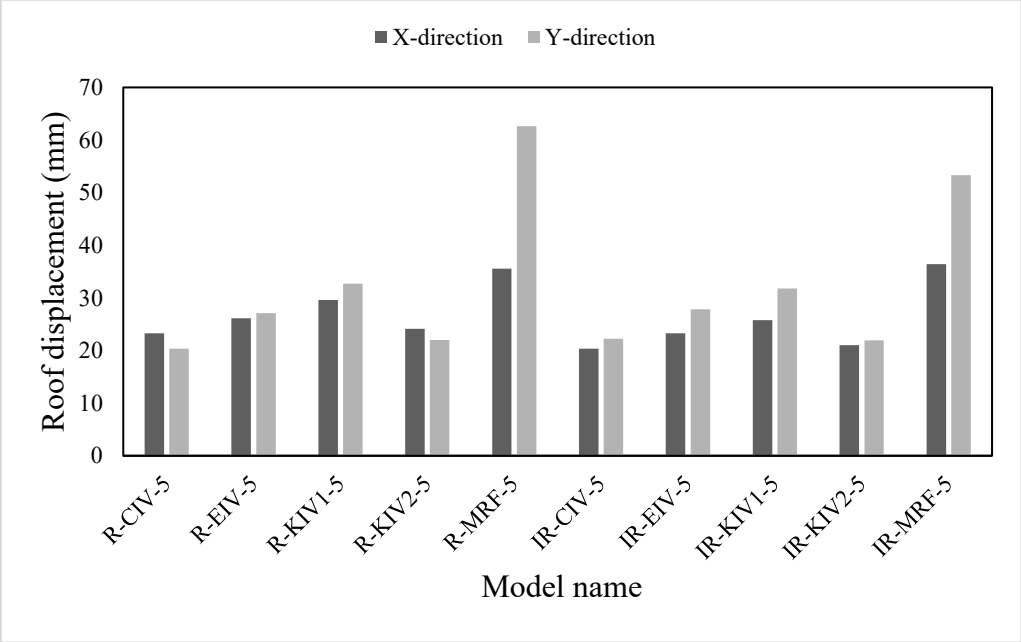

Figure 4.31: Roof displacement in X and Y directions for G+4 buildings (K.E)

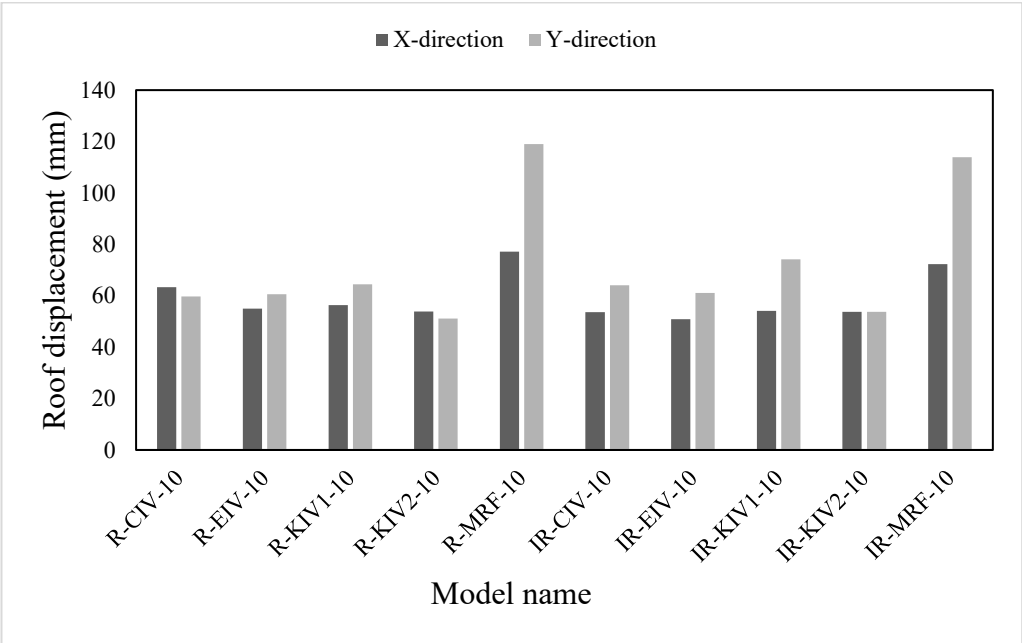

Figure 4.32: Roof displacement in X and Y directions for G+9 buildings (K.E)

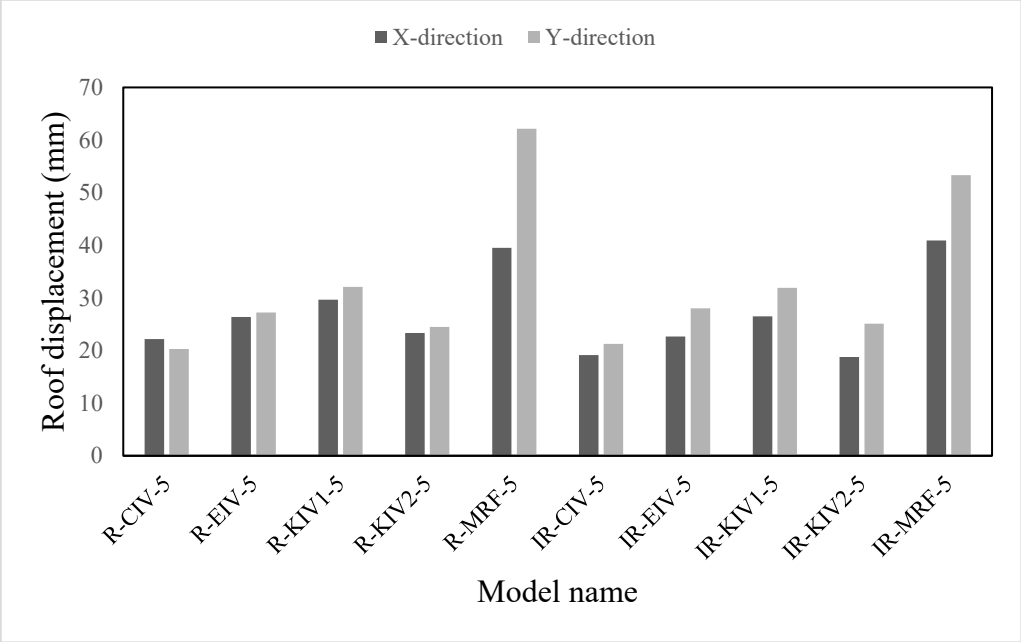

Figure 4.33: Roof displacement in X and Y directions for G+4 buildings (S.E)

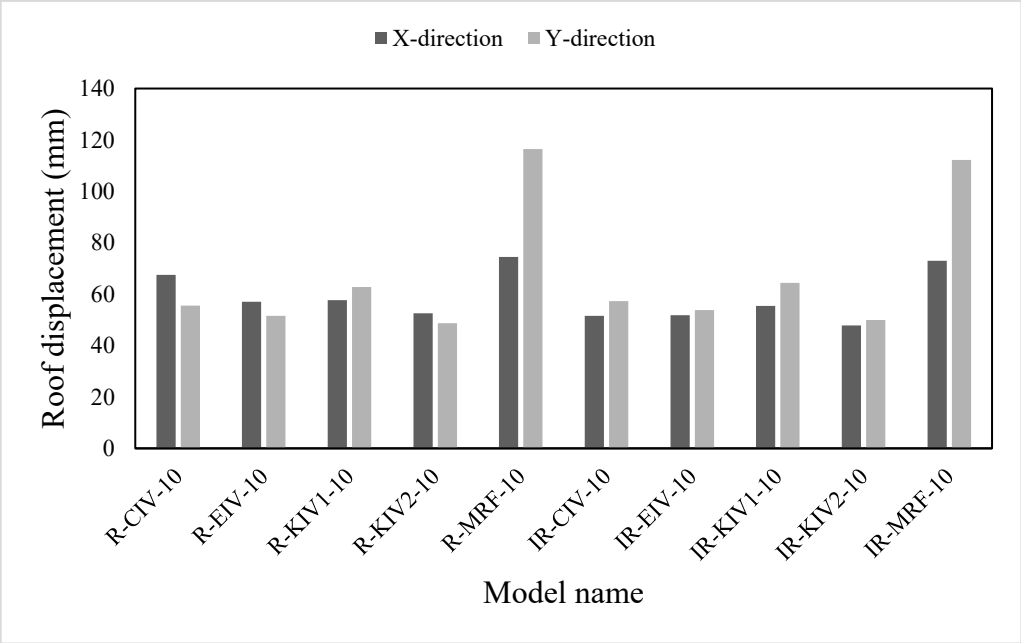

Figure 4.34: Roof displacement in X and Y directions for G+9 buildings (S.E)

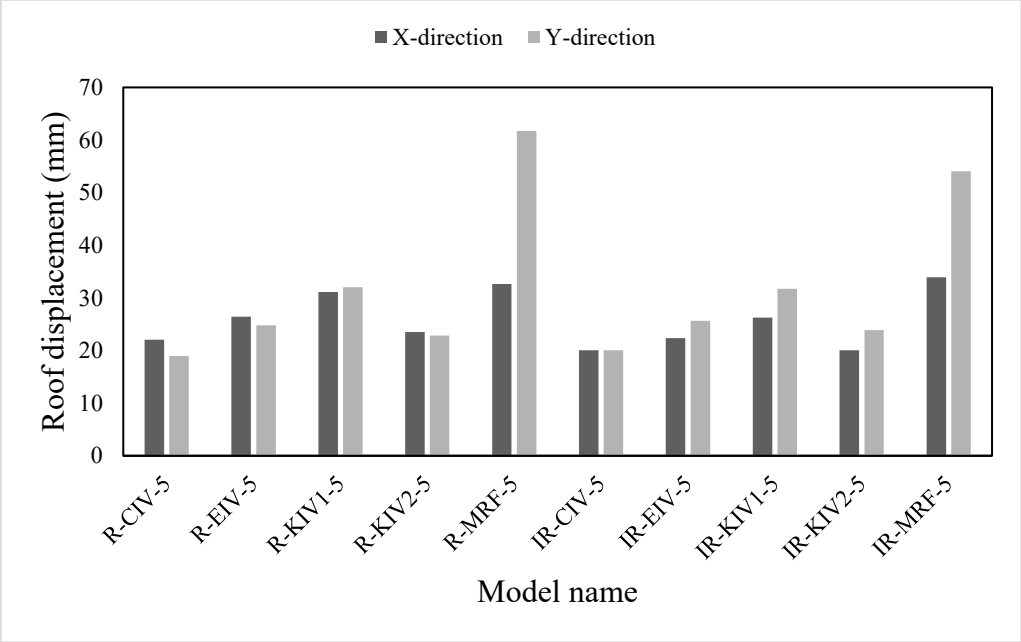

Figure 4.35: Roof displacement in X and Y directions for G+9 buildings (E.E)

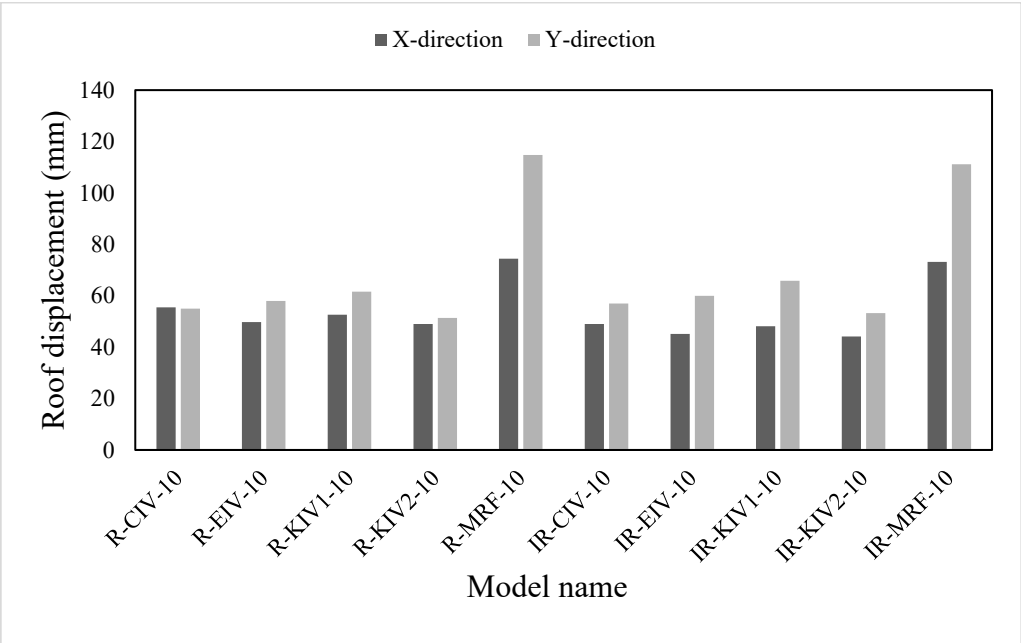

Figure 4.36: Roof displacement in X and Y directions for G+9 buildings (E.E)

Table 4.15: The percent reduction of roof displacement compared with the moment resisting frame (K.E)

Model Name	*(%) in (G+4)-X-direction	*(%) in (G+4) Y-direction	*(%) in (G+9) X-direction	*(%) in (G+9) Y-direction
R-CIV	34.6	67.6	18.0	49.9
R-EIV	26.5	56.8	28.8	49.1
R-KIV1	16.7	47.8	27.1	45.9
R-KIV2	32.1	64.9	30.1	57.0
IR-CIV	44.2	58.3	25.8	43.8
IR-EIV	36.0	47.8	29.7	46.3
IR-KIV1	29.2	40.3	25.2	34.9
IR-KIV2	42.3	58.9	25.7	52.8

$*(\%) = \left| \frac{Bracing\ disp - MRF\ disp}{MRF\ disp} \times 100 \right|$

Table 4.16: The percent reduction of roof displacement compared with the moment resisting frame (S.E)

Model Name	*(%) in (G+4)-X-direction	*(%) in (G+4) Y-direction	*(%) in (G+9) X-direction	*(%) in (G+9) Y-direction
R-CIV	43.9	67.3	9.3	52.3
R-EIV	33.3	56.2	23.3	55.8
R-KIV1	24.9	48.4	22.5	46.1
R-KIV2	40.9	60.6	29.3	58.2
IR-CIV	53.2	60.2	29.3	48.9
IR-EIV	44.7	47.4	29.0	52.1
IR-KIV1	35.3	40.1	24.0	42.6
IR-KIV2	54.1	52.9	34.4	55.4

$*(\%) = \left| \frac{Bracing\ disp - MRF\ disp}{MRF\ disp} \times 100 \right|$

Table 4.17: The percent reduction of roof displacement compared with the moment resisting frame (E.E)

Model Name	*(%) in (G+4)-X-direction	*(%) in (G+4) Y-direction	*(%) in (G+9) X-direction	*(%) in (G+9) Y-direction
R-CIV	32.5	69.3	25.4	52.1
R-EIV	19.0	59.8	33.1	49.5
R-KIV1	4.8	48.1	29.3	46.4
R-KIV2	27.9	62.9	34.2	55.3
IR-CIV	40.9	62.9	33.0	48.7
IR-EIV	34.1	52.6	38.4	46.1
IR-KIV1	2.6	41.3	34.3	40.8
IR-KIV2	0.9	55.8	39.7	52.1

$*(\%) = \left| \frac{Bracing\ disp - MRF\ disp}{MRF\ disp} \times 100 \right|$

4.4.3 Roof acceleration

Peak floor acceleration is used to estimate the damages of the non-structural components such as electrical wiring and pipeline system. The results of the nonlinear time history analysis show that roof acceleration is the highest for the CIV bracing system. On the other hand the least roof acceleration is governed by the MRF system since it has high ductility, which dissipates huge amount of the transmitted acceleration. This is observed in all of the ground motion records as shown in Figures 4.37-4.38-4.39-4.40-4.41-4.42. Also Tables 4.18-4.19-4.20 present the percent increment in the roof acceleration compared with the moment resisting frame.

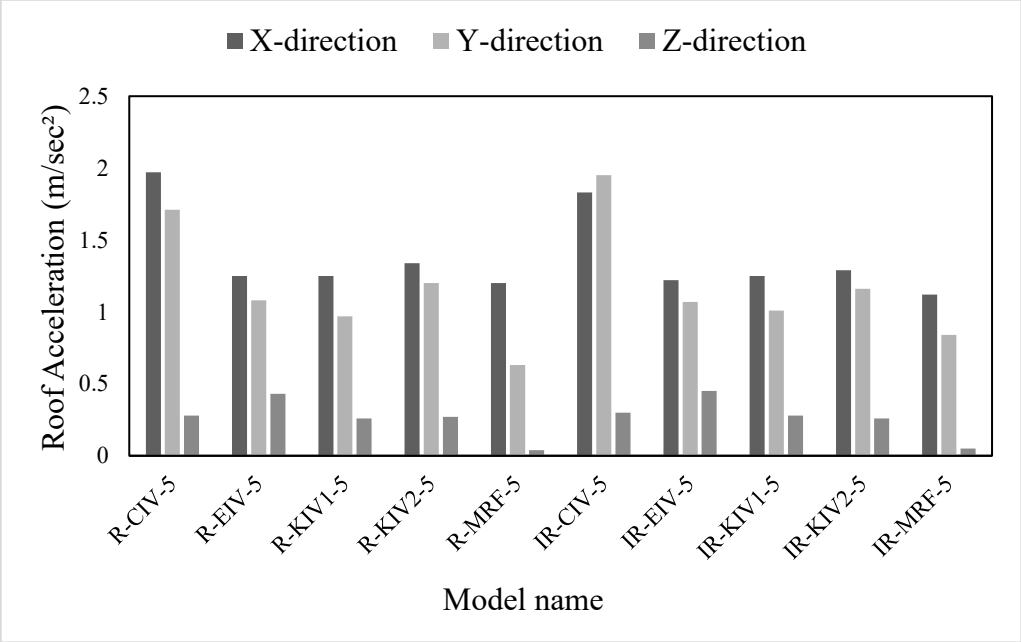

Figure 4.37: Roof acceleration in X and Y direction for G+4 buildings (K.E)

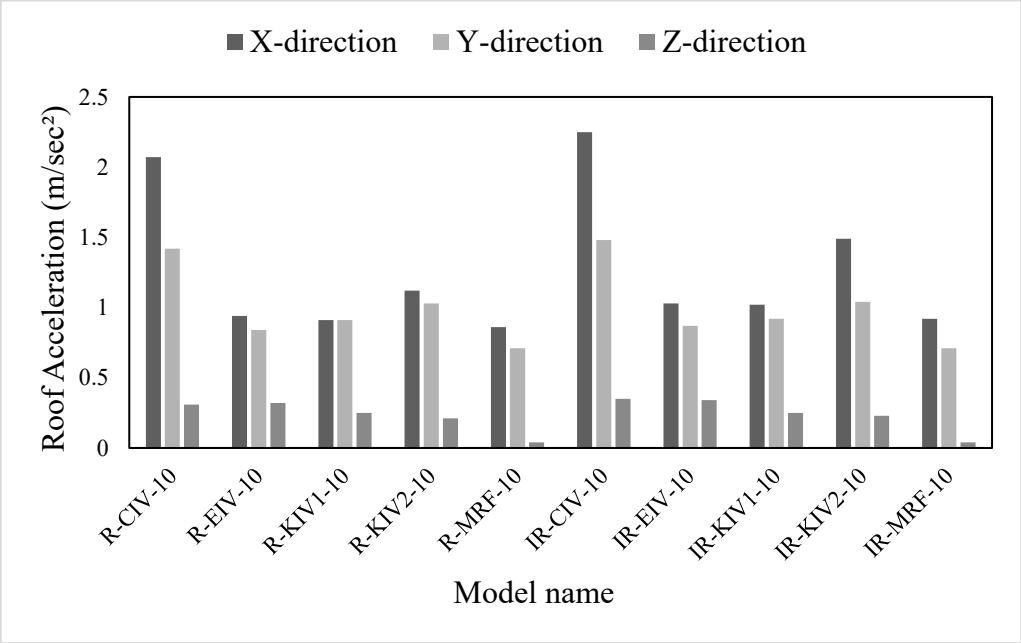

Figure 4.38: Roof acceleration in X and Y direction for G+9 buildings (K.E)

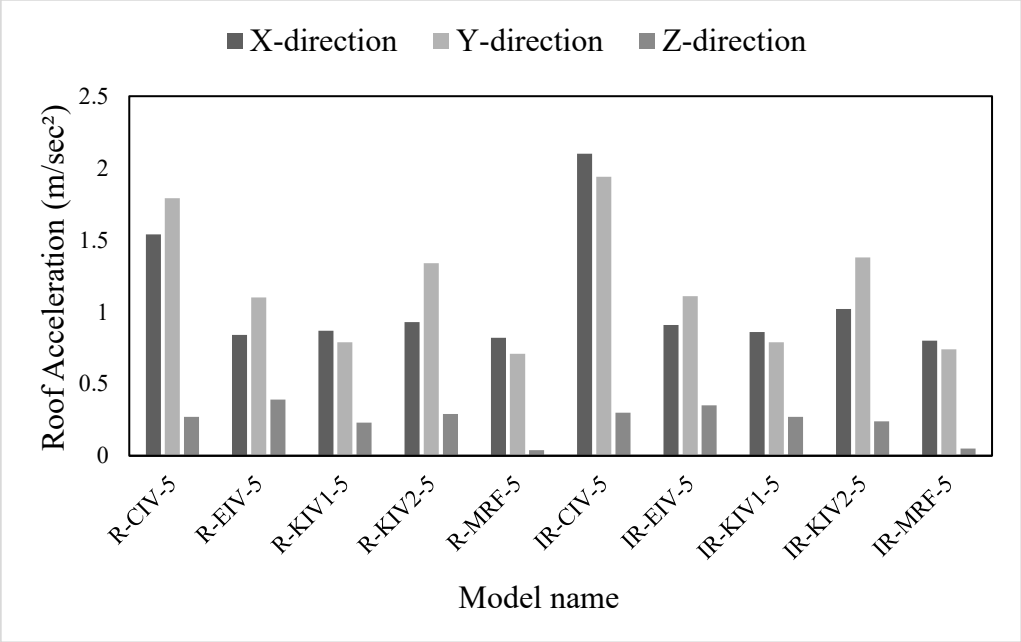

Figure 4.39: Roof acceleration in X and Y direction for G+4 buildings (S.E)

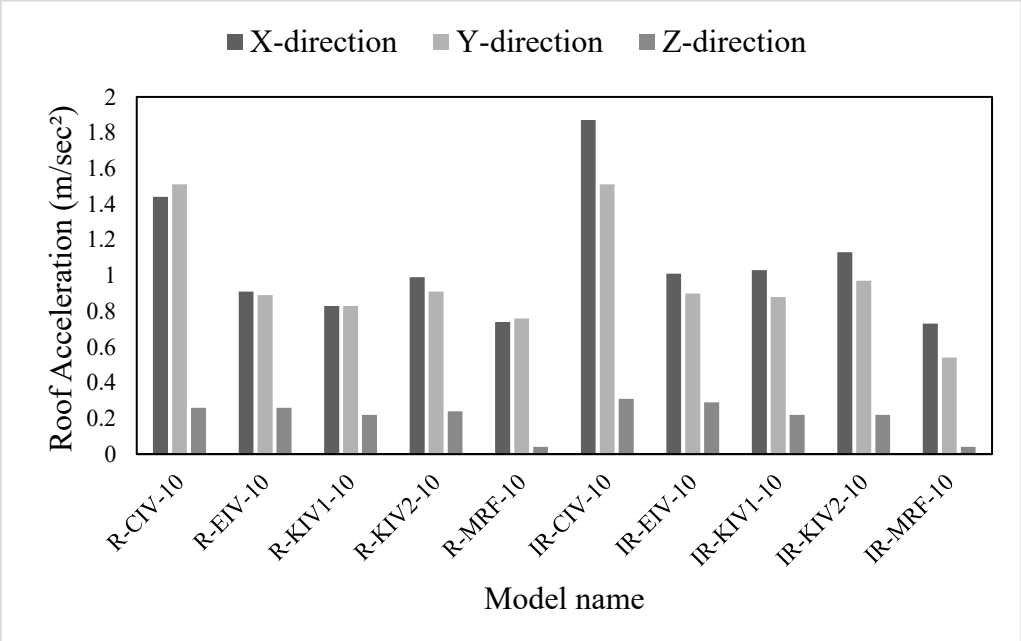

Figure 4.40: Roof acceleration in X and Y direction for G+9 buildings (S.E)

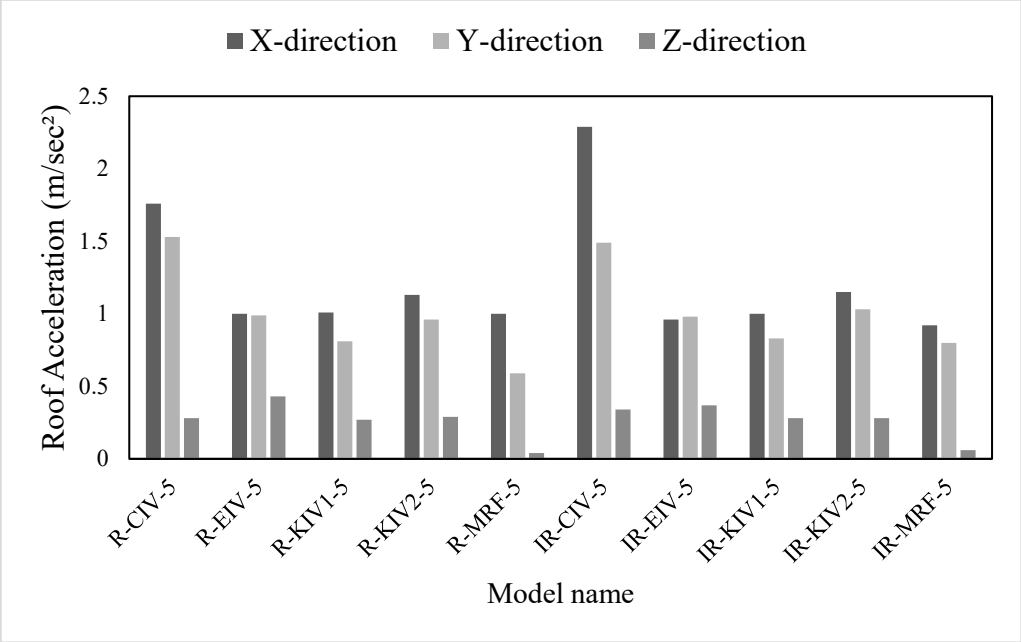

Figure 4.41: Roof acceleration in X and Y direction for G+4 buildings (E.E)

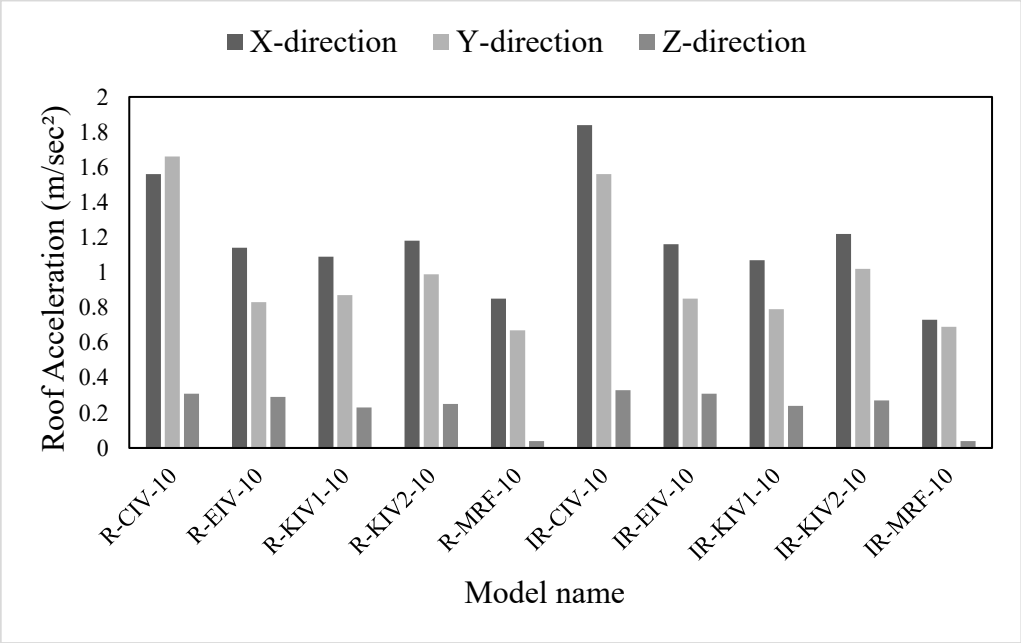

Figure 4.42: Roof acceleration in X and Y direction for G+9 buildings (E.E)

Table 4.18: The percent increment of roof acceleration compared with the moment resisting frame (K.E)

Model Name	*(%) in (G+4)-X	*(%) in (G+4)-Y	*(%) in (G+4)-Z	*(%) in (G+9)-X	*(%) in (G+9)-Y	*(%) in (G+9)-Z
R-CIV	64.2	171.4	600.0	140.7	100.0	675.0
R-EIV	4.2	71.4	975.0	9.3	18.3	700.0
R-KIV1	4.2	54.0	550.0	5.8	28.2	525.0
R-KIV2	11.7	90.5	575.0	30.2	45.1	425.0
IR-CIV	63.4	132.1	500.0	144.6	108.5	775.0
IR-EIV	8.9	27.4	800.0	12.0	22.5	750.0
IR-KIV1	11.6	20.2	460.0	10.9	29.6	525.0
IR-KIV2	15.2	38.1	420.0	62.0	46.5	475.0

$*(\%) = \frac{Bracing\ accel - MRF\ accel}{MRF\ accel.} \times 100$

Table 4.19: The percent increment of roof acceleration compared with the moment resisting frame (S.E)

Model Name	*(%) in (G+4)-X	*(%) in (G+4)-Y	*(%) in (G+4)-Z	*(%) in (G+9)-X	*(%) in (G+9)-Y	*(%) in (G+9)-Z
R-CIV	87.8	152.1	575.0	94.6	98.7	550.0
R-EIV	2.4	54.9	875.0	23.0	17.1	550.0
R-KIV1	6.1	11.3	475.0	12.2	9.2	450.0
R-KIV2	13.4	88.7	625.0	33.8	19.7	500.0
IR-CIV	162.5	162.2	500.0	156.2	179.6	675.0
IR-EIV	13.8	50.0	600.0	38.4	66.7	625.0
IR-KIV1	7.5	6.8	440.0	41.1	63.0	450.0
IR-KIV2	27.5	86.5	380.0	54.8	79.6	450.0

$*(\%) = \frac{Bracing\ accel - MRF\ accel}{MRF\ accel.} \times 100$

Table 4.20: The percent increment of roof acceleration compared with the moment resisting frame (E.E)

Model Name	*(%) in (G+4)-X	*(%) in (G+4)-Y	*(%) in (G+4)-Z	*(%) in (G+9)-X	*(%) in (G+9)-Y	*(%) in (G+9)-Z
R-CIV	76.0	159.3	600.0	83.5	147.8	675.0
R-EIV	0.0	67.8	975.0	34.1	23.9	625.0
R-KIV1	1.0	37.3	575.0	28.2	29.9	475.0
R-KIV2	13.0	62.7	625.0	38.8	47.8	525.0
IR-CIV	148.9	86.3	466.7	152.1	126.1	725.0
IR-EIV	4.3	22.5	516.7	58.9	23.2	675.0
IR-KIV1	8.7	3.7	366.7	46.6	14.5	500.0
IR-KIV2	25.0	28.8	366.7	67.1	47.8	575.0

$*(\%) = \frac{Bracing\ accel - MRF\ accel}{MRF\ accel.} \times 100$

CHAPTER 5

CONCLUSIONS & RECOMMENDATIONS

5.1 Overview

In the previous chapters, the seismic performance of steel structure that are equipped with various types of inverted-V bracing systems which are located within the boundary of Famagusta city. Both regular and irregular buildings with various storeys numbers are considered. For this purpose 20 structural models are analysed using ETABS 2016 software. Both linear and nonlinear behaviour of the steel structural buildings are discussed. This was achieved by conducting ELFM, pushover and time history analyses in accordance with NCSC2015 in order to obtain the optimum Inverted-V bracing systems.

5.2 Summary of the Results

The structural analysis results obtained using ETABS2016 software, are listed as follow:

1. Equivalent lateral force method

- Steel structures that are equipped with inverted-V bracing system have higher base shear compared with the MRF system. Especially, CIV bracing system, which resulted in the highest base shear among the other types.
- MRF system resulted in the highest roof displacement. On the other hand, the various types of the inverted-V bracing have no significant variation among themselves. However, CIV and KIV2 systems showed the least displacement.
- The total mass of the structure is also influenced by the bracing systems where moment resistant frame is the heaviest although it has lower number of the structural elements compared with buildings equipped with the bracing systems. The main mass reduction is observed in the columns masses. Ultimately, the reduction in beams masses are insignificant.

2. Non-linear static analysis

- The results of the base shear at the target displacement was highly influenced by the structural systems. MRF resulted the least base shear since it has low lateral stiffness and its stiffness is dramatically reduced due to the formation of collapse prevention plastic hinges. On the other hand, Inverted-V bracing systems had high base shear particularly the KIV-1 system where they developed the least amount of collapse prevention plastic hinges.
- CIV bracing system resulted in a significant enhancement of the initial stiffness compared with the other types of inverted-V bracing systems. However, this stiffness is suddenly reduced upon the development of the initial plastic hinges.
- The sequence from maximum to minimum displacement ductility factor is CIV, EIV, KIV2, KIV1 and MRF respectively.

3. Time history analysis

- Similar with the ELFM the maximum base shear is observed for CIV braced structures and the minimum values are observed for MRF buildings.
- Similar with the ELFM, moment resisting framed structure resulted in the highest displacement. However, CIV and KIV2 systems showed the minimum displacement for G+4 and G+9 respectively.
- Maximum storey acceleration for all the models in horizontal and vertical directions is observed in the case of CIV braced structures and minimum storey acceleration in all the directions are observed in the case of MRF buildings.

It can be concluded that KIV-2 is the optimum inverted-V bracing type where it has minimal cost compared with MRF, possess high performance compared with the other types of bracing and has higher ductility compared with CIV bracing system.

5.3 Recommendations

- Only mathematical modelling is applied within the content of the thesis. Since experimental validation through full scale modelling will add more value to the study outcomes.

- The study did not discuss the influence of different steel grade. Since different steel grade my results in a different behaviour.
- Only two different structure heights are considered. Hence, the behaviour of Inverted-V bracing systems in taller structure is still uncertain.
- The influence of the staircase was not consider regardless of the fact that it may increase the initial lateral stiffness of the building.
- Varying the bracing type along the elevation of the structure was not studied.

REFERENCES

Ahasan–ul–Haque, M., Masum, M. A., Ratul, M. M., & Tafheem, Z. EFFECT OF DIFFERENT BRACING SYSTEMS ON THE STRUCTURAL PERFORMANCE OF STEEL BUILDING.

Campbell, K. W., & Bozorgnia, Y. (2010). A ground motion prediction equation for the horizontal component of cumulative absolute velocity (CAV) based on the PEER-NGA strong motion database. Earthquake Spectra, 26(3), 635-650.

Chamber of Civil Engineers. (2015). *KKTC Deprem Bölgelerinde Yapılacak Binalar Hakkında Yönetmelik.* Lefkoşa: Inşaat Mühendisleri Odasi Chamber of Civil Engineers.

Council, B. S. S. (2000). Prestandard and commentary for the seismic rehabilitation of buildings. Report FEMA-356, Washington, DC.

CSI Analysis Reference Manual. (2013). CSI Analysis Reference Manual for SAP2000®, ETABS®, SAFE® and CSiBridge®

De Normalisation, C. E. (2005). European standard EN 1998-3 Eurocode 8: design of structures for earthquake resistance–part 3: assessment and retrofitting of buildings. Brussels, Belgium.

Duggal, S. K. (2013). Earthquake-Resistant Design of Structures. Oxford University Press.

Fahjan, Y. M. (2008). Selection and scaling of real earthquake accelerograms to fit the Turkish design spectra. Teknik Dergi, 19(3), 4423-4444.

Federal Emergency Management Agency. (2005). Improvement of nonlinear static seismic analysis procedures. FEMA 440, prepared by Applied Technology Council (ATC-55 Project).

Fukuta, T., Nishiyama, I., Yamanouchi, H., & Kato, B. (1989). Seismic performance of steel frames with inverted V braces. Journal of Structural Engineering, 115(8), 2016-2028.

Hashemi, B. H., & Alirezaei, M. (2018). On the Evaluation of the Use of EKBs to Improve Seismic Performance of Steel Frames. International Journal of Steel Structures, 18(1), 25-37.

Inel, M., Ozmen, H. B., & Bilgin, H. (2008). Re-evaluation of building damage during recent earthquakes in Turkey. Engineering Structures, 30(2), 412-427.

Kalibhat, M. G., Kamath, K., Prasad, S. K., & Pai, R. R. (2014). Seismic performance of concentric braced steel frames from pushover analysis. IOSR Journal of Mechanical and Civil Engineering, 67-73.

Kamble, P. S., Chavan, S. H., Kadam, S. S., Malve, D. S., Autade, T. S., & Choudhari, V. A. (2016). Lateral Load Analysis of a Building with & Without Knee Bracing. International Journal of Engineering Research and Applications, 6(5), 13-22.

Kotabagi, S., Manjunatha, K., Patil, H., & Dyavappanavar, S. P. (2015). A Comparative Study On Moment Resisting Steel Frames With & Without Bracings Subjected To Dynamic Loads For High Rise Buildings. IRJET) e-ISSN, 2395-0056

Kulkarni, Y. U., Chandak, P. G., Devtale, M. K., & Sayyed, S. S. (2016). Analysis of Various Steel Bracing Systems using Steel Sections for High Rise Structures. Int. J. Eng. Technol. Manag. Appl. Sci, 4(6), 220-227.

Londhe, R. S., & Baig, M. F. Non Linear Static Analysis Of Knee Bracing In Steel Frame Structures.

Miri, M., & Zare, A. (2009). Seismic Behaviour of Steel Frames Investigation with Knee Brace Based on Pushover Analysis. World Academy of Science, Engineering and Technology, International Journal of Civil, Environmental, Structural, Construction and Architectural Engineering, 3(2), 122-128.

Mahmoud, Y. M., Hassan, M. M., Mourad, S. A., & Sayed, H. S. (2018). Assessment of progressive collapse of steel structures under seismic loads. Alexandria engineering journal, 57(4), 3825-3839.

Mahmoudi, M., Montazeri, S., & Abad, M. J. S. (2018). Seismic performance of steel X-knee-braced frames equipped with shape memory alloy bars. Journal of Constructional Steel Research, 147, 171-186.

Mofid, M., & Lotfollahi, M. (2006). On the characteristics of new ductile knee bracing systems. Journal of Constructional Steel Research, 62(3), 271-281.

Naeemi, M., & Bozorg, M. (2009). Seismic performance of knee braced frame. World academy of science, engineering and technology, 50, 976-980.

Nourbakhs, S. M. (2011). Inelastic behavior of eccentric braces in steel structure (Doctoral dissertation, Eastern Mediterranean University).

Park, R. (1988, August). Ductility evaluation from laboratory and analytical testing. In Proceedings of the 9th world conference on earthquake engineering, Tokyo-Kyoto, Japan (Vol. 8, pp. 605-616).

Patel, B., Mali, R., Jadhav, P., & Ganesh, G. M. (2017). SEISMIC BEHAVIOR OF SYSTEMS IN HIGH RIS. International Journal of Civil Engineering, 8(3).

Patil, D. M., & Sangle, K. K. (2015, August). Seismic behaviour of different bracing systems in high rise 2-D steel buildings. In Structures (Vol. 3, pp. 282-305). Elsevier.

Popov, E. P., Kasai, K., & Engelhardt, M. D. (1987). Advances in design of eccentrically braced frames. Earthquake Spectra, 3(1), 43-55.

Tafheem, Z., & Khusru, S. (2013). Structural behavior of steel building with concentric and eccentric bracing: A comparative study. International Journal of Civil and Structural Engineering, 4(1), 12.

Turkish Standard Code of Practice for Design of Buildings and Structures for Agriculture. TS 498. Turkish Standards Institute; 1987 [in Turkish].

VA, M. C. (2016). Analysis of Moment Resisting Frame by Knee Bracing.

Sangle, K. K., Bajoria, K. M., & Mhalungkar, V. (2012). Seismic Analysis of High Rise Steel Frame with and without Bracing. 2012.

Siddiqi, Z. A., Hameed, R., & Akmal, U. (2016). Comparison of different bracing systems for tall buildings. Pakistan Journal of Engineering and Applied Sciences.

Yang, T. T., Sheikh, H., & Tobber, L. (2019). Influence of the Brace Configurations on the Seismic Performance of Steel Concentrically Braced Frames. Frontiers in Built Environment, 5, 27.

APPENDICES

APPENDIX 1

SEISMIC ZONES IN CYPRUS

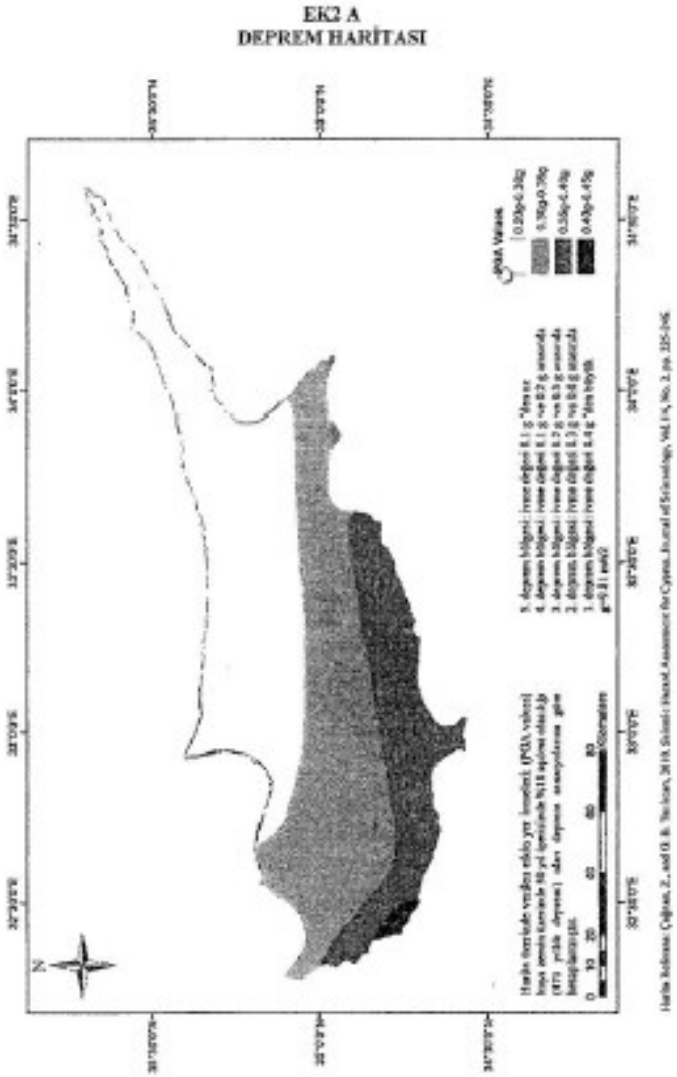

Belediye Hudutları Bazında
KKTC Deprem Bölgeleri Tablosu

Belediye	Deprem Bölgesi
Akdoğan	2
Akıncılar	2
Alayköy	3
Alsancak	3
Beyarmudu	2
Büyükkonuk	3
Çatalköy	3
Değirmenlik	3
Dikmen	3
Dipkarpaz	3
Esentepe	3
Gazimağusa	2
Geçitkale	3
Girne	3
Gönyeli	3
Güzelyurt	2
İnönü	3
İskele	3
Lapta	3
Lefke	2
Lefkoşa	3
Mehmetçik	3
Paşaköy	3
Serdarlı	3
Tatlısu	3
Vadili	2
Yeni Boğaziçi	3
Yeni Erenköy	3

APPENDIX 2

SOIL INVESTIGATION IN FAMAGUSTA CITY

➢ *Zeminin Mekanik Parametreleri;*

Zeminin Mekanik Parametreleri	*Doğu Akdeniz Üniversitesi Rekreasyon Projesi*		
	BLOK A (Bodrum + Zemin+ 8 kat)	***BLOK A (Zemin + 8 kat)***	***BLOK B (Zemin + 5 Kat)***
Ortalama Temel Taban Gerilmesi (ton/m^2)	23,05	20,61	14,63
Zemin Emniyet Gerilmesi (ton/m^2)	24,79	24,16	23,40
Zemin Yatak Katsayısı (ton/m^3)	2.974,80	2.899,20	2.808,00
Oturma Miktarı (cm)	3,77	3,38	2,52
Yeraltı Su Seviyesi (m)	6,15	6,00	5,15
Doğal Birim Hacim Ağırlık (kN/m^3)	19,23	19,15	19,25
Güvenlik Faktörü (Gs)	3	3	3
Zemin Grubu	B	B	B
Zemin Sınıfı	Z2	Z2	Z2
Spekrum karateristik periyotları	Ta=0,15 Tb=0,40	Ta=0,15 Tb=0,40	Ta=0,15 Tb=0,40
P_{GA}	0,28-0,30	0,28-0,30	0,28-0,30

APPENDIX 3

MATERIALS AND SLAB DECK PROPERTIES

Table 3.1: Yield strength and tensile strength for steel grade tested at 16 mm plate thickness.

Steel Grade	Yield Strength (MPA)	Tensile Strength (MPA)
S235	235 N/mm²	510 N/mm²
S275	275 N/mm²	530 N/mm²
S355	355 N/mm²	630 N/mm²

Table 3.2: Materials properties according to EC 3

Property	S275	C25/30
Weight per unit volume	77Kn/m³	25Kn/m³
Mass per unit volume	7850 kg/m³	2550kg/m³
Modulus of elasticity, E	210000N/mm²	31000 N/mm²
Poisson's 1ratio, U	0.3	0.2
Coefficient of Thermal expansion	0.0000117 1/C	0.00001 1/C
Shear modulus, G	80770 N/mm²	13000 N/mm²

Table 3.3: Equivalent between European steel grade and US steel grade.

European Steel grade	US grade
S235	A283C
S275	A570Gr40
S355	A572Gr50

Table 3.4: Slab deck dimensions, type (70/19)

Property Data	Value
Slab depth, tc	70 mm
Rip depth, hr	60 mm
Rip width top, wt	210 mm
Rip width bottom, wb	104 mm
Rip spacing, sr	305 mm
Deck shear thickness	1.2 mm
Deck unit weight	0.11 KN/m²
Shear stud diameter	19 mm
Shear stud height, hs	150 mm
Shear stud tensile strength, Fu	400 N/mm²

Table 3.5: The capacity of slab deck 915 type (KN/m²)

thickness (mm)	Span length (m)				
	1.5	2	2.5	3	3.5
0.7	7.46	4.74	3.29	2.42	1.85
0.8	9.11	5.75	3.97	2.91	2.22
0.9	10.83	6.79	4.67	3.41	2.60
1	12.61	7.87	5.39	3.93	2.99
1.1	14.45	8.98	6.13	4.45	3.39
1.2	16.33	10.11	6.88	4.99	3.79
1.3	18.26	11.26	7.65	5.54	4.20

APPENDIX 4

EARTHQUAKE PARAMETERS ACCORDING TO NCSC 2015

Table 4.1: Effective ground acceleration coefficient(A_0)

Seismic zone	(A_0)
1	0.4
2	0.3
3	0.2
4	0.1

The building importance factor (I) which depends on type and the purpose of the buildings.

Table 4.2: Buildings importance factor (I)

Buildings type and reasons of built	Importance factor
Buildings required to be utilized after the earthquake and buildings containing hazardous materials	1.5
Intensively and long-term occupied buildings and buildings preserving valuable goods	1.4
Intensively but short-term occupied buildings such as (Concert halls, cinema, theatre and sport facilities).	1.2
Other buildings	1

According to (NSCS-2015) seismic code the spectral acceleration coefficient A (T) that consider as the basis part for the determination of earthquake seismic loads is given by Equation (4.1).

$$A\,(T) \;=\; A_0\, I\, S\,(T) \qquad (4.1)$$

Where the spectrum coefficient S (T) which depending on the local site class conditions and the Structures natural period (T) determined by three Equations as shown below.

$$S\,(T) = 1 + 1.5\,\frac{T}{TA} \qquad (0 \le T \le TA)$$
$$S\,(T) = 2.5 \qquad (TA < T \le TB) \qquad (4.2)$$
$$S\,(T) = 2.5\left(\frac{TB}{T}\right)^{0.8} \qquad (TB < T)$$

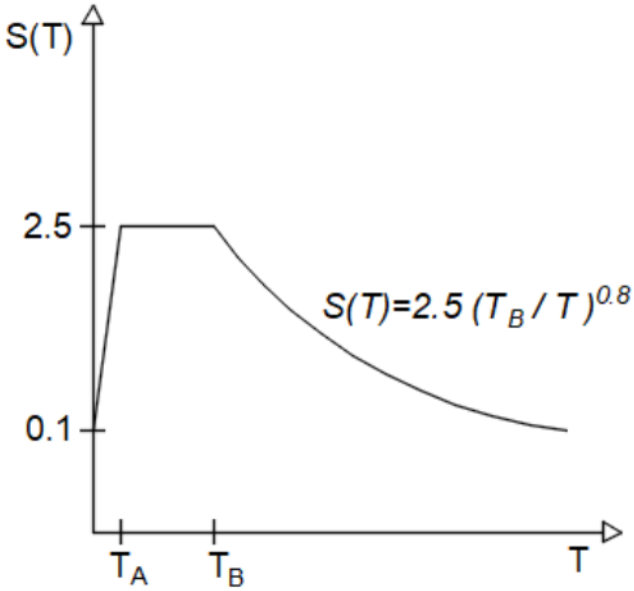

Figure 4.1: Spectrum coefficient curve according to (NCSC-2015)

T_B and T_A are the spectrum characteristic periods shown in the equation (3.2) depending on local site classes explaining in Table (4.3) shown below

Table 4.3: Spectrum characteristic periods (T_A, T_B)

Local site class	T_B (sec)	T_A (sec)
Z1	0.1	0.3
Z2	0.15	0.4
Z3	0.15	0.6
Z4	0.2	0.9

Soil group according to NCSC-2015 which depend on relative density, standard penetration shear wave velocity and compressive strength as display in Table (4.4).

Table 4.4: Soil group according to (NCSC-2015) code

Soil Group	Soil Group Description	relative density (%)	standard penetration (N/30)	Shear wave velocity (m/s)	compressive strength (kpa)
A	Massive volcanic rocks, unweather sound metamorphic rocks and stiff cemented sedimentary rocks	_	_	>1000	>1000
	Very dense sand and gravel...	8-100	> 50	>700	_
	Hard clay and silty clay	_	> 32	>700	>400
B	Soft volcanic rocks such as tuff and agglomerate and weathered cemented sedimentary rocks with planes of discontinuity	_	_	700-1000	500-1000
	Dense sand and gravel	65-85	30-50	400-700	_
	Very stiff clay and silty clay	_	16-32	300-700	200-400
C	Highly weathered soft metamorphic rocks and cemented sedimentary rocks with planes of discontinuity	_	_	400-700	<500
	Medium dense sand and gravel	35-65	10-30	200-400	_
	Stiff clay and silty clay	_	8-16	200-300	100-200
D	Soft and deep alluvial layers with high ground water level	_	_	<200	_
	Loose sand	<35	<10	<200	_
	Soft clay and silty clay	_	<8	<200	<100

Table 4.5: Local site classes according to (ncsc-2015) code

Local Site Class	Soil Group	Topmost Soil Layer Thickness (h1)
Z1	A	_
	B	h1 ≤ 15 m
Z2	B	h1 > 15 m
	C	h1 ≤ 15 m
Z3	C	15 m < h1 ≤ 50 m
	D	h1 ≤ 10 m
Z4	C	h1 > 50 m
	D	h1 > 10 m

Each structure has the ability to dissipate energy, the capacity to dissipate this energy vary among structure type. This capacity depend in the ductile behaviour of the elements. Where the structural seismic response reduced by the effective of ductility. According to (NCSC-2015) Ra is the seismic load reduction factor which calculated by using equation (4.2)

$$Ra\,(T) = 1.5 + (R - 1.5)\frac{T}{TA} \qquad (0 \le T \le TA)$$
$$Ra\,(T) = R \qquad (TA < T) \qquad (4.3)$$

Table 4.6: Live load participation factor according to NCSC-2015

Purpose of occupancy of structure	$\boldsymbol{n}$
Depot and warehouse	0.6
Dormitory, school, sport facility, theatre, cinema, concert hall, car park, restaurant and shop	0.8
Residence, hotel, office and hospital	0.3

Table 4.7: Minimum structure performance targets expected for different earthquakes levels

	Probability of the Earthquake to be exceeded		
The usage purpose and the Type of the structure	**50 % in 50 years**	**10 % in 50 years**	**2 % in 50 years**
The buildings that should be used after earthquakes such as (Health facilities, hospitals, fire stations, transportation stations, provincial and disaster management centres).	_	RU	LS
The buildings that people stay in for a long time period such as (Accommodations, schools,pensions, dormitories, military posts, prisons and museums).	_	RU	LS
The buildings that people visit densely and stay in for a short time period such as (Theatre and concert halls, cinema, culture ,centers and sports facilities.	RU	LS	_
The buildings containing hazardous materials.	_	RU	PC
Other structural buildings.	_	LS	_

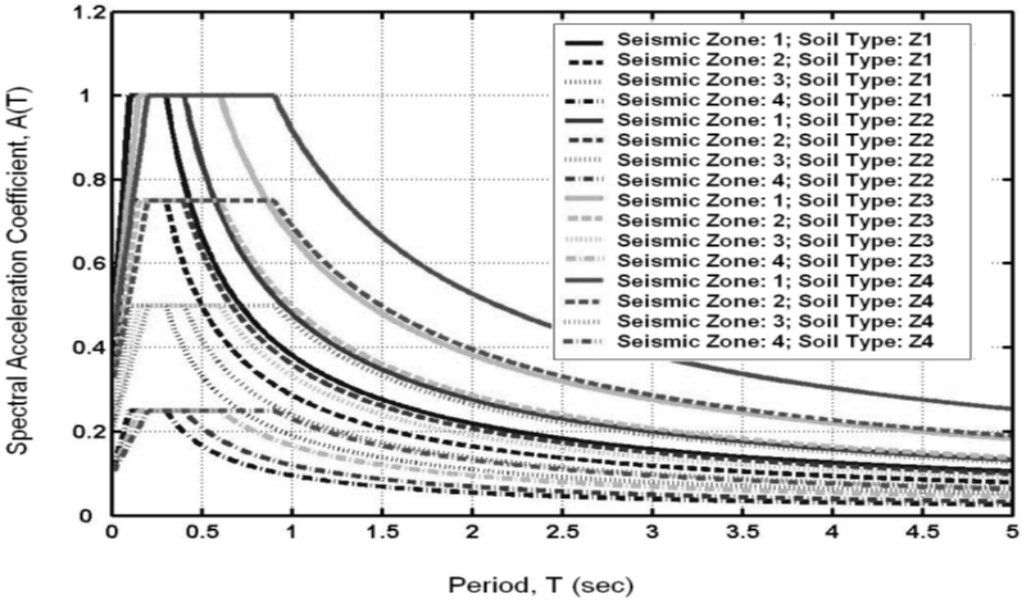

Figure 4.2: Spectral acceleration curves for all seismic zones and soil types according to (NCSC-2015)

APPENDIX 5

(STIFFNESS-BASE SHEAR) DISPLACEMENT CURVES

The results of stiffness-displacement curves with base shear displacement curve in Y-direction which is the columns flanges direction where the effect of bracings systems can be major are plotted below:

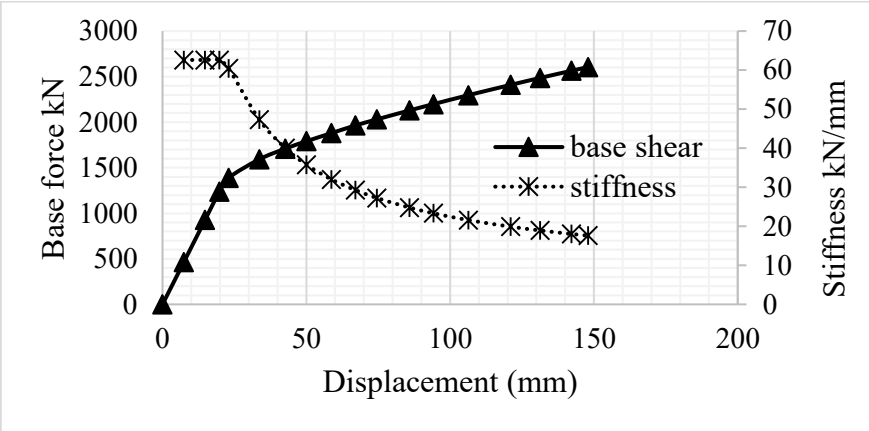

Figure 5.43: Stiffness –base shear-displacement curves in Y direction for (R-CIV-5) building

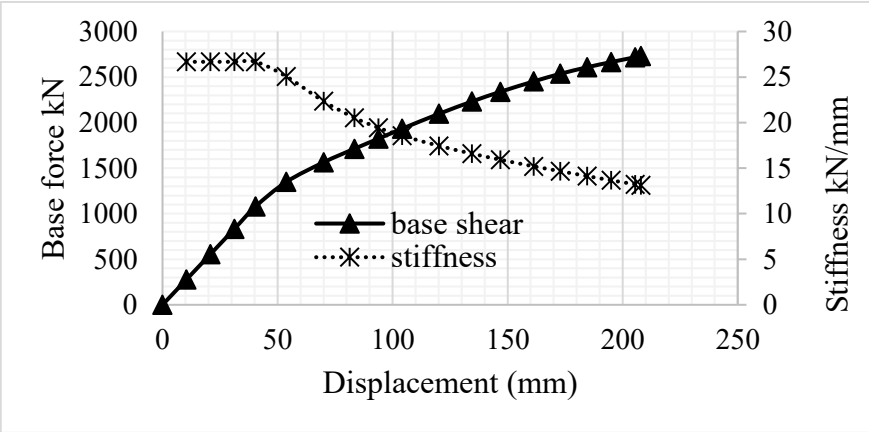

Figure 5.2: Stiffness –base shear-displacement curves in Y direction for (R-EIV-5) building

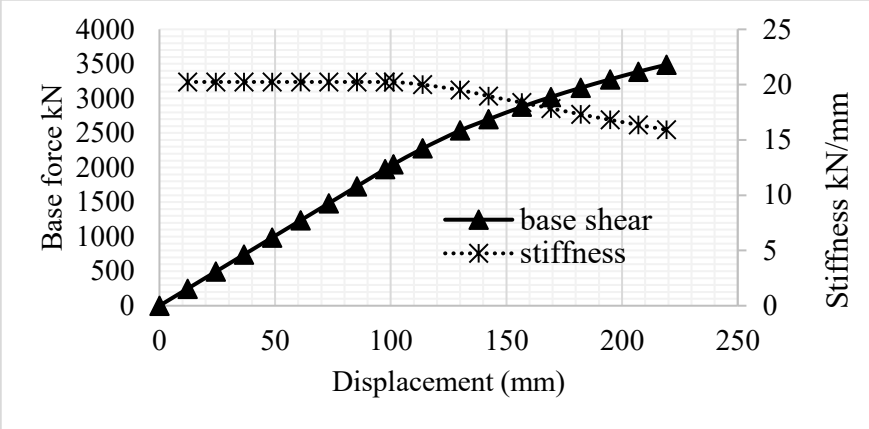

Figure 5.3: Stiffness –base shear-displacement curves in Y direction for (R-KIV1-5) building

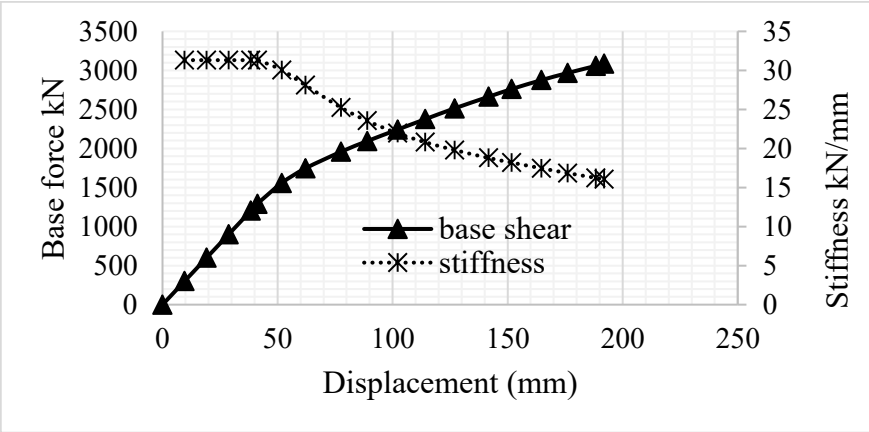

Figure 5.4: Stiffness –base shear-displacement curves in Y direction for (R-KIV2-5) building

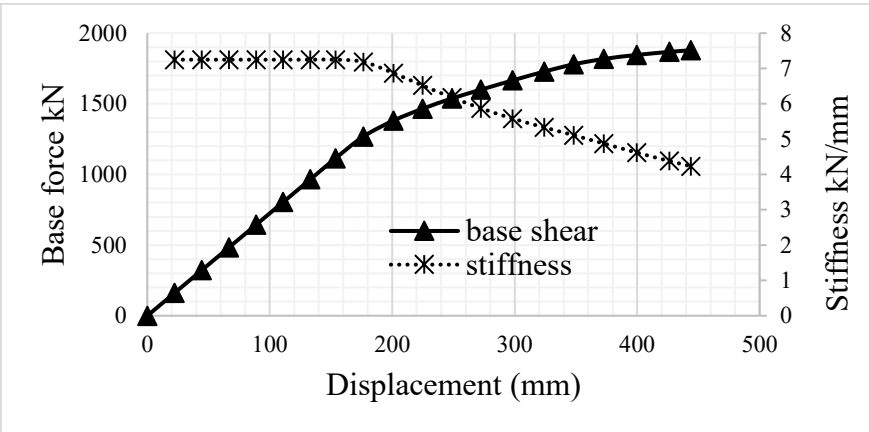

Figure 5.5: Stiffness –base shear-displacement curves in Y direction for (R-MRF-5) building

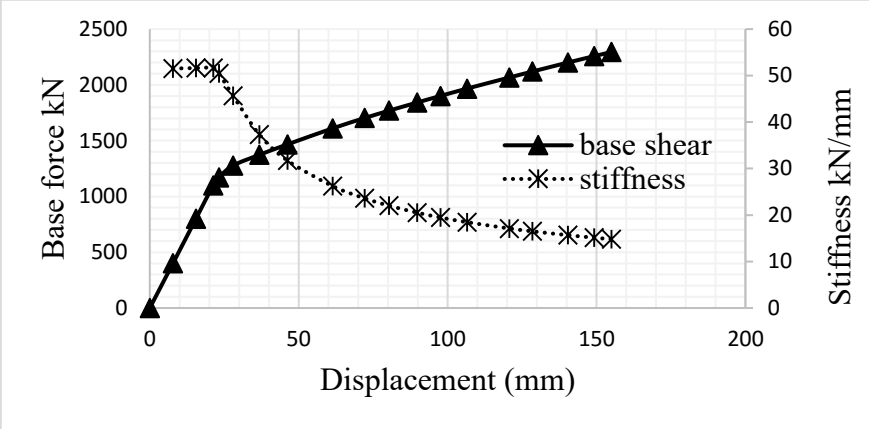

Figure 5.6: Stiffness –base shear-displacement curves in Y direction for (IR-CIV-5) building

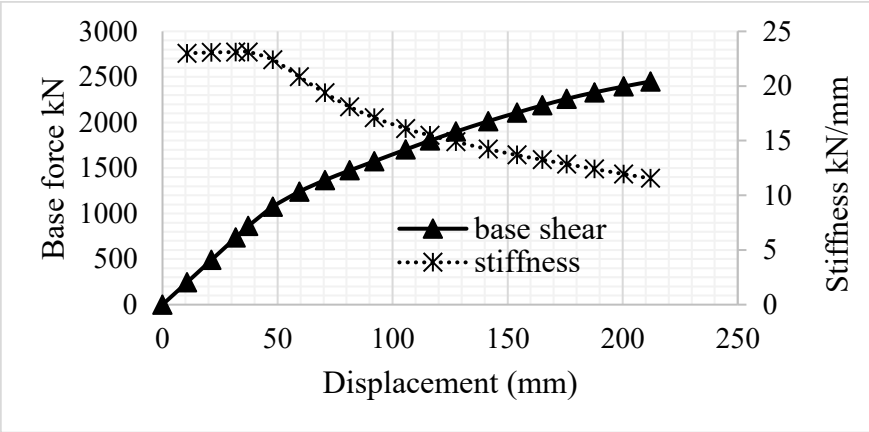

Figure 5.7: Stiffness –base shear-displacement curves in Y direction for (IR-EIV-5) building

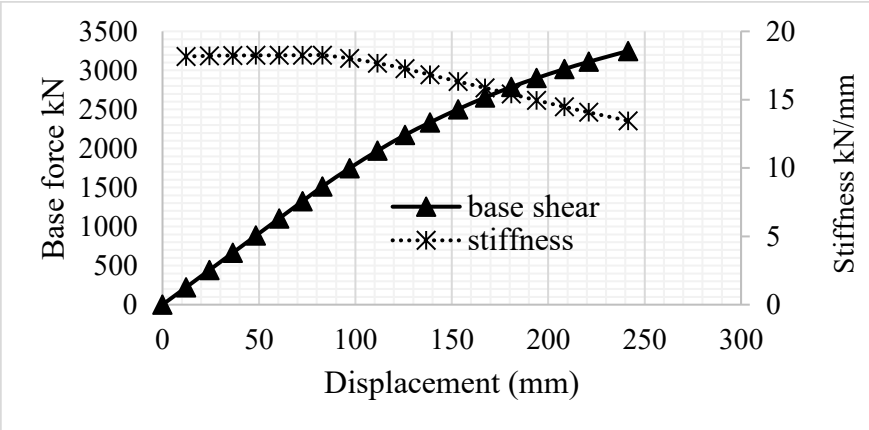

Figure 5.8: Stiffness –base shear-displacement curves in Y direction for (IR-KIV1-5) building

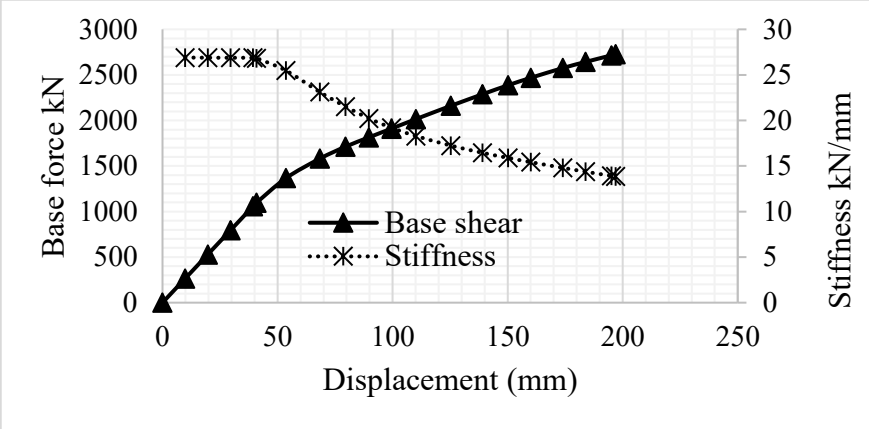

Figure 5.9: Stiffness –base shear-displacement curves in Y direction for (IR-KIV2-5) building

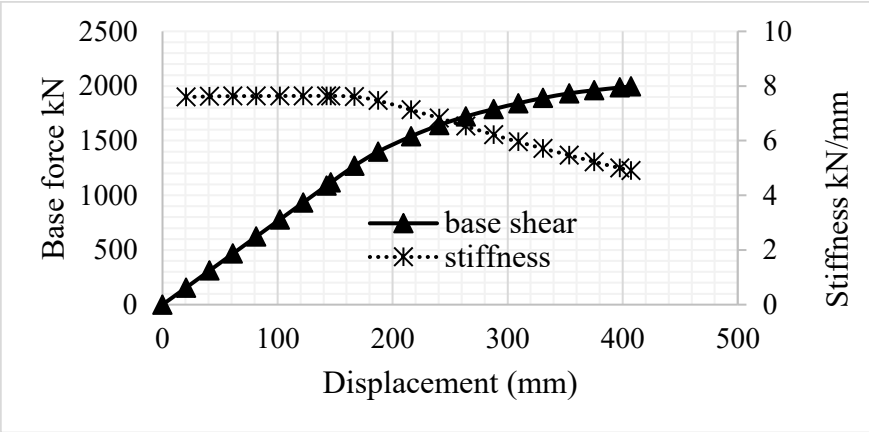

Figure 5.10: Stiffness –base shear-displacement curves in Y direction for (IR-MRF-5) building

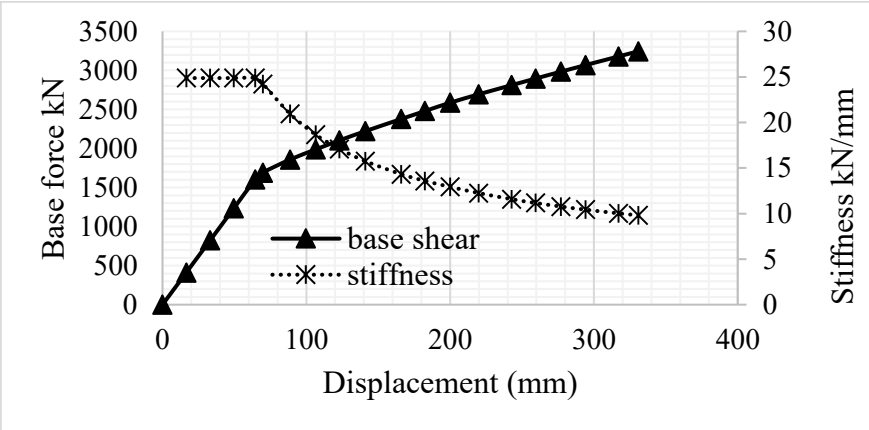

Figure 5.11: Stiffness –base shear-displacement curves in Y direction for (R-CIV-10) building

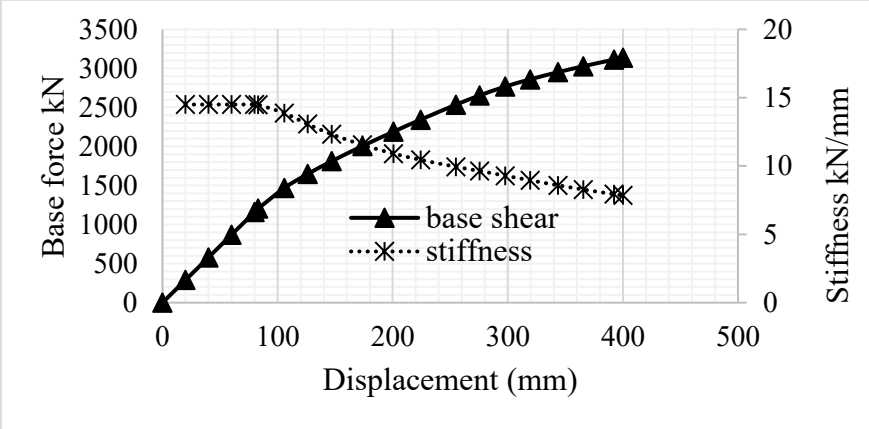

Figure 5.12: Stiffness –base shear-displacement curves in Y direction for (R-EIV-10) building

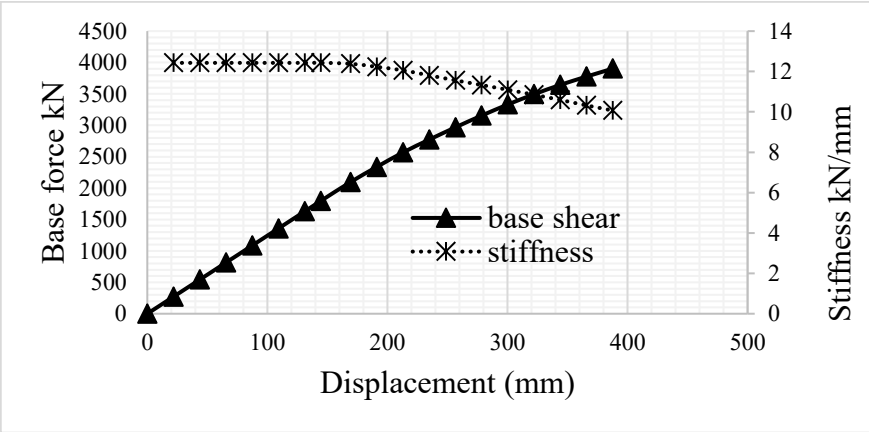

Figure 5.13: Stiffness –base shear-displacement curves in Y direction for (R-KIV1-10) building

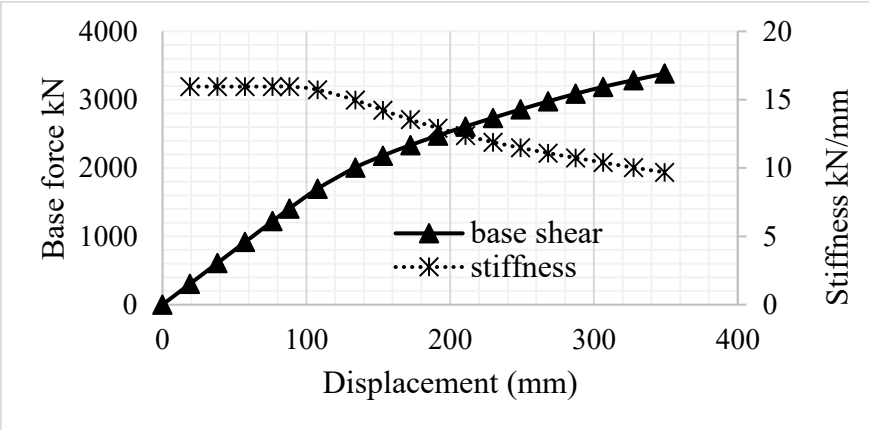

Figure 5.14: Stiffness –base shear-displacement curves in Y direction for (R-KIV2-10) building

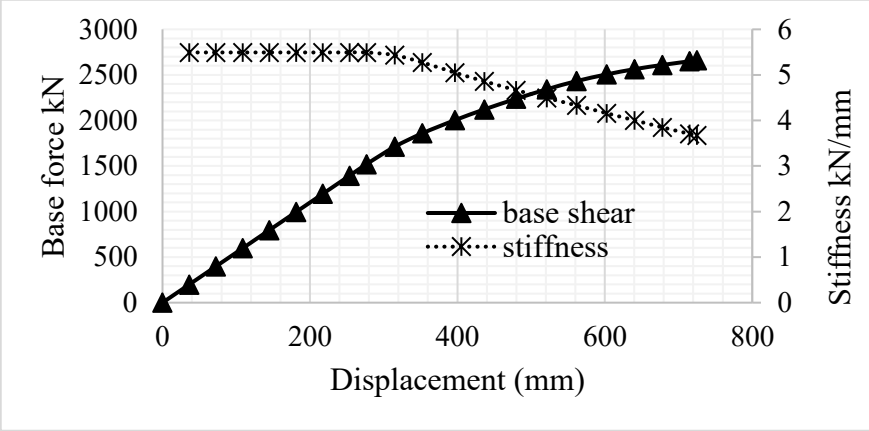

Figure 5.15: Stiffness –base shear-displacement curves in Y direction for (R-MRF-10) building

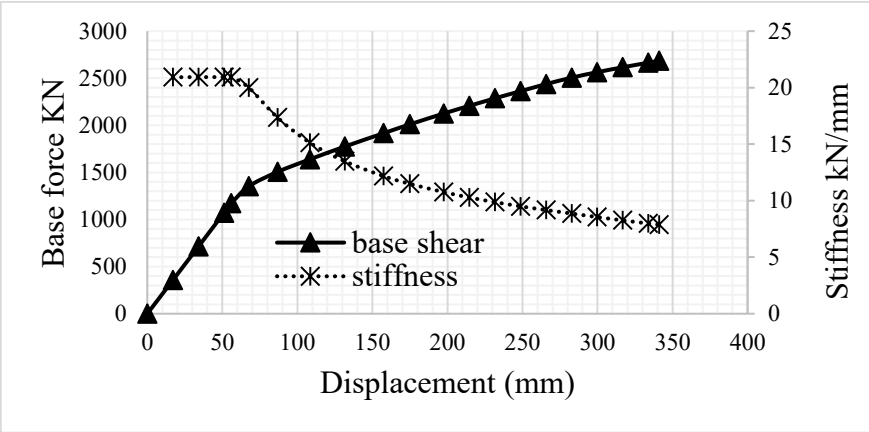

Figure 5.16: Stiffness –base shear-displacement curves in Y direction for (IR-CIV-10) building

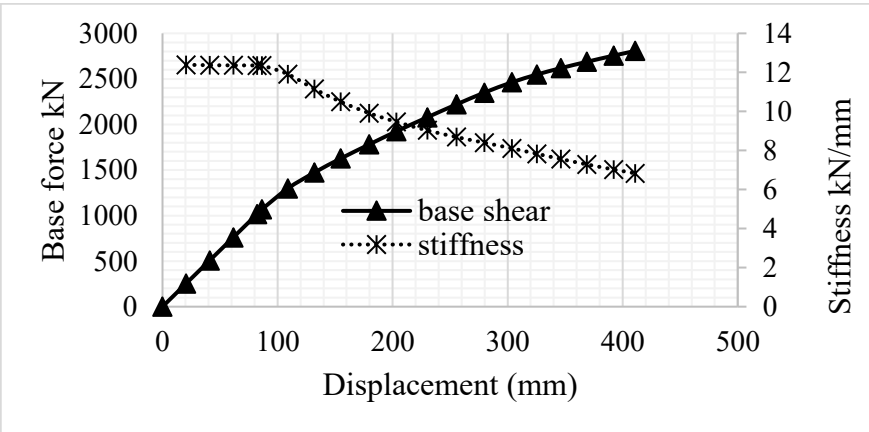

Figure 5.17: Stiffness –base shear-displacement curves in Y direction for (IR-EIV-10) building

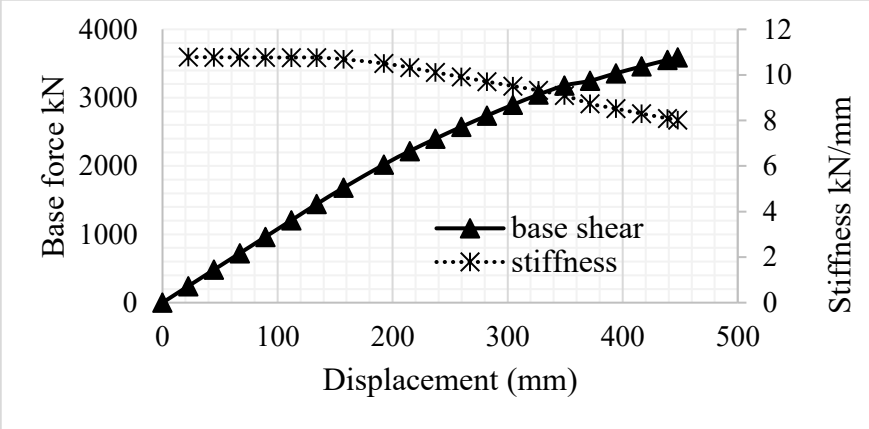

Figure 5.18: Stiffness –base shear-displacement curves in Y direction for (IR-KIV1-10) building

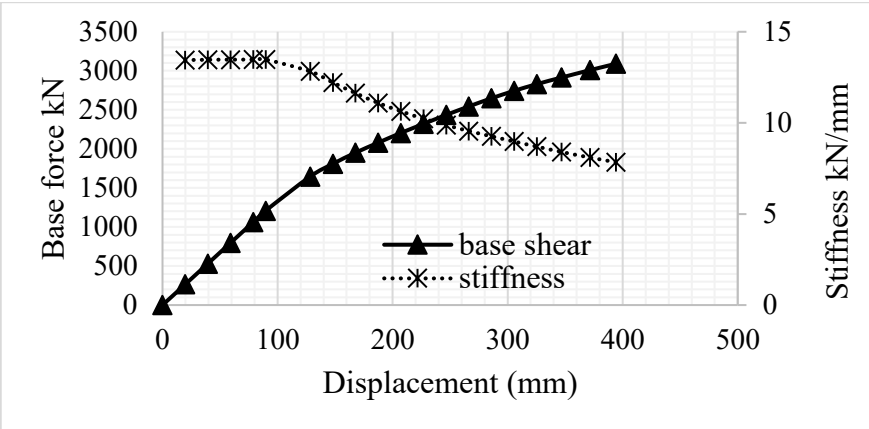

Figure 5.19: Stiffness –base shear-displacement curves in Y direction for (IR-KIV2-10) building

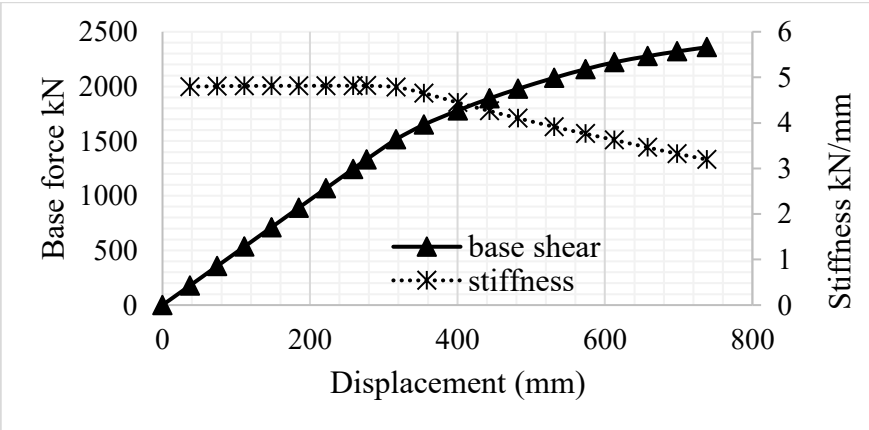

Figure 5.20: Stiffness –base shear-displacement curves in Y direction for (IR-MRF-10) building

APPENDIX 6

RESPONSE SPECTRUM CURVES

1. Response Spectrum Coefficient-NCSC-2015

period	S(T)	Damping	Seismic Zone	Site Class
0.000	1.000	0.05	Zone 2	Z2
0.050	1.383			
0.100	1.767			
0.150	2.500			
0.400	2.500			
0.500	2.091			
0.600	1.807			
0.700	1.598			
0.900	1.307			
1.000	1.201			
2.000	0.690			
4.000	0.396			
8.000	0.228			
10.000	0.190			
15.000	0.138			
20.000	0.109			
30.000	0.079			

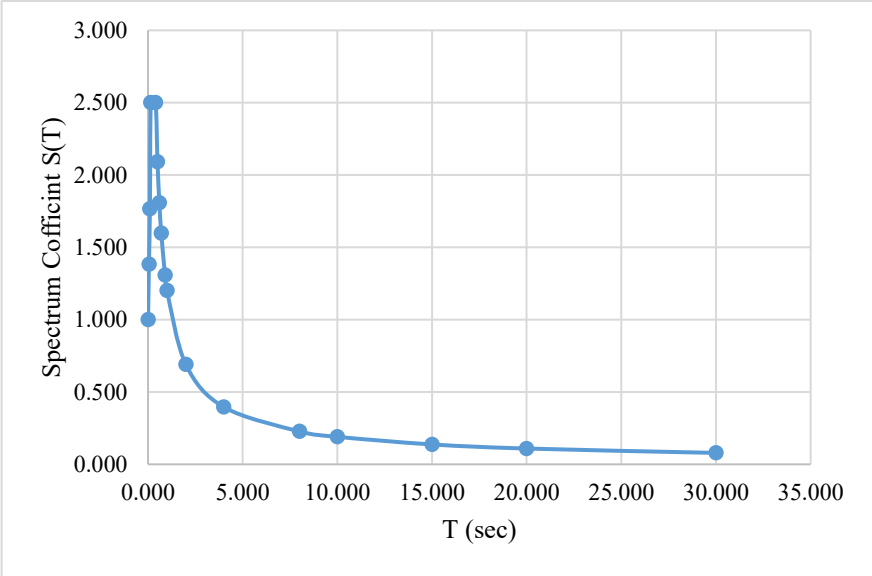

2. Response Spectrum Acceleration Coefficient -NCSC-2015

period	A(T)	Damping	Seismic Zone	Site Class	A_0
0.000	0.300	0.05	Zone 2	Z2	0.3
0.050	0.415				
0.100	0.530				
0.150	0.750				
0.400	0.750				
0.500	0.627				
0.600	0.542				
0.700	0.479				
0.900	0.392				
1.000	0.360				
2.000	0.207				
4.000	0.119				
8.000	0.068				
10.000	0.057				
15.000	0.041				
20.000	0.033				
30.000	0.024				

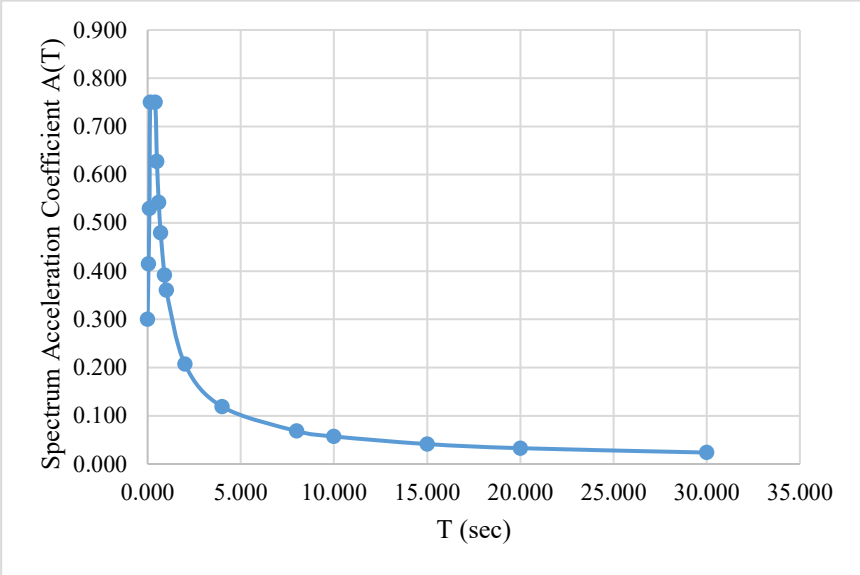

3. Response Acceleration Spectrum-NCSC-2015

period	Sa	Damping	Seismic Zone	Site Class	A_0	I	R	g	%
0.000	0.491	0.05	Zone 2	Z2	0.3	1	6	9.81	10
0.050	0.679								
0.100	0.867								
0.150	1.226								
0.400	1.226								
0.500	1.026								
0.600	0.887								
0.700	0.784								
0.900	0.641								
1.000	0.589								
2.000	0.338								
4.000	0.194								
8.000	0.112								
10.000	0.093								
15.000	0.068								
20.000	0.054								
30.000	0.039								

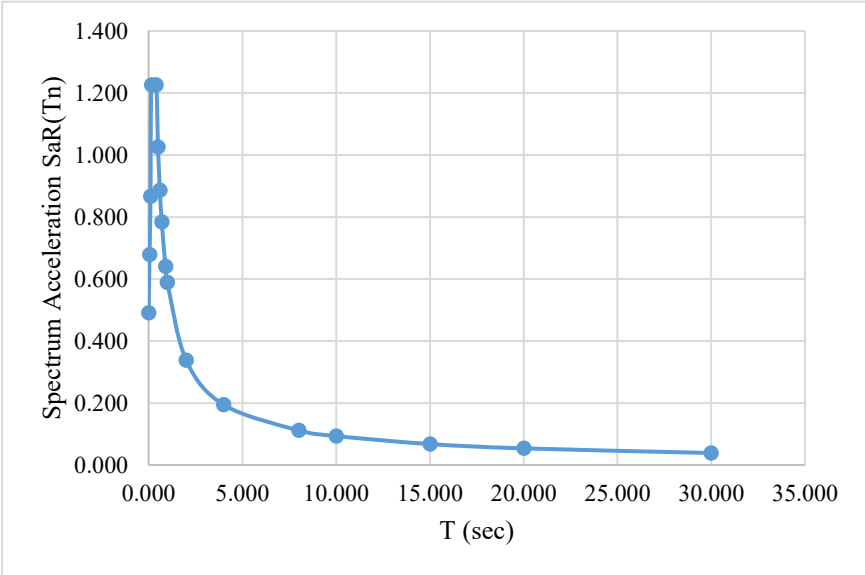

4. Response Acceleration Spectrum-NCSC-2015

period	Sa	Damping	Seismic Zone	Site Class	A_0	I	R	g	%
0.000	0.736	0.05	Zone 2	Z2	0.3	1	6	9.81	2
0.050	1.018								
0.100	1.300								
0.150	1.839								
0.400	1.839								
0.500	1.539								
0.600	1.330								
0.700	1.176								
0.900	0.961								
1.000	0.884								
2.000	0.508								
4.000	0.292								
8.000	0.167								
10.000	0.140								
15.000	0.101								
20.000	0.080								
30.000	0.058								

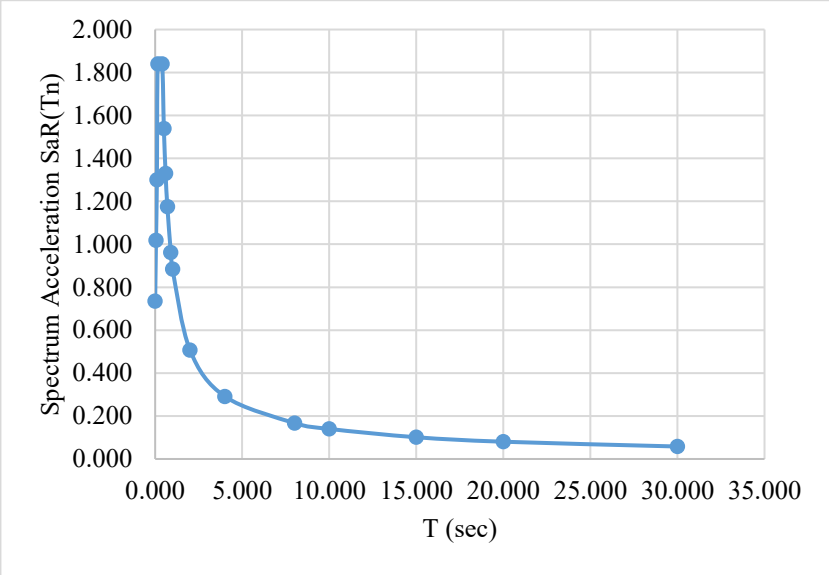

5. Response Acceleration Spectrum-NCSC-2015

period	Sa	Damping	Seismic Zone	Site Class	A_0	I	R	g	%
0.000	0.368	0.05	Zone 2	Z2	0.3	1	8	9.81	10
0.050	0.509								
0.100	0.650								
0.150	0.920								
0.400	0.920								
0.500	0.769								
0.600	0.665								
0.700	0.588								
0.900	0.481								
1.000	0.442								
2.000	0.254								
4.000	0.146								
8.000	0.084								
10.000	0.070								
15.000	0.051								
20.000	0.040								
30.000	0.029								

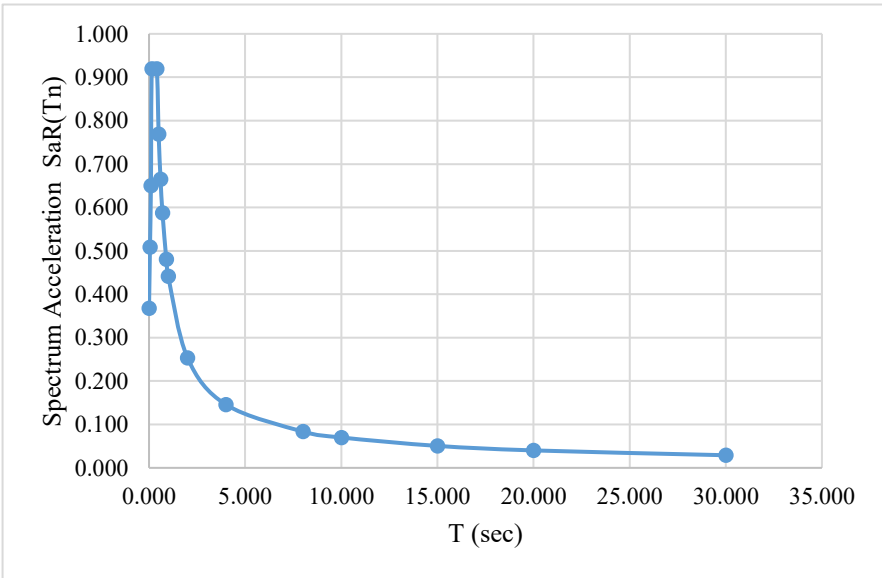

6. Response Acceleration Spectrum-NCSC-2015

pried	Sa	Damping	Seismic Zone	Site Class	A_0	I	R	g	%
0.000	0.552	0.05	Zone 2	Z2	0.3	1	8	9.81	2
0.050	0.763								
0.100	0.975								
0.150	1.380								
0.400	1.380								
0.500	1.154								
0.600	0.997								
0.700	0.882								
0.900	0.721								
1.000	0.663								
2.000	0.381								
4.000	0.219								
8.000	0.126								
10.000	0.105								
15.000	0.076								
20.000	0.060								
30.000	0.044